Functionally active serum and monoclonal antibody responses targeting the pre-erythrocytic stage of *Plasmodium falciparum* in Tanzanian adults after vaccination with purified, live-attenuated sporozoites

Inauguraldissertation

zur

Erlangung der Würde einer Doktorin der Philosophie

vorgelegt der

Philosophisch-Naturwissenschaftlichen Fakultät

der Universität Basel

von

Isabelle Madlen Zenklusen

aus Simplon-Dorf, VS

Basel, 2017

Genehmigt von der Philosophisch-Naturwissenschaftlichen Fakultät auf Antrag von Prof. Dr. Marcel Tanner, PD Dr. Claudia Daubenberger and Dr. Steffen Borrmann.

Basel, den 17. Oktober 2017 Prof. Dr. Martin Spiess

Summary

With 212 million cases worldwide and an estimated 429,000 deaths in 2015, malaria continues to be a serious global health threat. An effective vaccine could significantly decrease malaria-associated morbidity and mortality, especially in children under the age of five years. At present, there is no licensed malaria vaccine available. The most advanced malaria vaccine candidate, the RTS, S/AS01 subunit formulation, showed limited and short-term vaccine efficacy against clinical malaria in phase 3 clinical studies in malaria-endemic populations in sub-Saharan Africa.

The only vaccination approach that has ever induced complete sterile protection against controlled human malaria infection (CHMI) in malaria-naïve individuals, is the immunization with live, whole-attenuated sporozoites. The Sanaria® PfSPZ Vaccine (PfSPZ Vaccine) is a pre-erythrocytic vaccine, which is composed of live, radiation-attenuated, aseptic, purified, non-replicating, cryopreserved, whole *Plasmodium falciparum* (Pf) sporozoites (PfSPZ). In a study at the National Institutes of Health (NIH), the PfSPZ Vaccine was safe and well tolerated and protected 100% (6/6) of malaria-naïve volunteers against homologous CHMI when administered intravenously (IV) at 5 doses of 1.35 x 10^5 PfSPZ.

The overall aims of this thesis included i) the evaluation of the safety, immunogenicity and protective efficacy against homologous CHMI of the PfSPZ Vaccine by direct venous inoculation (DVI) of malaria pre-exposed volunteers from Tanzania and ii) the study of functionally active serum and monoclonal antibody responses against Pf sporozoites induced by malaria pre-exposed Tanzanian volunteers upon immunization with the PfSPZ Vaccine. Building on these objectives, the here presented thesis is structured around three manuscripts:

Manuscript 1: Safety, immunogenicity and protective efficacy against controlled human malaria infection of PfSPZ Vaccine in Tanzanian adults

This manuscript depicts the first clinical phase I trial on the safety, immunogenicity and protective efficacy against homologous CHMI of PfSPZ Vaccine performed in Africa. The study was conducted in healthy male volunteers aged 20 to 30 years in Bagamoyo, Tanzania. Similar regimen as tested in the NIH study of 5 doses of 1.35 x 10^5 (low-dose group) or 2.7 x 10^5 (high-dose group) of PfSPZ Vaccine was administered via DVI to Tanzanian adults.

Homologous CHMI was conducted at 3 and 24 weeks after the last vaccination. The PfSPZ Vaccine was safe and well tolerated, but less immunogenic and protective against CHMI as in malaria-naïve US Americans. In the low-dose group, 1 of 18 (6%) vaccinees was protected and 4 of 20 (20%) vaccinees were protected in the high-dose group at CHM1, 3 weeks past last vaccination. The 4 protected subjects from the high-dose group were still protected after repeated CHMI2, at 24 weeks past last vaccination. It is hypothesized that higher individual doses and altering intervals will be required to induce improved protective efficacy and immunogenicity in malaria endemic target populations.

Manuscript 2: Intravenous application of irradiation attenuated *Plasmodium falciparum* sporozoites elicits long-lived IgG and IgM invasion inhibitory antibodies in malaria pre-exposed volunteers

In this study we aimed i) to gain a better understanding of the vaccine-induced humoral immune responses in malaria pre-exposed individuals after immunization with DVI-administered PfSPZ Vaccine and ii) to investigate if sporozoite binding and invasion inhibitory IgM antibodies are induced following PfSPZ vaccination. To address this, we used serum and plasma samples collected from a subset of volunteers who participated in the PfSPZ Vaccine trial described in manuscript 1. Our findings demonstrate that malaria pre-exposed volunteers develop sporozoite invasion inhibitory antibodies and induce anti-CSP IgG and IgM antibodies after repeated PfSPZ vaccination. A subset of these plasma samples was depleted from IgG and IgA antibodies to obtain fractions containing only IgM antibodies. Depleted IgM antibody fractions of 3 volunteers demonstrated sporozoite invasion inhibitory capacity in *in vitro* inhibition of sporozoite invasion (ISI) assays. These results indicated for the first time that sporozoite-specific IgM antibodies could contribute to protection against malaria infection.

Manuscript 3: CSP-specific human monoclonal antibodies inhibiting *Plasmodium falciparum* liver stage infection target a distinct sequence at the N-terminus

To investigate the mechanisms of protection elicited by antibodies following PfSPZ vaccination, we isolated a panel of monoclonal antibodies from the PfSPZ-immunized Tanzanian volunteers who were found protected from homologous CHMI in the study

described in manuscript 1. Using an antigen-agnostic approach to identify antibodies that can bind the surface of intact sporozoites, we found that all monoclonal antibodies isolated target the circumsporozoite protein (CSP), confirming its known immunodominance. Functional characterization of these antibodies revealed, that the most effective antibodies reducing Pf liver burden in a humanized mouse model target a distinct epitope located at the junction between the N-terminal end and the NANP repeat, a region which is not included in the RTS, S vaccine. Our results suggest that this identified region could be a component of interest in the future design of effective second generation PfCSP subunit vaccines.

Acknowledgements

During my PhD studies I had the pleasure of working together with a number of people to whom I would like to express my deepest gratitude:

My supervisor Claudia Daubenberger for her guidance throughout these years, her support and helpful suggestions and all the scientific discussions we shared.

The former director of the Swiss TPH, Marcel Tanner, who made this PhD possible in the first place by connecting me with Claudia for this interesting project and for his time to evaluate this work.

Steffen Borrmann, who kindly agreed to be my Co-referee and for correcting my thesis and travelling to Basel to attend my PhD defense.

Antonio Lanzavecchia, Stefan Kappe, Stephen L. Hoffman, B. Kim Lee Sim and the whole Sanaria team for the great and fruitful collaborations.

Brandon Sack who did an excellent job as my supervisor during my stay at the Center for Infectious Disease Research in Seattle. It was a very interesting, educational and fun time!

My colleague Joshua Tan, for his support, the scientific discussions and the fun we had together at the IRB in Bellinzona.

The Kappe group: Ryan, Hayley, Brandon, Deba, Nana, Lander, Erika, Will, Dorender, Silvia, Ashley, Nelly, Matthew, Sebastian and the hard-working "sporozoite-production team", for the great atmosphere in the lab, for providing me with millions of sporozoites for my experiments. For their support and valuable scientific input and for making my stay in Seattle so pleasant. It was a pleasure being part of your group and I enjoyed it very much!

All my friends and colleagues from the Ifakara Health Institute in Bagamoyo, with special thanks to Jongo, Kamaka, Seif, Elena and the whole clinical study team. Asanteni sana for the wonderful team spirit during the busy times of the BSPZV1 trial. I learned a lot from you all and I will always remember this amazing experience. It was my greatest pleasure to work with you!

My dear colleagues from the Clinical Immunology Unit at the Swiss TPH: Tobias R. (Kaka T.), Dada Annethi, Catherine Mkindi (Mama D.), Julian, Damien, Kaka Max and Tobi S. for being so supportive and helpful during my PhD studies and for becoming such good friends.

My very good friends: Annie, Layla, David & Sämi. I am glad to have you here in Basel!

My dear family and brother for their never ending support throughout my life.
Very special thanks go to Julian for always being there, his kind support and his positive attitude to life!

Table of Contents

List of Abbreviations

ACT	Artemisinin-based combination therapy
α-Gal	Galα1-3Galβ1-4GlcNAc-R
BCR	B cell receptor
BCG	Bacille Calmette-Guerin
CHMI	Controlled human malaria infection
CHMP	Committee for Medical Products
CIDR1α	Cysteine-rich interdomain region 1α
CVac	Chemoprophylaxis vaccination
CPS	Chemoprophylaxis and sporozoites
CS	Circumsporozoite
CSP	Circumsporozoite protein
CSR	Class switch recombination
DC	Dendritic cell
DVI	Direct venous inoculation
EBV	Epstein Bar virus
E. coli	*Escherichia coli*
ELISA	Enzyme-linked immunosorbent assay
EMA	European Medicine Agency
GAPs	Genetically attenuated parasites
GC	Germinal center
GMP	Good Manufacturing Practices
ID	Intradermal
IDC	Intraerythrocytic developmental cycle
IFN-γ	Interferon gamma
iNOS	Inducible nitric oxidase synthase
IPTi	Intermittent preventive treatment in infants
IPTp	Intermittent preventive treatment in pregnancy
iRBC	Infected red blood cell
ISI	Inhibition sporozoite invasion
IFA	Immunofluorescence assay
ISTI	Inhibition of sporozoite traversal and invasion

ITN	Insecticide-treated bed-nets
IV	Intravenous/intravenously
LAG-3	Lymphocyte activation gene 3
LLPC	Long-lived plasma cell
LNVP	Liquid nitrogen vapor phase
LoD	Limit of detection
mAbs	Monoclonal antibodies
MBC	Memory B cell
MZ B	Marginal zone B cell
NAI	Naturally acquired immunity
NIH	National Institutes of Health
NK cells	Natural killer cells
NO	Nitric oxide
P. falciparum	*Plasmodium falciparum*
P. knowlesi	*Plasmodium knowlesi*
P. malariae	*Plasmodium malariae*
P. ovale curtisi	*Plasmodium ovale curtisi*
P. ovale wallikeri	*Plasmodium ovale wallikeri*
P. vivax	*Plasmodium vivax*
PBA	Polyclonal B cell activation
PBMC	Peripheral blood mononuclear cell
PD-1	Programmed cell death 1
Pf	*Plasmodium falciparum*
PfCS	*P. falciparum* circumsporozoite
PfEMP1	*P. falciparum* erythrocyte membrane protein 1
pfhrp2/*hrp3*	*P. falciparum* histidine rich protein 2/3
PfSPZ	*P. falciparum* sporozoites
pLDH	*Plasmodium* lactate dehydrogenase
RAS	Radiation-attenuated sporozoites
RBC	Red blood cell
RDT	Rapid diagnostic test
RUNMC	Radboud University Medical Center
RT	Room temperature
SC	Sub-cutaneous

SHM	Somatic hypermutation
SP	Sulfadoxine pryimethamine
TLR	Toll-like receptor
VSA	Variant surface antigen
WHO	World Health Organization

Chapter 1

Introduction

1.1 Malaria Overview

1.1.1 The global burden of malaria

To date, malaria is endemic in 91 countries and territories (Figure 1). Despite remarkable reductions in malaria morbidity and mortality due to improvements in vector control, therapeutics and diagnostics between the years 2000 and 2015, Malaria remains a disease of global health importance [1, 2]. In 2015, the World Health Organization (WHO) estimated 212 million new malaria cases globally, of which 429,000 were fatal. An estimated 92% of those deaths occurred in the WHO African region with 70% of all deaths reported in children under the age of 5 years [1].

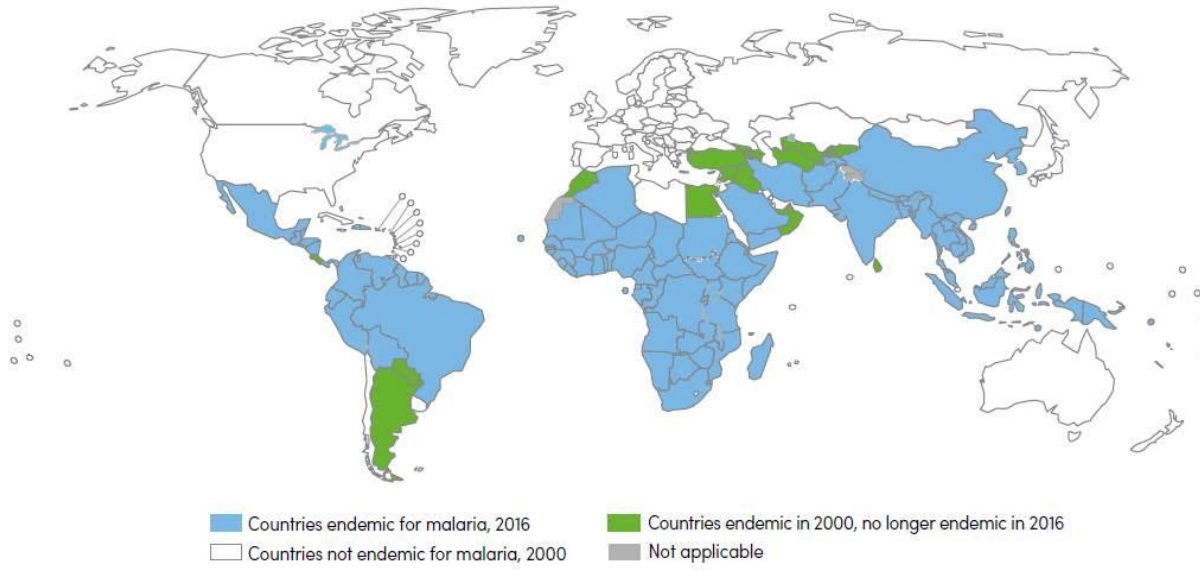

Figure 1 Countries endemic for malaria in the years of 2000 and 2016. Between 2000 and 2015 substantial reductions in malaria case incidence (41%) and malaria mortality rates (62%) have been achieved. The number of malaria-endemic countries and territories decreased from 108 in the year 2000 to 91 at the beginning of 2016 [1].

1.1.2 Malaria species infecting humans

Malaria is caused by *Plasmodium* parasites and transmitted to people through the bites of infected female *Anopheles* mosquitoes [3]. Six plasmodial species are infectious to humans: *P. falciparum* is the most prevalent parasite on the African continent and responsible for most malaria-related deaths globally [1]. *P. vivax* is a major cause of illness across large parts of the world, mainly outside of sub-Saharan Africa. Deaths due to this parasite have been underestimated in the past years [4]. *P. ovale curtisi*, *P. ovale wallikeri*, and *P. malariae* are considered as more benign species [1]. The zoonotic species *P. knowlesi* is a malaria parasite infecting long-tailed macaques and is largely found in Southeast Asia [5] and there is no clear evidence yet of human-to-human transmission [6]. Nevertheless, a study in Malaysia reported that this parasite can cause severe disease [6].

1.1.3 *P. falciparum* life cycle and pathogenesis

P. falciparum undergoes a complex life cycle and requires both human and mosquito hosts to complete transmission (Figure 2) [7]. The infection begins when female *Anopheles* mosquitoes inoculate a small number of sporozoites (10-100) into the human's dermis and blood stream while taking a blood meal (Figure 2A) [7]. A proportion of these sporozoites start to penetrate blood vessels, a process relying on gliding motility, in order to enter the bloodstream. Sporozoites remaining in the skin are destroyed and drained to regional lymph nodes [8]. Those that reach the circulation, quickly migrate to the liver tissue through a process called traversal. In the liver, the sporozoites first cross macrophage-like Kupffer cells and several hepatocytes before entering and taking residence in few hepatocytes (Figure 2B) [8, 9]. Inside the hepatocyte, the sporozoites start to replicate and differentiate for approximately 7 days until they give rise to tens of thousands of asexual blood-stage parasites called merozoites [10]. In each sporozoite-infected hepatocyte, around 40,000 merozoites are released into the blood-stream via the budding of parasite-filled vesicles called merosomes [10]. Throughout the whole pre-erythrocytic stage development in the liver, the infection remains clinically silent [9]. Clinical symptoms of malaria occur only during the asexual blood-stage infection (Figure 2C) and can develop as early as three days after merozoites are released from the liver. Once the merozoites are in the bloodstream, they start a 48 hour cycle of red blood cell (RBC) invasion, parasite replication and rupture, leading to the release of more merozoites that infect new RBC (Figure 2C), a process also known as asexual intraerythrocytic developmental cycle (IDC) [11]. The IDC includes four distinct stages: the

RBC-invasive merozoite stage; the ring-stage, which develops after RBC invasion and feeds on hemoglobin to form hemozoin crystal accumulations; the trophozoite stage, which is involved in the remodeling of the RBC architecture by the export of variant surface antigens (VSAs) such as PfEMP1 to the RBC surface; and the schizont stage, that is characterized by repetitive nuclear divisions in order to form new merozoites [9, 12]. VSAs act as receptors for endothelial cell surface expressed ligands, resulting in the binding (sequestration) of infected red blood cells (iRBCs) to the small blood vessels in various organs, which allows the parasite to avoid splenic clearance [9]. Sequestration of iRBCs is also associated with clinical syndromes of severe malaria like cerebral malaria where iRBC sequester in the brain or pregnancy-associated malaria, with iRBC sequestration in the placenta [9]. VSAs further contribute to disease by mediating rosetting of iRBCs to uninfected RBCs. Upon iRBC lysis, various parasite products are released that are thought to be responsible for the malaria symptoms like headaches, fever and lethargy [11]. A small number of blood-stage parasites will undergo gametocytogenesis and differentiate into male and female gametocytes (Figure 2D), which can be taken up by mosquitoes during a blood meal. In the mosquito midgut (Figure 2E), micro- and macrogametes fuse to form the zygote, which further differentiates into ookinetes that pass the midgut epithelium and ultimately encyst to form new sporozoites, that enter the mosquito's salivary glands - ready to be spread to the next human host [13]. Taken together, although the pathogenesis of malaria is not fully understood until today, the main effectors underlying this process are believed to be driven by both, parasite and host factors, which include the sequestration of iRBC in the blood vessels and the local and systemic inflammation [14].

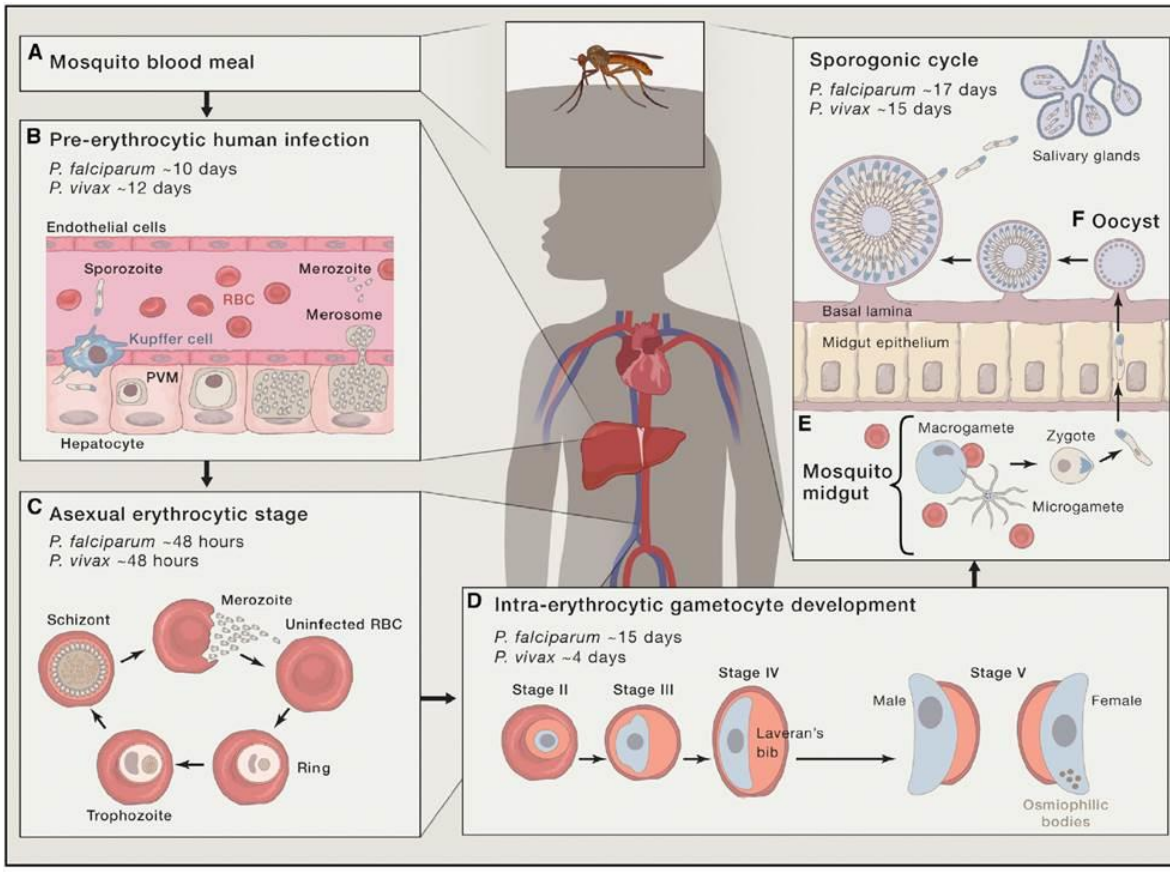

Figure 2 Life cycle of *Plasmodium falciparum* [9].

1.1.4 Malaria diagnosis and treatment

According to WHO, every suspected malaria case should be confirmed by microscopy or a rapid diagnostic test (RDT) before treatment is initiated, unless there is no parasite-based diagnostic testing available [1]. Both techniques show higher limits of detection (LoD) in comparison to PCR-based detection methods [15]. As a result of this limited sensitivity, sub-microscopic, low-density infections can be missed and a large proportion of transmission can be sustained [16]. These asymptomatic or chronic infections are particularly common in malaria pre-exposed individuals with naturally acquired immunity [17]. RDTs are immune chromatography-based assays that measure the presence of histidine-rich protein 2 (HRP2) for *P. falciparum* or lactate dehydrogenase for other *Plasmodium* species (pLDH) in peripheral blood [18]. In case of patient follow-up visits after treatment, these tests are not convenient, since they may lead to false positive results as the antigens can circulate up to 28 days after parasite death [18, 19]. Most importantly, malaria parasites with gene deletions of *pfhrp2*/*hrp3* begin to emerge in several South American countries, in the China-Myanmar

border, Ghana, the Democratic Republic of Congo, Eritrea, India, Uganda and Rwanda [1]. Consequently, new or better RDTs that target non-HRP2 antigens are needed [1].

Regarding treatment of uncomplicated *P. falciparum* malaria, WHO recommends for the treatment of children and adults (except pregnant women in their first trimester) an artemisinin-based combination therapy (ACT) [1]. To date, resistance to artemisinin has emerged in five countries in the Greater Mekong sub-region [1].

1.1.5 Current malaria control strategies

Current malaria prevention interventions include vector control, chemoprevention and potentially vaccination [1]. Among vector control, the use of insecticide-treated bed-nets (ITN) and indoor residual spraying (IRS) belong to the most frequently used methods in preventing mosquito bites [1]. Both strategies fundamentally contributed to the global decline in malaria burden since 2000 [2, 20, 21]. Chemoprevention consists of intermittent preventive treatment (IPT) of malaria in pregnant women (IPTp) and infants (IPTi) with sulfadoxine-pyrimethamine (SP) [1]. During IPT, antimalarial drugs are administered at specified time points without prior screening for parasites [22, 23]. IPTp and IPTi have demonstrated efficient reduction of placental malaria, low birth weight, clinical malaria in infants and anemia [24, 25]. Nevertheless, the remarkable gains of malaria prevention and control in the past 15 years are currently threatened by emerging resistance to anti-malarial drugs and insecticides [26]. Hence, there is an urgent need in taking action by the global malaria community in order to prevent any further spread of drug resistant vectors and parasites, and in maintaining the effectiveness of existing control interventions [26]. An alternative prevention strategy could be achieved through vaccination. To date, the most advanced malaria vaccine RTS,S/AS01 showed 39% efficacy against clinical malaria and 31.5% efficacy against severe malaria in infants aged 5-17 months at first vaccination in a large phase 3 clinical trial conducted in sub-Saharan Africa [27]. At present, the RTS,S/AS01 is considered a complementary malaria control tool to the core package of proven malaria interventions [1]. So far, the only immunogens that have ever induced high level protection (>90%) against controlled human malaria infection (CHMI) is the immunization with whole attenuated sporozoites [28–32]. This vaccination approach will be discussed more in detail in section 1.3.

1.2 The human immune response to *P. falciparum* infection

1.2.1 Humoral and cellular immune responses against *P. falciparum*

Powerful clinical research models such as CHMI studies, animal models of malaria and the study of immune responses to natural infection in malaria endemic settings with different transmission intensities, have led to an improved understanding of the immunobiology of *Plasmodium* infection in the past years [9]. Nevertheless, many open questions remain to be elucidated in terms of cellular and molecular mechanisms invovled in malaria immunity [9]. A summary of the main humoral and cellular immune responses controlling the different stages of the *P. falciparum* parasite are shown in Figure 3. In the skin, antibodies are known to be the main immune effectors that are capable of blocking or reducing sporozoite migration to the liver [9]. The proportion of sporozoites drained in lymph-nodes start to prime specific B and T cell responses while the live sporozoites that enter the blood stream and migrate to the liver travers Kupffer cells and invade hepatocytes [33]. During this clinically silent stage, no sterilizing immunity is known to be naturally acquired and the cellular and molecular mechanisms underlying lack of sterilizing immunity remains to be investigated [34]. In contrast, experimental infection of humans and mice with attenuated sporozoites have revealed that sterilizing immunity can be induced at this stage [9, 31, 35–37], and IFN-γ-producing CD8+ and CD4+ T cells, Natural killer (NK) cells and γδ T cells and inducible nitric oxidase synthase (iNOS) and nitric oxide (NO) secreted by macrophages are likely to be essential for this protection [9]. During blood stage infection, antibodies play a crucial role in the immune response against the asexual parasites [38]. The antibody-mediated protection involves the blocking of merozoites from RBC invasion [39, 40], opsonization of iRBC for phagocytic clearance [41, 42], monocyte-mediated antibody-dependent cellular killing [43], as well as complement-mediated lysis [44] and interference with the sequestration of iRBCs within the microvasculary blood vessels [45]. In addition, cytokine producing CD4+ T-cells, NK, NKT, γδ T cells, NO and iNOS-producing macrophages likely contribute to control of asexual blood-stage parasites [9]. Immune responses against the sexual stages (gametocytes, gametes, and ookinetes) are mainly driven by humoral immune effectors like complement-fixing antibodies that are taken up by the mosquito during the blood meal [9, 33, 46].

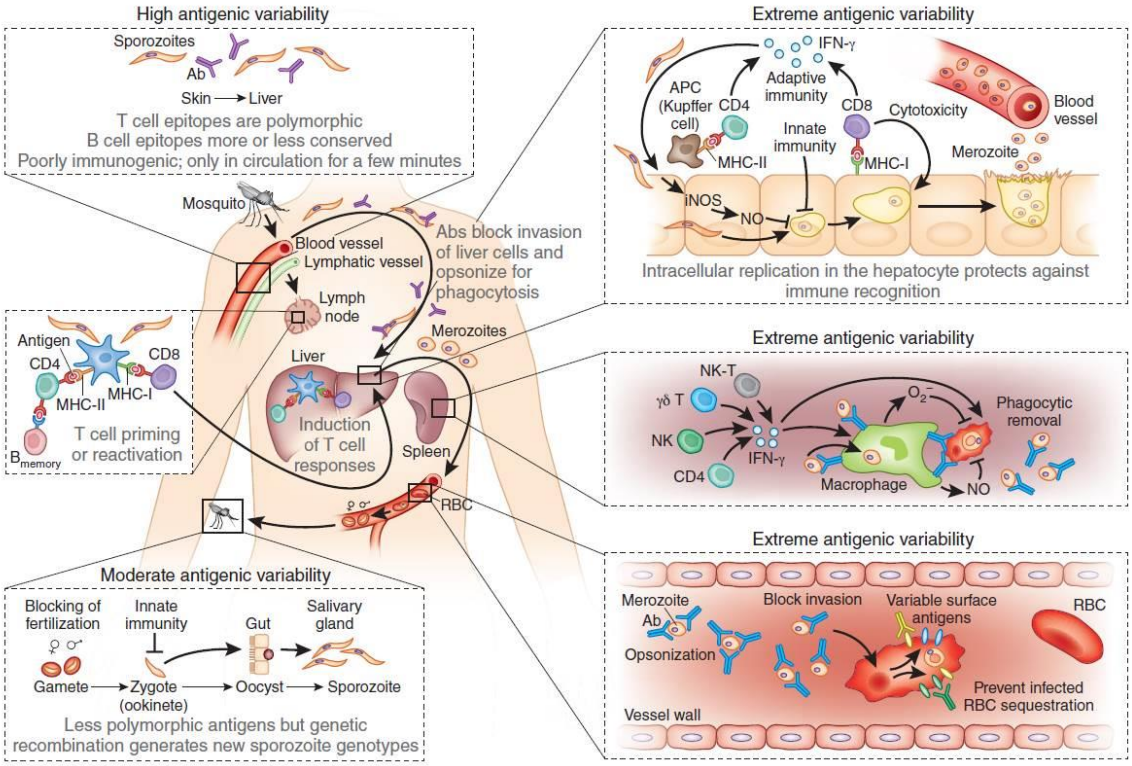

Figure 3 Humoral and cellular immune responses induced against the different stages of *P. falciparum* infection [33].

The complex life cycle and the high degree of genetic variability of *P. falciparum* pose several obstacles for the immune system [47]. Among the different parasite stages, asexual blood-stage parasites express the antigens with the highest variability, whereas surface proteins on sporozoites and sexual parasites are less or little polymorphic (Figure 3) [48]. As a result of antigenic polymorphism and genetic recombination, every new malaria infection can be genetically different and presents a new antigenic display to the immune system [33, 49]. Hence, during a natural infection, the induced immune responses may be highly stage- and genotype-specific [50]. Other challenges for the immune system are the obligate intracellular nature of the different parasite stages, which protects the parasite from antibody-mediated killing and the fast transition time of merozoites from one RBC to the next, as well as the short duration of each phase during the life cycle, which might be too short for the immune system to induce an effective antigen-specific immune response [51, 52].

1.2.2 Naturally acquired immunity

Naturally acquired immunity (NAI) to malaria is defined as the cumulative product of exposure to repeated infections over time, resulting in a sufficiently diverse repertoire of strain-specific immune responses in endemic populations [53]. NAI can be divided into clinical immunity and parasitological immunity [54]. Clinical immunity protects the individual from life-threatening disease and death and is normally obtained in children aged 5-10 years, who live in endemic areas with moderate to intense transmission [54]. Parasitological immunity is associated with the control and an incomplete clearance of the parasite, which can result in asymptomatic parasitemia that is commonly observed in adults living in endemic regions [54]. Importantly, NAI is slowly developed, non-sterile, and relatively short-lived [54, 55]. Albeit not yet fully understood, NAI is mainly antibody-driven and directed against the asexual blood stage parasite and it remains unclear whether NAI has an effect on pre-erythrocytic immune responses or against sexual parasite stages [13]. NAI depends on cell-mediated and humoral immune responses while the relative contributions of these immune mechanisms is incompletely understood and might differ between different human populations [56].

1.2.3 Inefficient acquisition of humoral immune memory to malaria in exposed people living in endemic countries

Humoral immune memory is composed of high-affinity memory B cells (MBCs) and long-lived antibody-producing plasma cells (LLPCs) [57]. Upon re-infection, MBCs are reactivated and rapidly start to proliferate and differentiate either into plasma cells that secrete high-affinity antibodies at high rates or re-enter germinal center reactions in order to acquire more affinity maturation to adapt to modified pathogens [58]. LLPCs reside in the bone marrow for long periods of time and constantly secrete protective antibodies which serve as a first line of defense against re-exposure to foreign proteins or pathogens [59, 60].

In contrast to other viral or bacterial pathogens (tetanus, smallpox, measles) which can induce long-lived protective antibodies for decades after a single exposure or vaccination [61–63], antibodies to *Plasmodium* antigens are slowly and inefficiently generated and rapidly lost in the absence of ongoing exposure in semi-immune individuals who live in malaria-endemic regions [64]. Likewise, a defective acquisition and maintenance of MBCs specific for malaria antigens compared to childhood vaccination-induced MBC has been reported in such endemic

populations [65]. In contrast, individuals living in areas of infrequent malaria exposure, stable malaria-specific MBC populations are described [66–69], suggesting that different levels of transmission might have an impact on the development and maintenance of MBCs. Despite a largely incomplete understanding of the immunological processes leading to this impaired and insufficient acquisition of LLPCs and MBCs in malaria, several mechanisms responsible for these defects in B cell immunological memory have been described in the past years [64]. The following paragraphs will summarize these main findings:

Clonal antigenic variation and the expression of highly polymorphic antigens on the surface of asexual blood stage parasites and iRBCs might be partially responsible for the sub-optimal acquisition of humoral immunity to malaria [64].

An expansion of a phenotypically similar memory B cell subset, so called atypical memory B cells, has been identified in various *P. falciparum*-exposed children and adults [68, 70]. The frequencies of these atypical MBCs seem to be positively correlated with the parasite's transmission intensity [70]. The immunological processes driving the development of atypical MBCs and whether these cells are detrimental or beneficial in humoral malaria immunity remains unclear. Different investigators have published contrary results in terms of the functional relevance of this MBC subset [71, 72]; *Muellenbeck et al. 2013*, reported a positive contribution of atypical MBC in malaria immunity by demonstrating that V_H and V_L genes cloned from atypical MBC from malaria-exposed individuals encoded broadly *P. falciparum* neutralizing antibodies [71]. However, further investigations are required on this finding, since direct antibody secretion by atypical MBCs could not be demonstrated. In contrast, according to studies published by *Portugal et al. 2015*, atypical MBCs express several inhibitory receptors and B cell receptor (BCR) signaling seems to be defective, which leads to an impaired B cell response including proliferation, cytokine production and antibody secretion [72]. Next-generation sequencing of the expressed V_H genes of atypical and classical MBCs revealed that V_H gene usage and the rates of somatic hypermutation (SHM) are similar, indicating that classical and atypical MBCs share a common precursor [72].

Another explanation for the functionally impaired B cell memory and the mechanisms driving expansion of atypical MBCs could be the direct modulation of B cell function by the parasite itself [65]. *In vitro* studies proved that the malaria parasite can directly interact with human B

cells through the cysteine-rich interdomain region 1α (CIDR1α), an extracellular domain of the variant surface antigen PfEMP1 expressed on the surface of iRBCs. $CD27^+$ B cells were the main responding population in these experiments, suggesting that MBC are particularly affected by CIDR1α. This interaction leads to T-cell-independent polyclonal B cell activation (PBA), resulting in MBC cell activation, proliferation and cytokine production [73, 74] and might induce altered Toll-like receptor (TLR) responsiveness and potentially lead to B cell exhaustion by reducing the B cell receptor activation threshold [75]. However, to confirm these findings further investigations are needed and it remains unclear whether the PfEMP1-CIDR1α-MBC interaction results in activation, exhaustion, or deletion of malaria-specific B cell memory responses [64].

It has also been discussed that systemic mediators responsible for B cell activation and survival, become modulated during a *P. falciparum* infection and thus, could potentially contribute to MBC dysfunction. One example of these mediators are the B cell activation factor BAFF and BAFF receptor [65, 76]. BAFF is a cytokine produced by mononuclear cells (monocytes, T cells, DCs) [77] and its production is mediated by the cytokines IL-10 and IFN-γ [78, 79], which are also up-regulated during an acute *P. falciparum* infection [76]. Increased plasma BAFF levels have been detected in children with acute *P. falciparum* infection [76] and in placental tissue from pregnant women infected with Pf malaria [80]. Parasite-induced BAFF secretion has been hypothesized to impair humoral B cell memory and B cell survival rates [65]. However, these findings are purely observational and the actual mechanisms and consequences underlying these modulations remain to be established [65].

The relatively insufficient acquisition of *P. falciparum*-specific humoral memory responses could also be linked to deficient immunological T cell help during a malaria infection [81]. $CD4^+$ T cells isolated from children of high-transmission settings for *P. falciparum,* have shown to express up-regulated levels of phenotypic markers for exhaustion, such as programmed cell death-1 (PD-1) and lymphocyte activation gene-3 (LAG-3) [82–84]. The expression of these inhibitory receptors appears to correlate with decreased proportion of MBCs in children with ongoing *P. falciparum* exposure [83] and up-regulated levels of PD-1 result in increased parasite burden during infection [84]. *In vivo* studies in mice further revealed that $CD4^+$ T cell exhaustion induced by *P. yoelii* infection can be restored through the blockade of PD-1 ligand and PD-L1 and the inhibitory receptors LAG-3 [82]. Nevertheless, whether these findings also count for humans remains unknown and further

investigations are needed in order to determine if the above described $CD4^+$ T cell phenotype is a reflection of exhaustion or of a compromised Tfh compartment during human malaria infection [64].

Studies in humans [85] and mice [86–88] indicated that severe malaria infection can dramatically affect the spleen's architecture by dissolution of the marginal zone, loss of B and T cells and reduced GC formation. These findings could partially explain the defective acquisition of MBCs and LLPCs in patients suffering from a fatal malaria infection [64].

In past years, great efforts in research on potential mechanisms responsible for this slow and inefficient acquisition of humoral immunity to malaria have provided important insights into this field. Nevertheless, many outstanding questions remain and thus, it is important to conduct further investigations on data collected from immune-epidemiological studies and as well from volunteers enrolled in vaccine trials and controlled human malaria infections to finally arrive at a better understanding of factors driving naturally acquired immunity to clinical malaria infection.

1.3 Malaria vaccine development

An effective malaria vaccine would be the ideal tool to reduce risk of contracting malaria in endemic populations, especially in areas where health-care delivery systems and vector control strategies are difficult to maintain due to political conflicts or natural disasters [89]. However, malaria vaccine development has been extremely hampered by the parasite's complex life cycle [33]. Several malaria vaccine candidates are currently tested in clinical trials and these are summarized in the global malaria vaccine pipeline shown in Figure 4. To date, the most clinically advanced malaria vaccine candidate is the subunit vaccine RTS,S/AS01, also known as Mosquirix [90]. The RTS,S/AS01 vaccine formulation is composed of the C-terminal portion of the *P. falciparum* circumsporozoite protein that is physically linked to the hepatitis B virus S antigen and an immune adjuvant (AS01) [91]. Results from phase 3 efficacy trial in seven different sub-Saharan African countries showed 26% reduction of clinical malaria in young infants aged 6-12 weeks, and 36% reduction in children aged 5-17 months at first vaccination, after a booster dose administration of 18 months after the primary series [27]. In 2015, the RTS,S/AS01 vaccine obtained positive

approval from the European Medicines Agency (EMA), followed by a WHO recommendation in 2016 to further evaluate RTS,S/AS01 vaccine in a larger scale pilot implementation study in children aged 5 to 9 months in sub-Saharan African settings of moderate to high parasite transmission [92]. The protective efficacy of the RTS,S/AS01 subunit vaccine demonstrated in the phase 3 clinical trial [27] are below the goal of 75% efficacy against clinical malaria set by the WHO Malaria Vaccine Technology Roadmap [93]. Thus, alternative vaccine approaches are needed in order to fulfill these goals.

So far, the only immunogens that have ever induced high-level protection against CHMI in humans is the immunization with live, whole sporozoites [28–30, 30, 32]. These vaccination approaches are discussed in detail in the paragraph below.

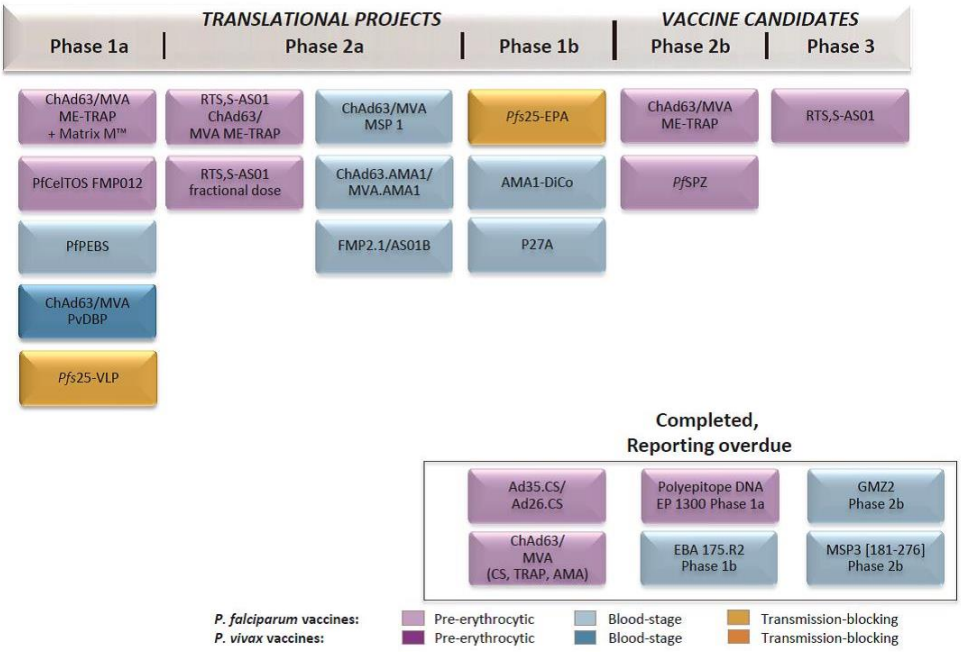

Figure 4 Global malaria vaccine pipeline (WHO rainbow table of global malaria vaccine projects).

1.3.1 Whole sporozoite immunization

Sterilizing immunity in humans and mice against experimental malaria infection after immunization by the bites of mosquitoes with radiation-attenuated sporozoites (RAS) has already been demonstrated in the late 1960's and early 1970's [28, 35]. During irradiation of infectious mosquitoes, the sporozoites' DNA becomes randomly damaged, resulting in

sporozoites that retain their capacity to invade hepatocytes, but are no longer capable of developing into mature liver-stage parasites and into disease-causing blood-stage parasites [35]. Besides radiation, other sporozoite attenuation approaches include genetic engineering of *Plasmodium* in order to generate live-attenuated parasites that cannot develop into asexual blood stage infections [94], or a combination of chemoprophylaxis and fully infectious sporozoites (CPS) [31]. However, this thesis will focus on RAS, since all the data generated in these studies come from RAS-immunized volunteers.

In earlier studies, where humans were exposed to infected irradiated mosquitoes, the mosquito-bite immunization approach was reasonably tolerable with mostly mild and moderate local and systemic adverse events. These studies also revealed that in order to achieve sterile immunity in humans, over 1,000 bites of irradiated mosquitoes during five or more immunization sessions are required [37]. Despite these promising findings, the development of an effective whole sporozoite based vaccine stalled because it was believed to be clinically and logistically impractical to generate such large numbers of irradiated mosquitoes for vaccinations of larger human populations. Moreover, it was also perceived to be impossible to produce, purify and preserve aseptic live sporozoites that meet regulatory standards [95]. Following the discovery and sequencing of the circumsporozoite protein (CSP) [96], efforts rather moved towards the development of a malaria subunit vaccine.

1.3.2 The Sanaria™ PfSPZ Vaccine

In 2003, scientists from the biotechnology company Sanaria Inc. re-started the efforts of developing an effective, aseptic, purified and potent irradiated whole sporozoite malaria vaccine suitable for injection to humans [95]. Six years later, Sanaria Inc. successfully managed to manufacture and release a metabolically active, non-replicating *P. falciparum* sporozoite (PfSPZ) Vaccine, the Sanaria™ PfSPZ Vaccine (PfSPZ Vaccine), that is biologically active and can be preserved in liquid nitrogen vapor phase (LNVP) [95]. The PfSPZ Vaccine is produced by raising adult *Anopheles stephensi* mosquitoes under aseptic conditions and feed them on human blood cultures that consist of aseptic *P. falciparum* gametocytes. Within the mosquitoes, the gametocytes develop into sporozoites in approximately two weeks. At this stage, the mosquitoes are exposed to radiation for attenuation. Immediately after radiation, the attenuated PfSPZ are isolated from the salivary glands by dissection under aseptic conditions, purified, vialed and cryopreserved into LNVP [95].

After the completion of pre-clinical studies, the first human clinical trial of the Sanaria™ PfSPZ Vaccine was conducted at the Naval Medical Research Center and University of Maryland at the Center for Vaccine Development in Maryland, U.S.; in 2009-2010 [97]. In this study, the vaccine was tested through the intradermal (ID) and subcutaneous (SC) administration route in 80 malaria-naïve adults. The results demonstrated that the vaccine was safe and well-tolerated, but protective efficacy and immunogenicity were low [97]. Thereafter, the administration route was changed from ID/SC to intravenous (IV) injection and first tested in animal models of non-human primates, rabbits and mice [29, 98]. The outcome of these experiments revealed that the vaccine was highly potent when administered IV. Following these promising results, the next goal was to test the safety, immunogenicity and protective efficacy of the IV-administered Sanaria™ PfSPZ Vaccine in humans. This was done in a phase 1 clinical trial at the Vaccine Research Center, National Institute of Allergy and Infectious Diseases, NIH, Maryland, U.S. in 2012 [29]. The IV injection was safe and well-tolerated in all the tested volunteers and most importantly, 100% protection against homologous CHMI was achieved when the vaccine was administered at 5 doses of 1.35 x 10^5 PfSPZ. Strikingly, there was a dose response in terms of antibody- and T-cell responses observed [29]. Animal studies further showed that the IV administration route was critical for the induction of hepatic PfSPZ-specific $CD8^+$, IFN-γ producing T cells, which are known to play an important role in the protective immune response against CHMI [97].

The next critical step was to assess the safety, immunogenicity and protective efficacy of the Sanaria™ PfSPZ Vaccine in malaria pre-exposed populations. These first safety and efficacy trials took place in Mali (NCT01988636), Tanzania (NCT02132299) (*Chapter 2*) and Equatorial Guinea (NCT02418962) between 2014 and 2015. In contrast to the high level, durable protection against homologous CHMI seen in malaria-naïve volunteers after IV administered PfSPZ immunization [29], the immune responses in *P. falciparum* pre-exposed African adults were sub-optimal and the efficacy was much lower. The Mali trial showed 28.5% protection against natural, field strain *P. falciparum* infection [99]. In the BSPZV1 trial in Tanzania (*Chapter 2*), 6% of volunteers in the low-dose group (5 x 1.35 x 10^5 PfSPZ) and 20% of volunteers in the high-dose group (5 x 2.7 x 10^5 PfSPZ) were protected against homologous controlled human malaria infection (CHMI) conducted 3 weeks post last vaccination (Jongo et al., manuscript submitted).

1.3.3 Controlled human malaria infection (CHMI)

The PfSPZ vaccine trials described above used the homologous CHMI model to assess the protective efficacy of the vaccine. CHMI is carried out under strictly controlled laboratory and clinical conditions, in which human volunteers are challenged with fully infectious sporozoites or blood-stage parasites using a defined dosing and malaria strain [100]. The experimental blood-stage infection approach is less established [101] than the sporozoite-induced challenge model and here we will focus on the CHMI studies using experimental sporozoite infection. CHMI has proven to be a powerful tool to determine the protective efficacy of malaria vaccines and antimalarial drugs [100]. And moreover, CHMI studies can accelerate the clinical malaria vaccine development in providing important preliminary information between phase I and phase II trials, and thus, substantial costs can be saved [100].

The first CHMI studies, using infectious mosquito bites or the IV or SC inoculation of dissected sporozoites suspended in media were already carried out in 1917 by Wagner von Jauregg as a treatment for patients with neurosyphilis, also known as "malariotherapy" [102]. With the advent of protocols for routine cultivation of *P. falciparum* and for the generation of gametocytes *in vitro,* CHMI studies using infected anopheles bites were practiced more routinely in the beginning of the 1980s [100]. The successful manufacture of aseptic, vialed, purified, cryopreserved, infectious PfSPZ by Sanaria Inc., made it possible to administer CHMI via needle and syringe inoculation. The first human trial using CHMI with infectious sporozoites via needle and syringe inoculation was carried out at the Radboud University Medical Center (RUNMC) in Nijmegen, in the Netherlands between 2010 and 2011 [103], followed by another trial in Tanzania [104]. In both studies, the volunteers were intradermally injected with the infectious PfSPZ. Importantly, the ID administration of the infectious PfSPZ challenge was safe and well-tolerated in all the participants, but the pre-patent period was longer than after mosquito-bite challenge and a 100% infection rate could not be achieved in neither of the two independent studies. To overcome these obstacles, the administration route was changed to IV or direct venous inoculation (DVI) and tested in a dose-finding trial in two centers, namely in Tübingen, Germany and Barcelona, Spain [105]. The two study sites found that 100% infection can be achieved when the infectious PfSPZ are intravenously administered at a dose of 3.2×10^3 sporozoites. The same CHMI dose regimen has also been used in Tanzanian adults and proved to be 100% infective in malaria pre-exposed volunteers (Jongo et al., manuscript submitted).

1.4 Aims of the thesis

As described in section 1.3.2, after the promising outcome of the vaccine trial in U.S. non-immune volunteers after intravenous administration of the Sanaria™ PfSPZ Vaccine with 100 % protection against homologous CHMI [29], the next indispensable step was to assess the safety, immunogenicity and protective efficacy of DVI administered PfSPZ Vaccine in endemic African populations. This includes the aim of the first part of this thesis. Between April 2014 and August 2015, we have conducted a phase 1, dose escalation, randomized controlled clinical trial to evaluate the safety, immunogenicity and protective efficacy against homologous CHMI of the PfSPZ Vaccine in Tanzanian male adults, in Bagamoyo, Tanzania (*Chapter 2*). The safety was determined by observation of adverse events including follow-up visits with clinical examination and laboratory tests. The immunogenicity was assessed by measurements of vaccine-induced antibody and T cell responses as described in *Chapter 2*. The vaccine efficacy was measured by CHMI via direct venous inoculation of 3,200 PfSPZ conducted 3 and 24 weeks after the last vaccination.

The aim of the second part of this thesis (*Chapter 3*) was to explore the impact of malaria pre-exposure on the humoral immune responses induced in Tanzanian adults after receiving active immunization with the PfSPZ Vaccine. Our primary objectives in *Chapter 3* were i) to determine the *ex vivo* induction of Pf sporozoite invasion inhibitory activity upon PfSPZ vaccination and ii) to investigate if antibodies of the non-IgG isotype, such as sporozoite-specific IgM antibodies are induced after vaccination and can potentially contribute to protection by preventing sporozoite invasion *in vitro*. *In vitro* inhibition of sporozoites invasion (ISI) assays were performed to assess the functional capacity of the vaccine-induced antibodies. PfSPZ-Vaccine-induced IgG and IgM antibodies were detected by enzyme-linked immunosorbent assasys (ELISA) using full length PfCSP. Plasma from a subset of volunteers was depleted from IgG and IgA antibodies in order to obtain IgM antibody fractions, which were tested in *in vitro* ISI assays to determine sporozoite-blocking activity and in immunofluorescence assays (IFA) to confirm binding against whole sporozoites.

The isolation and characterization of monoclonal antibodies has proven to be a powerful tool in diagnostics, therapeutics [106] and the identification of target antigens and conserved epitopes that can be formulated as a vaccine ("analytic vaccinology") [107]. As an example for malaria, monoclonal antibodies to CSP, AMA-1 and MSP-1 have been useful to explore the of process of sporozoite and merozoite invasion and for the identification of target

antigens of invasion inhibitory antibodies [108, 109]. Moreover, human monoclonal antibodies for MSP2, p27 and VAR2CSA, which is a PfEMP1 variant involved in placental malaria, have been isolated and functionally characterized [110–113]. The aim of the third part of this thesis (*Chapter 4*) was to isolate sporozoite-specific human monoclonal antibodies from Tanzanian adults, who have been experimentally infected with *P. falciparum* sporozoites. The PBMC samples for the isolation of memory B cells were obtained from the volunteers of the clinical trial described in *Chapter 2,* and memory B cells were immortalized with EBV and CpG in clonal conditions in 384-well plates. The culture supernatants of the B cell clones, containing the monoclonal antibodies, were screened for their capacity to bind to whole sporozoites using a high-throughput flow cytometer (IntelliCyte). Positive B cell clones were expanded and the produced antibodies were purified from the culture. cDNA was used to sequence the VH and VL genes and to produce recombinant antibodies in HEK293 cells transfected with appropriate human Ig vectors. Recombinant monoclonal antibodies were purified from the culture supernatants and produced in sufficient amounts to assess their biological function using *in vitro* and *in vivo* sporozoite blocking assays [32].

Chapter 2

Safety, immunogenicity and protective efficacy against controlled human malaria infection of PfSPZ Vaccine in Tanzanian adults

This chapter is an adapted version of the following publication:
Said A Jongo, Seif A Shekalage, LW Preston Church, Adam J Ruben, Tobias Schindler, **Isabelle Zenklusen**, Tobias Rutishauser, Julian Rothen, Anneth Tumbo, Catherine Mkindi, Maximilian Mpina, Ali T Mtoro, Andrew S Ishizuka, Kassim Kamaka Ramadhani, Florence A Mildano, Munira Qassim, Omar A Juma, Solomon Mwakasungula, Beatus Simon, Eric R James, Yonas Abebe, Natasha KC, Sumana Chakravarty, Elizabeth Saverino, Bakari M Bakari, Peter F Billingsley, Robert A Seder, Claudia Daubenberger, BKim Lee Sim, Thomas L Richie, Marcel Tanner, Salim Abdulla, Stephen L Hoffman. Safety, Immunogenicity and protective efficacy against controlled human malaria infection of PfSPZ Vaccine in Tanzanian adults. Submitted to *The Lancet Infectious Diseases*, 2017.

Safety, immunogenicity and protective efficacy against controlled human malaria infection of PfSPZ Vaccine in Tanzanian adults

Said A Jongo (MD)[1]§, Seif A Shekalage (MD)[1]§, LW Preston Church (MD)[2], Adam J Ruben (PhD)[2], Tobias Schindler (MSc)[3,4], **Isabelle Zenklusen (MSc)[3,4]**, Tobias Rutishauser (MSc)[3,4], Julian Rothen (MSc)[3,4], Anneth Tumbo (MSc)[1], Catherine Mkindi (MSc)[1], Maxmilian Mpina (PhD)[1], Ali T Mtoro (MD)[1], Andrew S Ishizuka (DPhil)[5], Kassim Kamaka Ramadhani (MPH)[1], Florence A Milando (MD)[1], Munira Qassim (MD)[1], Omar A Juma (MD)[1], Solomon Mwakasungula (MSc)[1], Beatus Simon (BPharm)[1], Eric R James (PhD)[2], Yonas Abebe (MS)[2], Natasha KC (BS)[2], Sumana Chakravarty (PhD)[2], Elizabeth Saverino (BS)[2], Bakari M Bakari (DCM)[1], Peter F Billingsley (PhD)[2], Robert A Seder (MD)[5], Claudia Daubenberger (DVM)[3,4], BKim Lee Sim (PhD)[2,6], Thomas L Richie (MD)[2], Marcel Tanner (PhD)[3,4], Salim Abdulla (MD)[1]†, Stephen L Hoffman (MD)[2]*†

[1]Ifakara Health Institute, Bagamoyo Research and Training Centre, Bagamoyo, Tanzania
[2]Sanaria Inc., Rockville, MD 20850
[3]Swiss Tropical and Public Health Institute (Swiss TPH), Basel, Switzerland
[4]University of Basel, Switzerland
[5]Vaccine Research Center (VRC), National Institute of Allergy and Infectious Diseases, National Institutes of Health, Bethesda, MD 20892
[6]Protein Potential LLC, Rockville, MD 20850

*Address correspondence to Stephen L. Hoffman, Sanaria Inc., 9800 Medical Center Drive, Rockville, MD 20850. E-mail: slhoffman@ sanaria.com

§ These authors contributed equally to this study.
† These authors contributed equally to this study.

2.1 Abstract

Background: We are using controlled human malaria infection (CHMI) by direct venous inoculation (DVI) of cryopreserved, infectious *Plasmodium falciparum* (Pf) sporozoites (SPZ) (PfSPZ Challenge) to reduce time and costs of developing PfSPZ Vaccine to prevent malaria in Africa. PfSPZ Vaccine gave 65% vaccine efficacy (VE) at 24 weeks against mosquito bite CHMI in US adults and 52% (time-to-event) or 29% (proportional) VE over 24 weeks against naturally transmitted Pf in Mali. We assessed the identical regimen in Tanzanians for VE against PfSPZ Challenge.

Methods: 20 to 30 year old men were randomized to DVI of 5 doses normal saline or 1.35 x 10^5 or 2.7 x 10^5 (US/Mali dose) PfSPZ of PfSPZ Vaccine in a double blind clinical trial. VE was tested 3 and 24, or 24, weeks later.

Findings: Adverse events were similar in vaccinees and controls. Antibody responses to Pf circumsporozoite protein were 4.3-fold lower than in US, but higher than in Malians. 1/18 (6%) and 4/20 (20%) vaccinees were protected (1.35 x 10^5, 2.7 x 10^5 groups, respectively) at 3 week CHMI. Four protected volunteers were protected again at 24 weeks, compared to 0/5 undergoing first CHMI at 24 weeks. All 18 controls developed Pf parasitemia.

Interpretation: PfSPZ Vaccine was safe, well tolerated, and induced durable immunity in 4 subjects. CHMI by DVI of PfSPZ Challenge appeared more stringent over 24 weeks (VE 0-20%) than mosquito bite CHMI (VE 65%) or natural exposure (VE 52%/29%), providing a rigorous test of VE in Africa.

Funding: Swiss TPH, Ifakara Health Institute, Tanzanian Commission for Science and Technology, U.S., NIAID, NIH, Sanaria.

2.2 Introduction

In 2015 >$2.5 billion were invested in malaria control. Yet, in 2015 there were an estimated 438,000-730,000 deaths caused by malaria.[1-3] *Plasmodium falciparum* (Pf) is the cause of > 98% of malaria deaths and >80% of malaria cases in sub-Saharan Africa. Our goal is to field a vaccine that will prevent infection with Pf and thereby prevent all manifestations of Pf malaria and parasite transmission from humans to mosquitoes.[4] When used in mass vaccination program campaigns such a vaccine could eliminate Pf from geographically defined areas. Pf sporozoites (SPZ) are the only immunogens that have ever prevented Pf infection in >90% of recipients. This was initially done by mosquito bite administration of radiation attenuated PfSPZ.[5-7] Sanaria® PfSPZ Vaccine, radiation attenuated, aseptic, purified, cryopreserved PfSPZ, was then developed.[8,9] When administered by rapid intravenous injection, PfSPZ Vaccine protected 100% (6/6) of subjects against controlled human malaria infection (CHMI) with Pf parasites similar to those in the vaccine (homologous) 3 weeks after last immunization.[10] PfSPZ Vaccine protected against, 1) homologous CHMI for at least 59 weeks,[11] 2) heterologous (parasites different than in vaccine) CHMI for 3 weeks[12] and then for at least 33 weeks.[13] PfSPZ Vaccine also prevented naturally transmitted heterogeneous Pf in adults in Mali for at least 24 weeks.[14] We used the same dosage regimen as in the U.S. and Mali to evaluate the tolerability, safety, immunogenicity, and vaccine efficacy (VE) of PfSPZ Vaccine in young adult Tanzanians. Previously, we had conducted the first modern CHMI in Africa and showed that injection of aseptic, purified, cryopreserved PfSPZ, Sanaria® PfSPZ Challenge, consistently infected Tanzanian volunteers.[15-20] In this study we took advantage of this capability to assess the VE of PfSPZ Vaccine by CHMI with PfSPZ Challenge. To our knowledge this was the first time CHMI has ever been used to assess a malaria vaccine in Africa. The results showed the same dosage regimen of PfSPZ Vaccine was less immunogenic and protective against CHMI in Tanzanians than in non-malaria exposed US Americans,[12] and VE against homologous CHMI in Tanzania was lower (or similar) to VE against intense field exposure to heterogeneous Pf parasites in Mali.[14]

2.3 Materials and Methods

2.3.1 Study design and population

This double blind, randomized, controlled trial was conducted in Bagamoyo, Tanzania between April 2014 and August 2015. 67 healthy male volunteers 18 to 35 years of age were recruited from higher learning institutions in Dar es Salaam through sensitization meetings. After initial screening, prospective volunteers were invited to the Bagamoyo Clinical Trial Unit (BCTU) of the Ifakara Health Institute (IHI) to complete informed consent and screening. All had to complete a 20-question assessment of trial understanding with a 100% correct response rate on the first or second attempt (Table S1) to be eligible. Volunteers were screened using predetermined inclusion and exclusion criteria based on medical history, clinical examinations and laboratory tests (Tables S2, S3). History of malaria in the previous 5 years was an exclusion criterion; antibodies to PfEXP1 by ELISA above a pre-specified level (see below) 5 were considered evidence of recent or substantial past malaria infection and an exclusion criterion. Hematology, biochemistry, and parasitology testing, including malaria thick blood smear (TBS), stool and urine by microscopy was done. Tests for HIV, hepatitis B and C were performed after counseling; volunteers were excluded if positive and referred for evaluation and management. Volunteers were excluded if they had significant abnormalities on electrocardiograms.

The trial was performed in accordance with Good Clinical Practices. The protocol was approved by institutional review boards (IRBs) of the Ifakara Health Institute (Ref. No. IHI/IRB/ No:02-2014), the National Institute for Medical Research Tanzania (NIMR/ HQ/R.8a/Vol.IX/1691) and the Ethikkommission Basel (EKNZ), Basel, Switzerland (reference number 261/13). The protocol was approved by the Tanzania Food and Drug Authority (TFDA) (Ref. No. TFDA 13/CTR/0003), registered at Clinical Trials.gov (NCT02132299) and conducted under U.S. FDA IND 14826.

2.3.2 Investigational products

The investigational products (IPs) were Sanaria® PfSPZ Vaccine [8-14] and Sanaria® PfSPZ Challenge,[15-20] both comprised of the NF54 strain of Pf. PfSPZ Vaccine consists of aseptic, purified, vialed, metabolically active, non-replicating (radiation attenuated) cryopreserved PfSPZ. It was stored, thawed, diluted and administered by direct venous inoculation (DVI) in

0·5 mL through a 25 gauge needle.[12,14,18,20] PfSPZ Challenge is identical to PfSPZ Vaccine except it is not radiation attenuated. It was handled and administered like PfSPZ Vaccine. Preparation of IPs was supervised by the study pharmacist. After labeling the syringe, the pharmacist handed it to the nurse through a window.

2.3.3 Allocation and randomization

Volunteers were allocated to 5 groups (Table 1, Figure 1). Forty-nine received PfSPZ Vaccine, 8 were normal saline (NS) controls, and 10 were additional infectivity controls. The clinical team and volunteers were blinded to assignment to vaccine or NS until study end.

Group 1. 3 volunteers received consecutive doses of 3×10^4, $1{\cdot}35 \times 10^5$, and $2{\cdot}7 \times 10^5$ PfSPZ of PfSPZ Vaccine at 4-week intervals to assess safety.

Group 2. Volunteers were randomized to receive $1{\cdot}35 \times 10^5$ PfSPZ of PfSPZ Vaccine (N=20) or NS (N=4) at 0, 4, 8, 12 and 20 weeks.

Group 3. Volunteers were randomized to receive $2{\cdot}7 \times 10^5$ PfSPZ of PfSPZ Vaccine (N=20) or NS (N=4) at 0, 4, 8, 12 and 20 weeks.

Group 4. 6 volunteers were immunized with $2{\cdot}7 \times 10^5$ PfSPZ of PfSPZ Vaccine on the same schedule as Group 3.

Group 5. 10 volunteers served as unblinded infectivity controls during CHMIs (see below); two with CHMI #1, two with CHMI #2 and six with CHMI #3.

2.3.4 Vaccine efficacy (VE)

CHMI: VE was assessed by CHMI by DVI of $3{\cdot}2 \times 10^3$ PfSPZ of PfSPZ Challenge. CHMI #1 was 3 weeks after last immunization in Group 2. CHMI #2 was 3 weeks after last immunization in Group 3. CHMI #3 was 24 weeks after last immunization in Group 4 and included the 4 volunteers in Group 3 who did not develop parasitemia after CHMI #2. Volunteers were inpatients from day 9 after PfSPZ Challenge injection for observation until diagnosed and treated for malaria or until day 21; daily outpatient monitoring for TBS

negative volunteers continued until day 28. TBSs were obtained every 12 hours on days 9-14 after CHMI and daily on days 15-21 until positive or until day 21. TBSs could be performed more frequently, if volunteers had symptoms/signs consistent with malaria. After initiation of treatment, TBSs were assessed until two consecutive daily TBSs were negative, and on day 28.

Diagnosis: Slide preparation and reading for TBSs were performed following a standard procedure.[19] Sensitivity was 2 parasites/μL blood unless the volunteer was symptomatic, in which case twice as many fields were read. Parasitemia was also determined by quantitative polymerase chain reaction (qPCR) using two previously published qPCR assays. All samples were measured using a multiplex assay, detecting *Plasmodium spp*. 18S genes and the human RNaseP gene as endogenous control.[21] Following first qPCR assays, negative samples were analyzed using the Pf specific telomere-associated repetitive element 2 (TARE-2).[22] The WHO International Standard for Pf DNA Nucleic Acid Amplification Techniques (NIBSC, Hertfordshire, UK) was used as standard for calculation of parasite densities. DNA was extracted from 100μL whole blood and eluted with 50μL Elution Buffer using Quick-gDNA Blood MicroPrep Kit (Zymo Research, Irvine, USA). Blood samples collected during CHMI #1 were analyzed retrospectively after storing at –80 °C. During CHMI #2 and CHMI #3 qPCR results were provided to physicians within 12 hours of blood collection. To exclude field strain infections, parasite genotyping was performed on 10% of samples randomly chosen as described.[23]

2.3.5 Adverse events (AE)

Volunteers were observed as inpatients for 48 hours after administration of IP and discharged home with diaries and thermometers for recording AEs and temperatures and followed with daily telephone calls. Symptoms and signs (solicited and unsolicited) were recorded and graded by physicians: mild (easily tolerated), moderate (interfere with normal activity), severe (prevents normal activity) or life threatening. Axillary temperature was grade 1 (> 37·5–38·0 °C), grade 2 (> 38·0–39·0°C), grade 3 (39·1-40·0°C) or grade 4 (>40·0°C). Hematological and biochemical abnormalities were also assessed.

During the first 7 days after injection of IP pre-specified local (site of injection) and systemic AEs were solicited. Open-ended questioning was used to identify unsolicited AEs through day 28 (Table S4). All AEs were assessed for severity and relatedness to IP administration.

For CHMIs, volunteers returned on day 9 for admission to the ward for assessment of safety and diagnosis and treatment of malaria. Events during the 8 to 28 day period were assessed for relationship to Pf infection, and considered related if the event was within 3 days prior to and 7 days after TBS was first positive.

2.3.6 Antibody assays

Sera were assessed for antibodies by enzyme-linked immunosorbent assay (ELISA), immunofluorescence assay (aIFA), and inhibition of sporozoite invasion (aISI) assay as described (see Table S5).[24] ELISA for PfEXP1 was used to screen volunteers for possible malaria exposure (Table S6). Any subject with an OD 1·0 of >600 was excluded.

2.3.7 T cell assays

T cell responses in cryopreserved PBMCs were measured by flow cytometry in a single batch after the study as described.[11] After stimulation, cells were stained as described.[25] The staining panels are shown in Table S7 and the antibody clones and manufacturers are shown in Table S8. All antigen-specific frequencies are reported after background subtraction of identical gates from the same sample incubated with control antigen. Data were analyzed with FlowJo v9·9·3 (TreeStar) and graphed in Prism v7·0a (GraphPad).

2.3.8 Statistical analysis

Comparisons of categorical variables between groups were analyzed using 2-tailed Fisher's exact test. Comparisons of continuous variables between groups were analyzed by 2-tailed non-parametric tests. For multiple group comparisons Kruskal-Wallis test was used. Time to event was assessed by Kaplan Meier curves and log rank test. Analysis of variance was utilized to analyze differences in trends between groups. Analyses of immunological data are described with the data.

2.3.9 Role of the funding source

The funders were involved in the study design, study management, data collection, data analysis, data interpretation and writing the report. SA and SLH had full access to all the data in the study and had final responsibility for the decision to submit for publication.

2.4 Results

2.4.1 Study population and experience with DVI

57 Tanzanian men (Table 1, Figure 1) met criteria (Table S2, S3), and received PfSPZ Vaccine (n=49) or NS (n=8). All volunteers had AA hemoglobin and normal G6PD activity. 31 volunteers (46%) were heterozygous for α-thalassemia; 21 had evidence of latent tuberculosis infection by Quantiferon testing, but showed no evidence of active tuberculosis. One volunteer (group 2, NS) had a *Strongyloides stercoralis* on screening and was successfully treated prior to vaccination (Table 1).

Of 237 immunizations with PfSPZ Vaccine, 234 were completed with a single injection (98·7%). 230 injections (97·0%) were considered painless by the volunteer. For NS subjects, 39 of 40 immunizations (97·5%) were completed in a single injection and 39 of 40 (97·5%) considered painless by the volunteers. The nurse performing immunizations considered the procedure to be simple in 265 of 273 single injections (97·1%).

One subject in Group 2 received four immunizations. The third immunization was withheld while the subject was evaluated for what was diagnosed as benign ethnic neutropenia. One subject in Group 4 missed his second immunization when he left town. All other subjects received 5 immunizations.

2.4.2 Safety

Among 49 volunteers who received 237 doses of PfSPZ Vaccine, there were 17 solicited AEs possibly related to IP (17/237=7·2%) in 10 of the 49 vaccinees (20·4%) (Table 2a). Among 8 volunteers who received 40 doses of NS, there were two solicited AEs (2/40=5·0%) in one volunteer (12·5%) possibly related to IP (Table 2a). There were no local or serious AEs. Systemic AEs included headache (10), abdominal pain (3), chills (1), fever (2) and atypical chest pain (1). One episode each of headache and fever were grade 2; all other solicited AEs were grade 1. Seven episodes of headache were observed in Group 2 volunteers who received $1{\cdot}35 \times 10^5$ PfSPZ; 4/7 episodes occurred after the 3rd vaccine dose and did not recur with 4th or 5th doses. No factor was identified to account for this apparent clustering of headache. None of the comparisons of AEs between vaccinees and controls or between Group 2 (1·35 x

10^5 PfSPZ) with Groups 3 and 4 (2·7 x 10^5 PfSPZ) was significant (Table 2a). 26 of 49 vaccinees (53·1%) experienced 43 unsolicited AEs (0·88/individual) in the 28 days following injections #1-#4, and the 21 days before CHMI after injection #5. Seven of 8 controls (87·5%) experienced 14 unsolicited AEs (2/individual) during this period. No vaccinee or control experienced an unsolicited, related AE within 28 days of an immunization.

No significant laboratory abnormalities were attributed to PfSPZ (Table 2b). Three abnormalities during immunization were deemed clinically significant or grade 3. One was diagnosed as benign ethnic neutropenia. One was lymphopenia associated with an infected foot laceration, and one was eosinophilia associated with *Fasciolopsis buski* and *S. stercoralis* infection. Lymphopenia and eosinophilia resolved with treatment. Two Group 4 volunteers had asymptomatic hookworm infections diagnosed prior to CHMI; one was co-infected with *Enterobius vermicularis*. No volunteer had malaria during screening or during the trial other than from CHMI. A cyclic variation in total bilirubin following each immunization was observed in volunteers receiving vaccine or NS (see Figure S1).

2.4.3 Tolerability, Safety and VE during CHMI

46 vaccinees, 8 NS controls, and 10 infectivity controls underwent homologous CHMI. All subjects were negative by TBS and qPCR for Pf infection on day of CHMI. Two volunteers were excluded from primary analysis - a Group 2 volunteer who left the area two days after administration of PfSPZ Challenge and a Group 4 volunteer who left 9 days after. Both volunteers were located and treated pre-emptively.

Tolerability and safety of administration of PfSPZ Challenge: CHMI was well tolerated with no local solicited AEs and 3 systemic solicited AEs (grade 1 headache in Group 3, grade 2 headache in Group 4 and grade 1 arthralgia in an infectivity control) in the 7 days post administration of PfSPZ Challenge.

Parasitemia:
Controls: The 18 NS and infectivity controls developed Pf infection after CHMI (16 TBS and qPCR positive, 2 TBS negative and qPCR positive) (Figure 2a-d and Table S9). These included, four NS and 2 infectivity controls in CHMI #1 and CHMI #2, and six infectivity

controls in CHMI #3. All received the same lot of PfSPZ Challenge. Thus, results from all 18 were pooled for assessment of statistical significance.

Group 2 (1.35 x 10^5 PfSPZ): 17/18 volunteers who received five doses and 1/1 volunteer who received 4 doses developed parasitemia (Figure 2a), 15 positive by TBS and qPCR and 3 by qPCR only (CHMI #1). One volunteer (5·3%) was negative through day 28 by TBS and qPCR (p=1, Fisher's exact test, 2-tailed as compared to 18 controls).

Group 3 (2.7 x 10^5 PfSPZ):

1st CHMI at 3 weeks (CHMI#2): 16/20 volunteers who received five doses developed parasitemia (Figure 2b), all positive by TBS and qPCR. Four volunteers (20%) were negative through day (p=0.11).

2nd CHMI at 24 weeks (CHMI #3): The four protected volunteers from the first CHMI underwent a second CHMI 24 weeks after last vaccine dose (Figure 2c). Three were asymptomatic and negative by TBS and qPCR through day 28 day. The 4th volunteer, also asymptomatic, was reported to have a positive TBS on day 12 and treated. The sample with positive TBS was negative by retrospective qPCR. Re-evaluation of the TBS indicated an error in slide reading (false positive). P values for all 18/18 positive controls (CHMIs #1, #2, #3) vs. 0/3 or 0/4 vaccinees positive were 0·0008 (95% CI: 43·85%, 100%) and 0·0001 (95% CI: 51·01%, 100%), respectively. If only the six control volunteers at CHMI #3 are used, p values were 0·0119 (95% CI: 43·85%, 100%) and 0·0048 (95% CI: 51·01%, 100%), respectively.

Group 4 (2·7 x 10^5 PfSPZ):

1st CHMI at 24 weeks after last vaccine dose (CHMI #3): 4/5 vaccinees developed parasitemia by TBS and qPCR. The fifth was negative by TBS, but positive by qPCR. There was one excluded volunteer (see above) (Figure 2c).

Volunteers heterozygous for α-thalassemia were no more likely to be TBS negative and qPCR positive than volunteers without α-thalassemia (3 of 27 vs. 3 of 34, p=1·0). Protection from CHMI did not correlate with α-thalassemia status; 3/37 with normal hemoglobin and 2/29 heterozygous for α-thalassemia protected.

Prepatent periods and parasite densities: The median pre-patent period in the 16 TBS positive NS and infectivity controls was 12·2 days. In the vaccinees in Groups 2-4 respectively they were 14·0, 14·0, and 15·3 days (p=0·1066) (Table S9). The parasite densities by qPCR and TBS at time of diagnosis for each individual are in Table S10. The median parasite density in controls vs. vaccinees at time of first positivity were 0·5 vs. 0·4 parasites/μL for qPCR (p=0·5714) and 11·2 vs 15·0 parasites/μL for TBS (p=0·1492). All parasites tested were PfNF54.

Tolerability and Safety of Parasitemia During CHMI:

Controls: 16 controls developed parasitemia by TBS; 9 (56%) never had symptoms (Table S11). Headache occurred in 7/7 symptomatic individuals. One of two control volunteers only positive by qPCR did not have any symptoms; the second had headache 8 days after qPCR spontaneously reverted to negative. No volunteer had symptoms at time of first positive qPCR.

Vaccinees: 35 immunized volunteers developed parasitemia by TBS; 20 (57%) never had symptoms. Three volunteers had temperature > 39·0ºC; all other clinical manifestations were grade 1 or 2. Fever (28·6%) and headache (31·4%) were most common. Compared with controls, elevated temperature was more common in vaccinees with positive TBSs (9/35 vs. 0/16, p=0·043). There was no significant difference in frequency of headache between controls and vaccinees. In the 3 volunteers in Group 2 who were qPCR positive and TBS negative, one developed headache 3 days after qPCR positivity. No volunteer had symptoms at time of first positive qPCR.

Clinical labs: No unexpected changes in clinical values were observed following CHMI. Declines in lymphocyte counts were observed in TBS positive controls and vaccinees (mean decline 1110 ± 720 cells/μl and 1180 ± 680 cells/μl, respectively) on day of first positive TBS. Absolute lymphocyte counts less than 1000 cells/μl were observed in 8/16 and 16/35 TBS positive controls and vaccinees. All lymphocyte counts returned to baseline by day 28. There were mild decreases in platelet counts in TBS positive subjects, but all platelet counts were > 100 x 10^3 cells/μl.

Treatment: Volunteers with positive TBS were treated with either atovaquone/proguanil (n=43) or artemether/lumefantrine (n=8) within 24 hours of first positive TBS. NS and infectivity controls who were TBS negative (n=2) were treated at day 28.

2.4.4 Immunogenicity

Antibody Responses:
PfCSP and PfSPZ: Antibodies against PfCSP by ELISA (a), PfSPZ by aIFA (b), and PfSPZ by ISI (c) in sera taken 2 weeks after last vaccine dose and just prior to CHMI (20-23 days after last dose) for Groups 2 (CHMI #1) and 3 (CHMI #2) are in Figure 3a-c. The median response and those uninfected and infected by qPCR are shown.

For all three assays median antibody responses prior to first CHMI were higher in uninfected than in infected vaccinees. There was a significant difference in median net aIFA responses between infected and uninfected volunteers in Group 3 prior to CHMI #1 ($p = 0{\cdot}0499$, Wilcoxon Rank Sum Test). For Group 3 the p value for PfCSP ELISA results in uninfected (N=4) and infected (N=16) volunteers was 0·2902 and for ISI was 0·2485.

In sera collected prior to CHMI #3 (170-171 days after last vaccine dose), antibodies by the 3 assays for Group 4 and for the 4 volunteers in Group 3 uninfected in CHMI #1 who underwent CHMI#2 are in Figure 3d-f. All data appear in Table S12.

After the 5^{th} dose, in the PfCSP ELISA, volunteers were considered to have seroconverted if their net OD 1·0 and OD 1·0 ratio, calculated, respectively, by subtracting or dividing by the pre-vaccination antibody OD 1·0, were ≥ 50 and ≥ 3·0. By these criteria, 15/18 volunteers (83%) in Group 2, 20/20 (100%) in Group 3, and 5/5 (100%) in Group 4 seroconverted, median net OD 1·0 of positives of 1189, 2685, and 961, and median OD 1·0 ratio of positives of 11·50, 21·15, and 37·83, respectively (Table S13). In the aIFA, volunteers with a net AFU 2 x 10^5 of ≥150 and a ratio of post to pre AFU 2 x 10^5 of ≥ 3·0 were considered positive (Table S13). By these criteria, 17/18 volunteers (94%) in Group 2, 18/20 (90%) in Group 3, and 5/5 (100%) in Group 4 seroconverted, median net OD 1·0 of positives of 2844, 1165, and 1820, and median OD 1·0 ratio of positives of 1193·00, 552·88, and 224·86, respectively (Table S13). For the ISI, volunteers with a net ISI activity of ≥10% and ratio of post to pre ISI activity of ≥ 3·0 were considered positive. By these criteria, 3/18 volunteers (17%) in Group

2, 8/20 (40%) in Group 3, and 3/5 (60%) in Group 4 were positive, median net OD 1·0 of positives of 22·05, 38·92, and 12·44, and median OD 1·0 ratio of positives of 19·79, 12·53, and 13·44, respectively (Table S13).

Other Antigens: Two weeks after 5th dose in Groups 2 (1·35 x 10^5 PfSPZ) and Groups 3 and 4 (2·7 x 10^5 PfSPZ), there were antibodies to: 1) PfCSP in 15/18 and 25/25 subjects; 2) PfCelTOS in 1/18 and 1/25; 2) PfMSP5 in 2/18 and 3/25; 4) PfAMA1 in 2/18 and 10/25; 5) PfEXP1 in 0/18 and 0/25; 6) PfLSA1 in 0/18 and 1/25; 7) PfMSP1 in 1/18 and 4/25; and 8) PfEBA175 in 1/18 and 1/25, respectively (Table S14). The presence of antibodies against proteins first expressed in late liver stages (PfMSP1 and PfEBA175) was unexpected; results were confirmed. No antibody responses were associated with protection.

*T cell responses***:** T cells against liver-stage malaria parasites in mice and non-human primates immunized with radiation-attenuated sporozoites mediate protection,[9,26-28] and likely in humans.[11] T cell responses were measured prior to immunization, two weeks after first and two weeks after final immunization in Group 2 (1·35 x 10^5 PfSPZ). For technical reasons the other groups could not be studied. CD8 and CD4 T cell responses generally peak after first vaccination with PfSPZ Vaccine.[13]

After the first vaccination, the percent of PfRBC-specific and PfSPZ-specific cytokine producing memory CD4 T cell responses increased by 0·25 ± 0·06 (mean ± s.e.m.) and 0·24 ± 0·04 respectively (Figure 4a,b). After final vaccination, at week 22, the CD4 T cell responses were above pre-vaccine responses by 0·17 ± 0·05 and 0·18 ± 0·05 percentage points, respectively. These responses were significantly lower than after the same immunization regimen in malaria- nnaïve U.S. adults.[10]

PfRBC-specific CD8 T cells were not significantly above pre-vaccine levels, and PfSPZ-specific CD8 T cells were slightly above background (Figure 4c,d). These responses were lower than in U.S. adults.

In contrast to other PfSPZ Vaccine trials,[10,11,13,14] there was negligible change in frequency of circulating γδ T cells (Figure 4e), or activation as measured by change in expression of the activation markers HLA-DR and CD38 following immunization (Figure 4f). To identify potential explanations for lower cellular immune responses in Tanzanians, we examined

frequency of T regulatory cells (Treg) ($CD4^+Foxp3^+CD25^+CD127^-$) expressing the activation marker CD137 (also known as 4-1BB) [29] after stimulation with PfRBC. There was no difference in pre-vaccine frequency of PfRBC-specific Tregs in the Tanzanians as compared to Americans[10] (Figure 4g). Consistent with CD4 and CD8 T cell responses, PfRBC-specific Tregs were highest after first immunization in Tanzanians (Figure 4h). Last, the pre-vaccine frequency of total memory T cells relative to total naïve T cells was significantly higher in Tanzanians compared to Americans (Figure 4i).

2.5 Discussion

To our knowledge this is the first assessment of the VE of a malaria vaccine in Africa by CHMI; the first CHMI in Africa with Sanaria® PfSPZ Challenge was conducted by the Tanzanian/SwissTPH team.[19] PfSPZ Vaccine was well tolerated and safe, but less immunogenic and protective in Tanzanian men than in U.S. volunteers. 4/20 (20%) recipients of 5 doses of 2·7 x 10^5 PfSPZ were protected against homologous CHMI by DVI 3 weeks after last immunization. In contrast, 12/13 (92·3%) volunteers in the U.S. who received 5 doses of 2·7 x 10^5 PfSPZ were protected against homologous CHMI by mosquito bite 3 weeks after last vaccine dose.[12] When the four protected Tanzanian volunteers underwent repeat homologous CHMI at 24 weeks after last dose, all four (100%) were protected. In the U.S. 7/10 previously protected volunteers were protected when they underwent homologous CHMI at 24 weeks[12] and all 5 volunteers in the U.S. who were protected at 21 weeks after last immunization (4 doses of 2·7 x 10^5 PfSPZ) were protected against repeat mosquito administered CHMI at 59 weeks.[11] However, none of the volunteers in this Tanzanian study who only underwent CHMI at 24 weeks were protected.

The same regimen (5 doses of 2·7 x 10^5 PfSPZ) was assessed for VE against intense field transmission of heterogeneous Pf in Mali. VE against infection with Pf on TBS was 52·1% by time to event and 28·5% by proportional analysis during 24 weeks after last vaccine dose.[14] This was higher than the 20% VE against homologous CHMI in Tanzania. This suggests that CHMI by DVI of PfSPZ Challenge may provide a potentially more rigorous test of VE than field transmission.

Vaccine-induced antibody responses and T cell responses in the Tanzanians were significantly lower than in malaria naïve Americans. Two weeks after last dose, the median antibody responses to PfCSP, the major protein on the surface of PfSPZ, were 4.3 times lower

in the Tanzanians than in Americans,[12] but higher than in Malians who received the same immunization regimen[14] (Figure 3g). The T cell responses were also lower than in Americans.[10,11] (Figure 4). The Tanzanians had a significantly higher proportion of total memory T cells compared to total naïve T cells at baseline than did the Americans. This higher frequency of memory cells compared to naïve cells may explain the lower immunogenicity due to less available naïve cells for expansion during the vaccinations. Moreover, the greater frequency of non-Pf-specific memory T cells may compete for infected cell contacts during pathogen surveillance.[30] These data suggest that PfSPZ Vaccine immunogenicity may be dependent on cumulative history of Pf exposure. Another explanation is that an activated immune microenvironment in the Tanzanians as compared to the Americans reduced immune responses.[31] Helminth infections have been associated with reduced immune responses to malaria,[32] the paucity of helminth infections in this population does not support helminth infection as a cause of the reduced immune responses.

There were no differences between vaccine and NS placebo recipients in regard to vaccine tolerability or AEs. 97.1% of the DVI administrations were rated painless and no volunteer experienced any local AE. Systemic AEs, most commonly headache, were mild, infrequent and of short duration, with a similar frequency in NS controls as in vaccinees.

Among the controls, 16 of 18 were positive for Pf by TBS after CHMI. However, all 18 were positive by qPCR. This is consistent with findings in Gabon after CHMI (B. Lell, submitted). It is likely that pre-existing asexual blood stage immunity limits Pf replication in some individuals. Thus, they never reach the threshold for detection by TBS. In our CHMI studies in Bagamoyo we now use qPCR to confirm positive TBS, and retrospectively or in real time assess parasitemia in all volunteers by qPCR.

We propose that increasing the numbers of PfSPZ per dose and altering intervals between doses will lead to overcoming the down regulation of humoral and cell-mediated immunity most likely due to previous exposure to Pf and thereby increase immune responses to PfSPZ Vaccine and VE. Based on work in the U.S., we are also reducing to three doses of PfSPZ Vaccine and conducting CHMI with heterologous as well as homologous Pf strains.[12,13]

Contributors: SA, SLH, MT, and TLR conceived the study. BKLS directed manufacture of the investigational product and syringe preparation in Bagamoyo. ERJ, PFB, and YA participated in manufacture of IP and syringe preparation. SAJ, SAS, ATM, KKR, FAM, MQ, MM and LWPC managed clinical data collection. NKC and SC conducted antibody analyses. ASI and RAS conducted cellular immune analyses. MM, SM, IZ, TS, TR, JR and CD

conducted clinical laboratory and parasitology analyses. AJR, ASI and LWPC conducted the statistical analyses. AJR and ASI generated figures. All authors helped to interpret the data. SLH, LWPC, SAS, SAJ, TLR, and PFB wrote the manuscript and all authors reviewed the manuscript.

Declaration of interests: Sanaria Inc. manufactured PfSPZ Vaccine and PfSPZ Challenge, and Protein Potential LLC is affiliated with Sanaria. Thus, all authors associated with Sanaria or Protein Potential have potential conflicts of interest. There are no other conflicts of interest.

Acknowledgements: The Tanzanian Commission on Science and Technology (COSTECH), the Ifakara Health Institute, and the Swiss Tropical Public Health Institute provided funding for this clinical trial. The development, manufacturing, and quality control release and stability studies of PfSPZ Vaccine and PfSPZ Challenge were supported in part by NIAID Small Business Innovation Research grant 5R44AI055229. Sanaria supported transport of PfSPZ Vaccine and PfSPZ Challenge to the study site and syringe preparation.

The authors would like to thank first and foremost the study volunteers for their participation in the study. We also thank the entire study team at the Bagamoyo branch of the Ifakara Health Institute and the manufacturing, quality control, regulatory and clinical teams at Sanaria, Inc. for their contributions to the conduct of this trial. We would also like to thank the members of the data safety monitoring board for their thoughtful oversight.

2.6 Figure legends

Figure 1: Volunteer participation (CONSORT 2010 diagram)**.**

Figure 2: Kaplan-Meier survival curves in immunized volunteers vs. controls as assessed by qPCR. Kaplan-Meier curves in volunteers undergoing CHMI 3 weeks after the last of 5 doses with 1.35 x 10^5 (Group 2) (a) or 2.7 x 10^5 (Group 3) (b) PfSPZ of PfSPZ Vaccine. Panel (c) volunteers undergoing either first (Group 4) or second (Group 3) CHMI 24 weeks after the 5^{th} immunization with 2.7 x 10^5 PfSPZ of PfSPZ Vaccine. (d) Protective efficacy and pre-patent period results.

Figure 3: Antibody responses to PfSPZ and PfCSP prior to CHMI. For all assays, uninfected subjects are shown as filled (black) circles and infected subjects are open circles. For each of the defined subject groups, the interquartile ranges and the median values of response of subjects in each group are shown. Assessment of antibodies was performed in sera from subjects before immunization and prior to CHMI #1 (~2 weeks after last dose of PfSPZ Vaccine or NS) and/or CHMI #2 (~24 weeks after last dose of PfSPZ or NS) (a, d). Antibodies to PfCSP by ELISA are reported as net OD 1.0 (the difference in OD 1.0 between pre-CHMI and pre-immunization sera). (b, e) Antibodies to PfSPZ by aIFA are reported as net AFU 2 x 10^5, the reciprocal serum dilution at which the fluorescent units were 2 x 10^5 (AFU 2 x 10^5) in pre-CHMI minus pre-immunization sera. (c, f) Results of inhibition of sporozoite invasion (ISI) assay are reported as serum dilution at which there was 80% reduction of the number of PfSPZ that invaded a human hepatocyte line (HC-04) in the presence of pre-CHMI as compared to pre-immunization sera from the same subject. Panels a-c show Groups 2 (5 doses of 1.35 x 10^5 PfSPZ) and 3 (5 doses of 2.7 x 10^5 PfSPZ) prior to short-term CHMI (2 weeks after last dose of PfSPZ or NS); panels d-f show those volunteers in Groups 3 (5 doses of 2.7 x 10^5 PfSPZ) and 4 (5 doses of 2.7 x 10^5 PfSPZ) who underwent long-term CHMI (24 weeks after last dose of PfSPZ). Panel g shows net OD 1.0 anti-PfCSP antibodies by ELISA comparing vaccinated Tanzanian volunteers to volunteers in other trials receiving the same regimen. After 5 doses of 2.7 x 10^5 PfSPZ/dose, volunteers in BSPZV1 (N = 25) had a 4.3-fold lower median net OD 1.0 than those in the U.S.-based clinical trial WRAIR 2080 (N = 26) but a 6.6-fold higher median OD 1.0 than volunteers in 14-I-N010 in Bamako, Mali (N = 42), where malaria transmission rates are higher.

Figure 4: PfSPZ-specific T cell responses in vaccine recipients receiving 1.35 × 10^5 PfSPZ. (**a–d**) PfSPZ-specific T cell responses. Frequency of cytokine-producing memory CD4 T cells responding to (**a**) PfRBC or (**b**) PfSPZ. Frequency of cytokine producing memory CD8 T cells responding to (**c**) PfRBC or (**d**) PfSPZ. Results are the percentage of memory T cells producing IFN-γ, IL-2, and/or TNF-α following stimulation minus the percentage of cells following control stimulation. (**e**) Frequency of the $V\delta2^+$ sub-family of γδ T cells out of total lymphocytes. Results are expressed as fold-change from the pre-vaccine frequency. (**f**) γδ T cell activation *in vivo*. Data are the percentage of memory γδ T cells expressing HLA-DR and CD38 as measured on PBMCs following incubation with control stimulation (vaccine diluent). (**g**) Pre-vaccine frequency of PfRBC-specific Tregs in Tanzania compared to malaria-naive U.S. subjects from the VRC 314 study. (**h**) Frequency of PfRBC-specific Treg. Results are the percentage of $CD4^+Foxp3^+CD25^+CD127^-$ T cells expressing CD137 (also known as 4-1BB) after stimulation with PfRBC minus the percentage of cells following stimulation with uninfected RBC. (**i**). Percentage of total CD4 (left) or CD8 (right) T cells that are naïve (gray bar; $CCR7^+CD45RA^+$) or memory (blue bar; not $CCR7^+CD45RA^+$) phenotype assessed pre-vaccination in all 48 subjects vaccinated in Tanzania or in 14 healthy U.S. subjects from the VRC 314 study[13]. For **a**–**f** and **h**, $n = 24$, and statistical difference was by Wilcoxon matched-pairs signed rank test. For **g** and **i**, statistical difference was by Mann-Whitney *U* test. *P*-values are reported as not significant (ns), <0.05 (*), <0.01 (**) or <0.001 (***). Data are mean ± SEM. Time points are pre-vaccine, two weeks after the first vaccination, and two weeks after the final vaccination. Black arrowhead designates PfSPZ Vaccine administration.

2.7 Figures and Tables

Table 1 Demographic characteristics of volunteers.

	Vaccinees	Normal Saline Controls	Infectivity Controls
Number of volunteers	49	8	10
Percent males	100%	100%	100%
Mean age in years (range)	24 (20, 30)	23 (20, 28)	25 (21, 28)
Percent Africans	100%	100%	100%
Mean Body Mass Index (range)	22·33 (18·00, 29·70)	21·91 (19·00, 24·20)	21·68 (18·40, 24·30)
Number (%) heterozygous for alpha thalassemia	22 (44·9%)	4 (50%)	5 (50%)
Number (%) with LTBI (QuantiFERON positive)	17 (34·7%)	3 (36·5%)	1 (10%)
Number (%) positive on screening of urine or stool for parasitic infection	0 (0%)	1 (12·5%)	0 (0%)
Number (%) students	49 (100%)	8 (100%)	10 (100%)

Table 2 a) Solicited adverse events (AEs) by group considered possibly related to administration of the investigational product during the first 7 days post immunization. b) Summary of abnormal laboratory values and severity grades.

2a	Group 1 (Dose Escalation)	Group 2 ($1{\cdot}35x10^5$ PfSPZ)	Group 3 ($2{\cdot}7x10^5$ PfSPZ)	Group 4 ($2{\cdot}7x10^5$ PfSPZ)	Total PfSPZ Vaccine	Normal Saline Controls
No. of volunteers	3	20	20	6	49	8
Total no. of injections	9	99	100	29	237	40
Number of local AEs	0	0	0	0	0	0
Numbers of systemic AEs (% of total immunizations)						
All	1 (11%)	10 (10·1%)	6 (6%)	0	17 (7·2%)	2 (5·0%)
Headache	1 (11%)	7 (7%)	2 (2%)	0	10 (4·2%)	1 (2·5%)
Abdominal pain	0	2 (2%)	1 (1%)	0	3 (1·3%)	0
Chills	0	0	1 (1%)	0	1 (0·4%)	0
Fever	0	0	2 (2%)	0	2 (0·8%)	0
Diarrhea	0	0	0	0	0	1 (2·5%)
Chest pain	0	1 (1%)	0	0	1 (0·4%)	0
Other	0	0	0	0	0	0
Systemic AEs - # volunteers with ≥1 event (% of volunteers)						
Any	1 (33%)	7 (35%)	2 (10%)§	0	10 (20·4%)	1 (13%)
Headache	1 (33%)	6 (30%)	2 (10%)§	0	9 (18·4%)	1 (13%)
Abdominal pain	0	2 (10%)	1 (5%)§	0	3 (6·1%)	0
Chills	0	0	1 (5%)§	0	1 (2·0%)	0
Fever	0	0	2 (10%)§	0	2 (4·1%)	0
Diarrhea	0	0	0	0	0	1 (13%)
Chest pain	0	1 (5%)	0	0	1 (2·0%)	0
All other	0	0	0	0	0	0

2b Lab parameter	Vaccinees in Group 2 ($1{\cdot}35x10^5$ PfSPZ) (n=20)		Vaccinees in Groups 3 and 4 ($2{\cdot}7x10^5$ PfSPZ) (n=26)		Normal Saline Controls (n=8)		P values: Vaccinees (n=46) vs Controls (n=8)
	#	%	#	%	#	%	
Leukocytosis	1	5	2	7·7	3	37·5	0·0358
Leukopenia	6	30	7	27	1	12·5	>0·05
Neutropenia	6	30	5	19	2	25	>0·05
Lymphopenia	3	15	3	11·5	2	25	>0·05
Eosinophilia*	0	0	2	7·7	3	37·5	0·0194
Decreased hemoglobin	1	5	0	0	0	0	>0·05
Thrombocytopenia	1	5	0	0	0	0	>0·05
Elevated creatinine	2	10	4	15·4	2	25	>0·05
Low total bilirubin	4	20	7	27	1	12·5	>0·05
Elevated total bilirubin	2	10	2	7·7	2	25	>0·05
Elevated alkaline phosphatase	1	5	2	7·7	0	0	>0·05
Elevated ALT	3	15	5	19	2	25	>0·05
Elevated AST	0	0	3	11·5	0	0	>0·05

Table 2a

- There were no significant differences between vaccinees and normal saline controls for any or all adverse events.
- All AEs were grade 1, except one headache and one fever.
- Local solicited AEs were injection site pain, tenderness, erythema, swelling, or induration.
- Systemic solicited adverse events = allergic reaction (rash, pruritus, wheezing, shortness of breath, bronchospasm, allergy related edema/angioedema, hypotension, anaphylaxis), abdominal pain, arthralgia, chest pain/discomfort, chills, diarrhea, fatigue, fever, headache, malaise, myalgia, nausea, pain (other), palpitations, shortness of breath, vomiting.

Table 2b

- P values calculated using Fisher's exact test (2-tailed).
- One volunteer who received saline developed grade 3 eosinophilia attributed to *S. stercoralis* infection, which improved with anthelminthic therapy. This volunteer had a baseline of mild eosinophilia, which persisted throughout the clinical trial.
- All other laboratory abnormalities were grade 2 or less. There was no association between laboratory abnormalities and time after a dose or increasing number of doses.

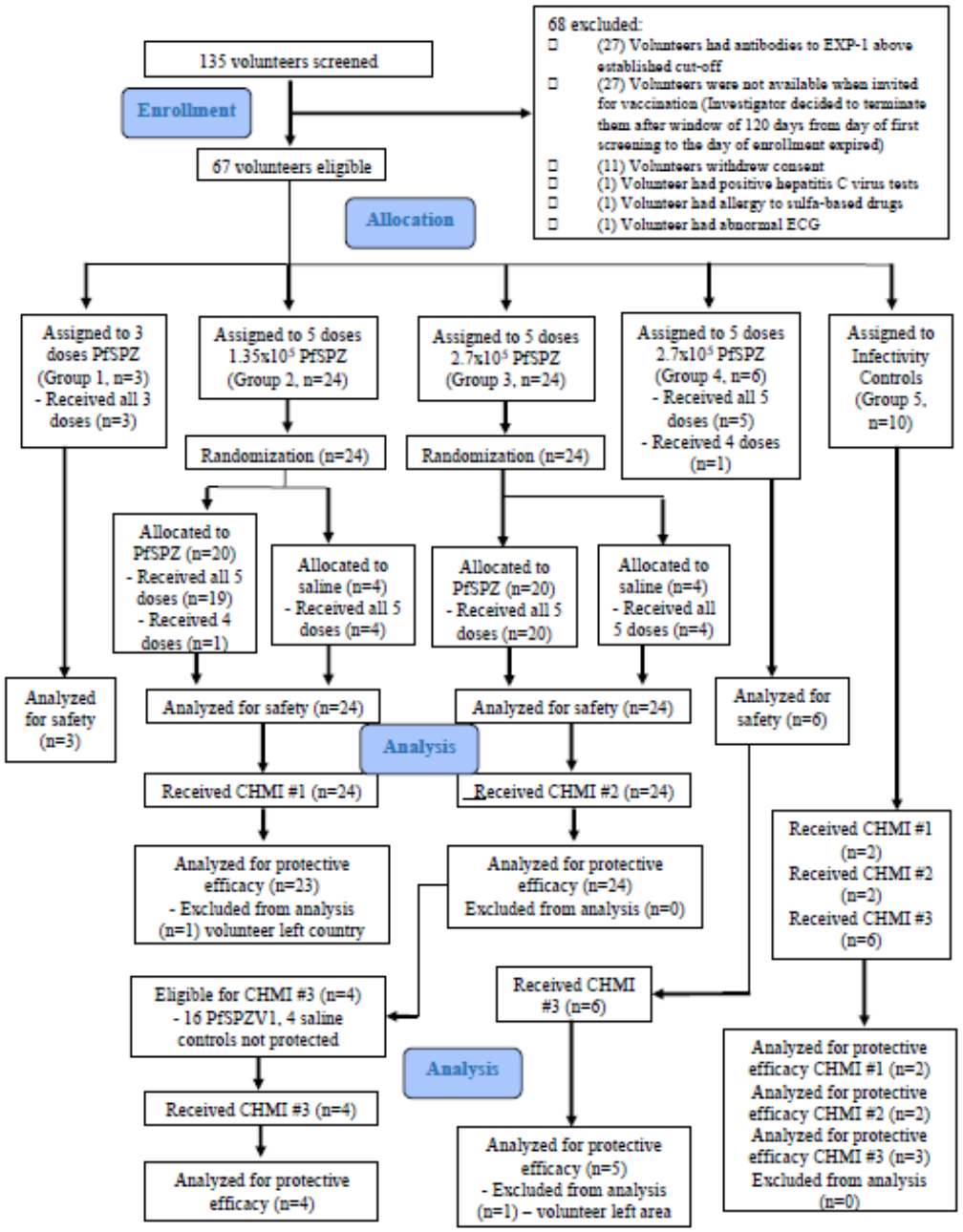
135 volunteers screened
Enrollment
68 excluded:
(27) Volunteers had antibodies to EXP-1 above established cut-off
(27) Volunteers were not available when invited for vaccination (Investigator decided to terminate them after window of 120 days from day of first screening to the day of enrollment expired)
(11) Volunteers withdrew consent
(1) Volunteer had positive hepatitis C virus tests
(1) Volunteer had allergy to sulfa-based drugs
(1) Volunteer had abnormal ECG
67 volunteers eligible
Allocation
Assigned to 3 doses PfSPZ (Group 1, n=3) - Received all 3 doses (n=3)
Assigned to 5 doses 1.35x10⁵ PfSPZ (Group 2, n=24)
Assigned to 5 doses 2.7x10⁵ PfSPZ (Group 3, n=24)
Assigned to 5 doses 2.7x10⁵ PfSPZ (Group 4, n=6) - Received all 5 doses (n=5) - Received 4 doses (n=1)
Assigned to Infectivity Controls (Group 5, n=10)
Randomization (n=24)
Randomization (n=24)
Allocated to PfSPZ (n=20) - Received all 5 doses (n=19) - Received 4 doses (n=1)
Allocated to saline (n=4) - Received all 5 doses (n=4)
Allocated to PfSPZ (n=20) - Received all 5 doses (n=20)
Allocated to saline (n=4) - Received all 5 doses (n=4)
Analyzed for safety (n=3)
Analyzed for safety (n=24)
Analyzed for safety (n=24)
Analyzed for safety (n=6)
Analysis
Received CHMI #1 (n=24)
Received CHMI #2 (n=24)
Received CHMI #1 (n=2) Received CHMI #2 (n=2) Received CHMI #3 (n=6)
Analyzed for protective efficacy (n=23) - Excluded from analysis (n=1) volunteer left country
Analyzed for protective efficacy (n=24) Excluded from analysis (n=0)
Eligible for CHMI #3 (n=4) - 16 PfSPZV1, 4 saline controls not protected
Received CHMI #3 (n=6)
Analysis
Received CHMI #3 (n=4)
Analyzed for protective efficacy (n=4)
Analyzed for protective efficacy (n=5) - Excluded from analysis (n=1) – volunteer left area
Analyzed for protective efficacy CHMI #1 (n=2) Analyzed for protective efficacy CHMI #2 (n=2) Analyzed for protective efficacy CHMI #3 (n=3) Excluded from analysis (n=0)

Figure 1

a

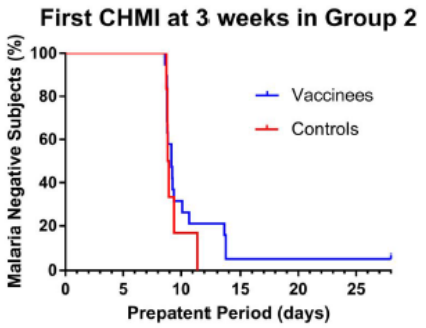

b

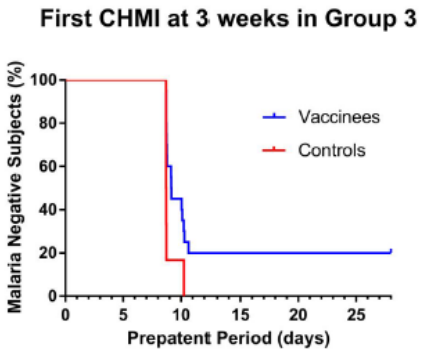

c

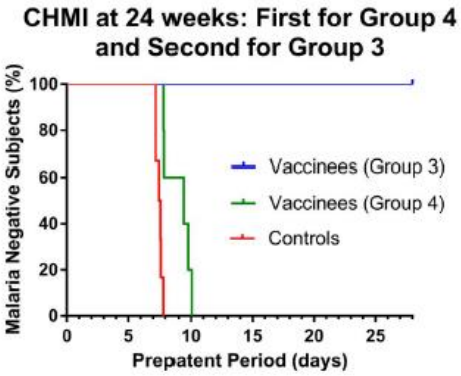

d

Group	Timing of CHMI	# protected/ # underwent CHMI	Protective efficacy	95% CI	p	Median prepatent period by qPCR of positives (days)
2 ($1.35x10^5$ PfSPZ)	3 weeks after 5th immunization	1/18	5.56%	(-55.8%, 25.76%)	>0.999	9.2
3 ($2.7x10^5$ PfSPZ)	3 weeks after 5th immunization	4/20	20%	(-34.2%, 41.6%)	0.543	9.0
3 ($2.7x10^5$ PfSPZ)	24 weeks after 5th immunization*	3/3 or 4/4**	100% (20% overall)	(43.85, 100%) or (51.01%, 100%)**	0.012 or 0.005**	n/a
4 ($2.7x10^5$ PfSPZ)	24 weeks after 5th immunization	0/5	0%	(-64%, 43.45%)	>0.999	8.7

*This was the second CHMI for the 4 volunteers in Group 3 who were protected after the first CHMI at 3 weeks.
**One volunteer was inappropriately treated on day 13 for a false positive TBS. Without this volunteer, 3/3 protected. With this volunteer 4/4 were protected.

Figure 2

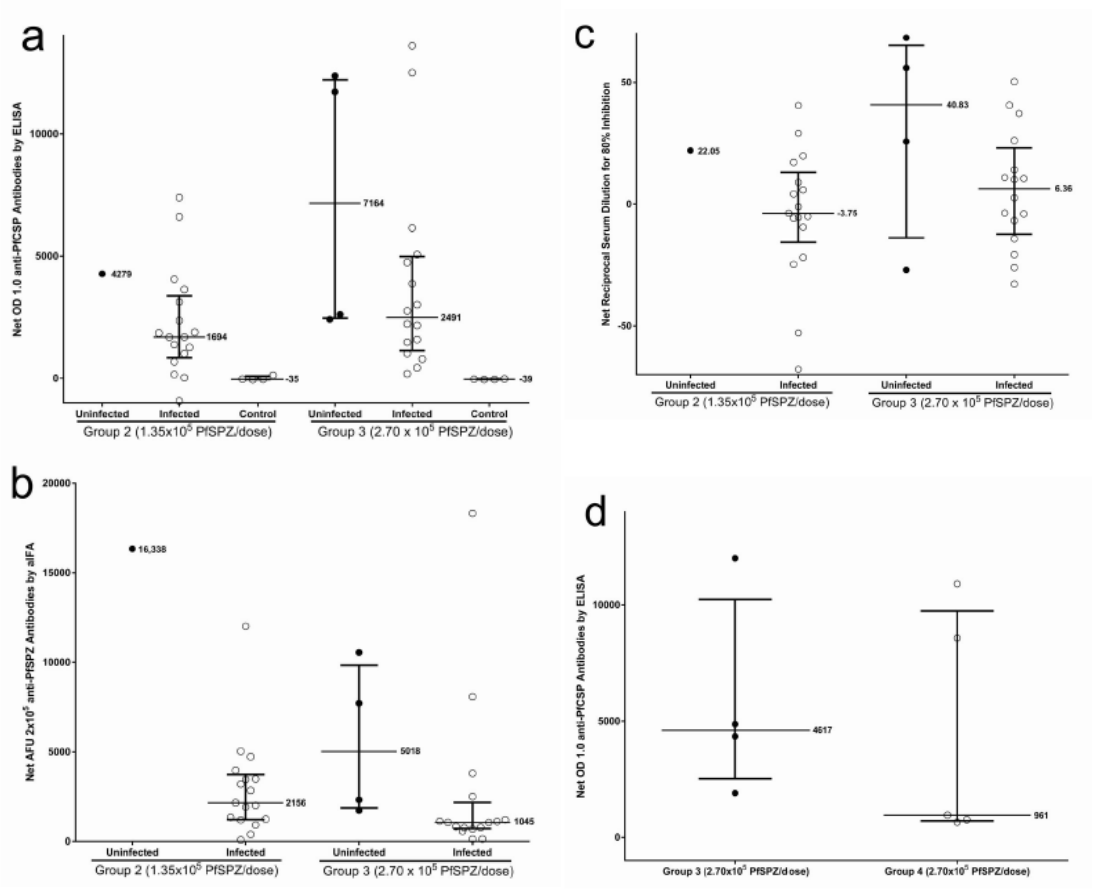
a
Net OD 1.0 anti-PfCSP Antibodies by ELISA
10000
5000
0
4279
1694
-35
7164
2491
-39
Uninfected
Infected
Control
Uninfected
Infected
Control
Group 2 (1.35x10^5 PfSPZ/dose)
Group 3 (2.70 x 10^5 PfSPZ/dose)
c
Net Reciprocal Serum Dilution for 80% Inhibition
50
0
-50
22.05
-3.75
40.83
6.36
Uninfected
Infected
Uninfected
Infected
Group 2 (1.35x10^5 PfSPZ/dose)
Group 3 (2.70 x 10^5 PfSPZ/dose)
b
Net AFU 2x10^5 anti-PfSPZ Antibodies by aIFA
20000
15000
10000
5000
0
16,338
2156
5018
1045
Uninfected
Infected
Uninfected
Infected
Group 2 (1.35x10^5 PfSPZ/dose)
Group 3 (2.70 x 10^5 PfSPZ/dose)
d
Net OD 1.0 anti-PfCSP Antibodies by ELISA
10000
5000
0
4617
961
Group 3 (2.70x10^5 PfSPZ/dose)
Group 4 (2.70x10^5 PfSPZ/dose)

Figure 3

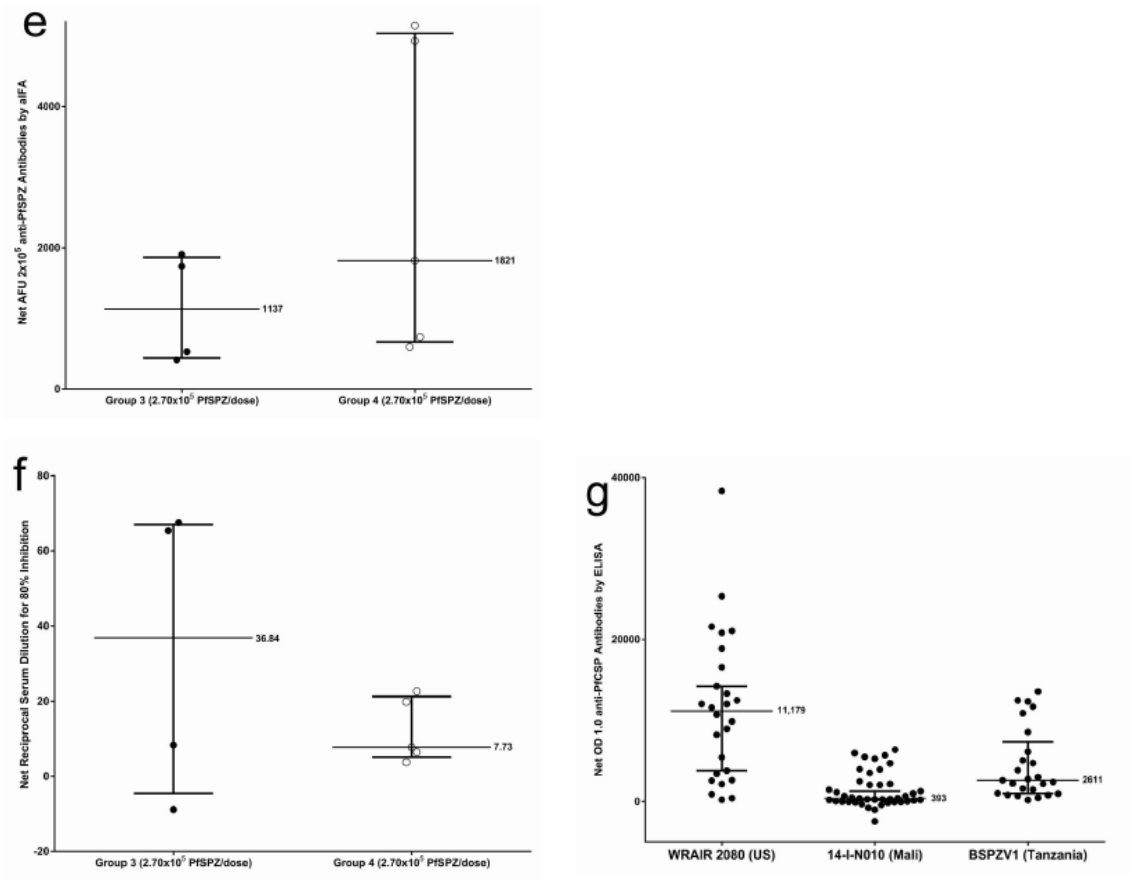
e
Net AFU 2x10^5 anti-PfSPZ Antibodies by aIFA
4000
2000
0
1137
1821
Group 3 (2.70x10^5 PfSPZ/dose)
Group 4 (2.70x10^5 PfSPZ/dose)
f
Net Reciprocal Serum Dilution for 80% Inhibition
80
60
40
20
0
-20
36.84
7.73
Group 3 (2.70x10^5 PfSPZ/dose)
Group 4 (2.70x10^5 PfSPZ/dose)
g
Net OD 1.0 anti-PfCSP Antibodies by ELISA
40000
20000
0
11,179
393
2611
WRAIR 2080 (US)
14-I-N010 (Mali)
BSPZV1 (Tanzania)

Figure 3

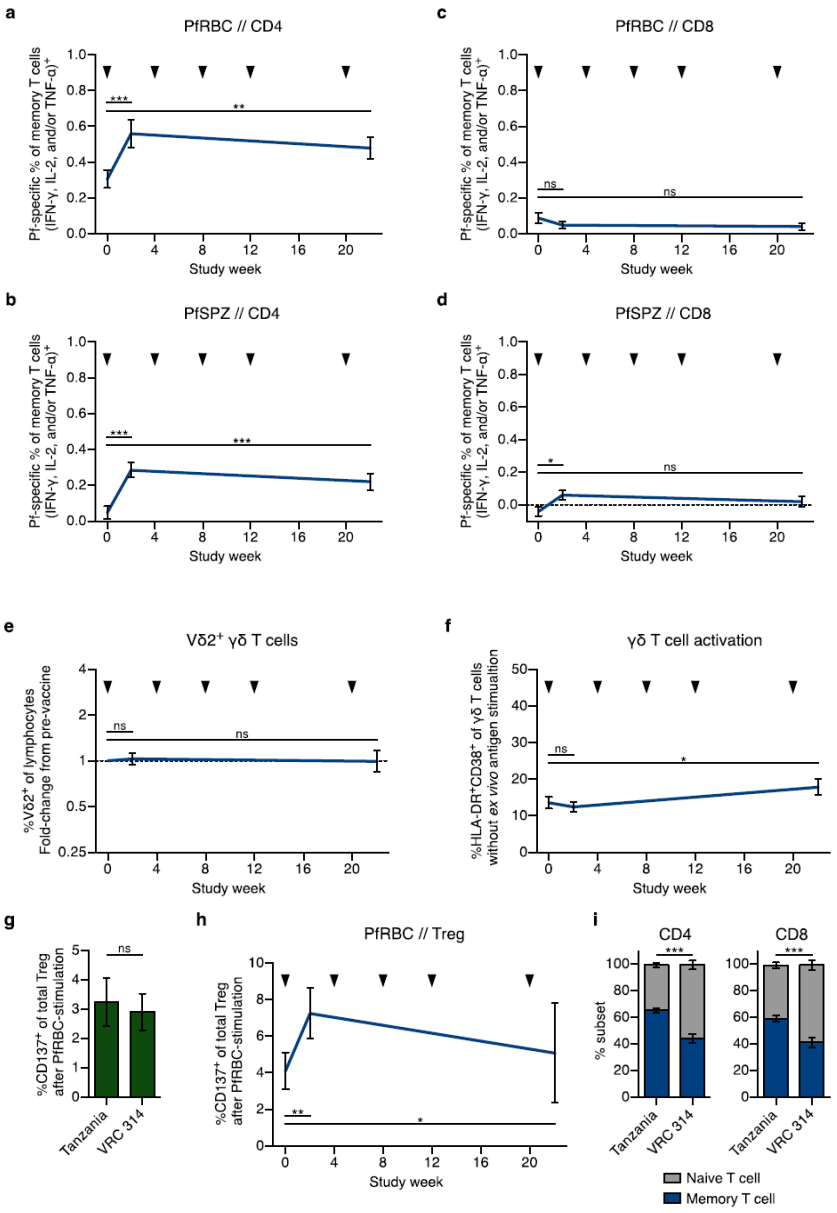
a
PfRBC // CD4
Pf-specific % of memory T cells (IFN-γ, IL-2, and/or TNF-α)+
Study week
c
PfRBC // CD8
b
PfSPZ // CD4
d
PfSPZ // CD8
e
Vδ2+ γδ T cells
%Vδ2+ of lymphocytes Fold-change from pre-vaccine
f
γδ T cell activation
%HLA-DR+CD38+ of γδ T cells without ex vivo antigen stimualtion
g
%CD137+ of total Treg after PfRBC-stimulation
Tanzania
VRC 314
h
PfRBC // Treg
i
CD4
CD8
% subset
Naive T cell
Memory T cell

Figure 4

2.8 References

1. World Health Organization. Global Malaria Programme. World malaria report 2015, Geneva: World Health Organization. 2015.

2. GBD 2015 Mortality and Causes of Death Collaborators. Global, regional, and national life expectancy, all-cause mortality, and cause-specific mortality for 249 causes of death, 1980-2015: a systematic analysis for the Global Burden of Disease Study 2015. *Lancet* 2016; **388**(10053): 1459-544.

3. Gething PW, Casey DC, Weiss DJ, et al. Mapping Plasmodium falciparum Mortality in Africa between 1990 and 2015. *N Engl J Med* 2016; **375**(25): 2435-45.

4. Richie TL, Billingsley PF, Sim BK, et al. Progress with Plasmodium falciparum sporozoite (PfSPZ)-based malaria vaccines. *Vaccine* 2015; **33**(52): 7452-61.

5. Clyde DF, Most H, McCarthy VC, Vanderberg JP. Immunization of man against sporozoite-induced falciparum malaria. *Am J Med Sci* 1973; **266**: 169-77.

6. Rieckmann KH, Carson PE, Beaudoin RL, Cassells JS, Sell KW. Sporozoite induced immunity in man against an Ethiopian strain of *Plasmodium falciparum*. *Trans R Soc Trop Med Hyg* 1974; **68**: 258-9.

7. Hoffman SL, Goh LM, Luke TC, et al. Protection of humans against malaria by immunization with radiation-attenuated *Plasmodium falciparum* sporozoites. *J Infect Dis* 2002; **185**(8): 1155-64.

8. Hoffman SL, Billingsley P, James E, et al. Development of a metabolically active,nonreplicating sporozoite vaccine to prevent *Plasmodium falciparum* malaria. *Human Vaccines* 2010; **6**(1): 97-106.

9. Epstein JE, Tewari K, Lyke KE, et al. Live attenuated malaria vaccine designed to protect through hepatic CD8+T cell immunity. *Science* 2011; **334**(6055): 475-80.

10. Seder RA, Chang LJ, Enama ME, et al. Protection against malaria by intravenous immunization with a nonreplicating sporozoite vaccine. *Science* 2013; **341**(6152): 1359-65.

11. Ishizuka AS, Lyke KE, DeZure A, et al. Protection against malaria at 1 year and immune correlates following PfSPZ vaccination. *Nat Med* 2016; **22**(6): 614-23.

12. Epstein JE, Paolino KM, Richie TL, et al. Protection against Plasmodium falciparum malaria by PfSPZ Vaccine. *JCI Insight* 2017; **2**(1): e89154.

13. Lyke KE, Ishizuka AS, Berry AA, et al. Attenuated PfSPZ Vaccine induces straintranscending T cells and durable protection against heterologous controlled human malaria infection. *Proc Natl Acad Sci U S A* 2017; **114**(10): 2711-6.

14. Sissoko MS, Healy SA, Katile A, et al. Safety and efficacy of PfSPZ Vaccine against Plasmodium falciparum via direct venous inoculation in healthy malaria-exposed adults in Mali: a randomised, double-blind phase 1 trial. *Lancet Infect Dis* 2017; **17**(5): 498-509.

15. Roestenberg M, Bijker EM, Sim BK, et al. Controlled Human Malaria Infections by Intradermal Injection of Cryopreserved *Plasmodium falciparum* Sporozoites. *Am J Trop Med Hyg* 2013; **88**(1): 5-13.

16. Sheehy SH, Spencer AJ, Douglas AD, et al. Optimising Controlled Human Malaria Infection Studies Using Cryopreserved Parasites Administered by Needle and Syringe. *PLoS One* 2013; **8**(6): e65960.

17. Hodgson SH, Juma EA, Salim A, et al. Evaluating Controlled Human Malaria Infection in Kenyan Adults with Varying Degrees of Prior Exposure to Plasmodium falciparum using sporozoites administered by intramuscular injection. *Frontiers in Microbiology* 2014; **5**: 686.

18. Mordmüller B, Supan C, Sim KL, et al. Direct venous inoculation of *Plasmodium falciparum* sporozoites for controlled human malaria infection: a dose-finding trial in two centres. *Malar J* 2015; **14**: 117.

19. Shekalaghe S, Rutaihwa M, Billingsley PF, et al. Controlled human malaria infection of Tanzanians by intradermal injection of aseptic, purified, cryopreserved *Plasmodium falciparum* sporozoites. *Am J Trop Med Hyg* 2014; **91**(3): 471-80.

20. Gomez-Perez GP, Legarda A, Munoz J, et al. Controlled human malaria infection by intramuscular and direct venous inoculation of cryopreserved Plasmodium falciparum sporozoites in malaria-naive volunteers: effect of injection volume and dose on infectivity rates. *Malar J* 2015; **14**: 306.

21. Kamau E, Alemayehu S, Feghali KC, Saunders D, Ockenhouse CF. Multiplex qPCR for detection and absolute quantification of malaria. *PLoS One* 2013; **8**(8): e71539.

22. Hofmann N, Mwingira F, Shekalaghe S, Robinson LJ, Mueller I, Felger I. Ultra-sensitive detection of Plasmodium falciparum by amplification of multi-copy subtelomeric targets. *PLoS Med* 2015; **12**(3): e1001788.

23. Anderson TJ, Su XZ, Bockarie M, Lagog M, Day KP. Twelve microsatellite markers for characterization of Plasmodium falciparum from finger-prick blood samples. *Parasitology* 1999; **119 (Pt 2)**: 113-25.

24. Mordmuller B, Surat G, Lagler H, et al. Sterile protection against human malaria by chemoattenuated PfSPZ vaccine. *Nature* 2017; **542**(7642): 445-9.

25. Lamoreaux L, Roederer M, Koup R. Intracellular cytokine optimization and standard operating procedure. *Nat Protoc* 2006; **1**(3): 1507-16.

26. Schofield L, Villaquiran J, Ferreira A, Schellekens H, Nussenzweig RS, Nussenzweig V. Gamma-interferon, CD8+ T cells and antibodies required for immunity to malaria sporozoites. *Nature* 1987; **330**: 664-6.

27. Weiss WR, Sedegah M, Beaudoin RL, Miller LH, Good MF. CD8+ T cells (cytotoxic/suppressors) are required for protection in mice immunized with malaria sporozoites. *Proc Natl Acad Sci U S A* 1988; **85**(2): 573-6.

28. Weiss WR, Jiang CG. Protective CD8+ T lymphocytes in primates immunized with malaria sporozoites. *PLoS One* 2012; **7**(2): e31247.

29. Schoenbrunn A, Frentsch M, Kohler S, et al. A converse 4-1BB and CD40 ligand expression pattern delineates activated regulatory T cells (Treg) and conventional T cells enabling direct isolation of alloantigen-reactive natural Foxp3+ Treg. *J Immunol* 2012; **189**(12): 5985-94.

30. Fernandez-Ruiz D, Ng WY, Holz LE, et al. Liver-Resident Memory CD8+ T Cells Form a Front-Line Defense against Malaria Liver-Stage Infection. *Immunity* 2016; **45**(4): 889-902.

31. Muyanja E, Ssemaganda A, Ngauv P, et al. Immune activation alters cellular and humoral responses to yellow fever 17D vaccine. *J Clin Invest* 2014; **124**(7): 3147-58.

32. Hartgers FC, Yazdanbakhsh M. Co-infection of helminths and malaria: modulation of the immune responses to malaria. *Parasite Immunol* 2006; **28**(10): 497-506.

33. Purkins L, Love ER, Eve MD, et al. The influence of diet upon liver function tests and serum lipids in healthy male volunteers resident in a Phase I unit. *Br J Clin Pharmacol* 2004; **57**(2): 199-208.

Chapter 3

Intravenous application of irradiation attenuated *Plasmodium falciparum* sporozoites elicits long-lived IgG and IgM invasion inhibitory antibodies in malaria pre-exposed volunteers

---

This chapter is an adapted version of the following article:
Isabelle Zenklusen, Said Jongo, Salim Abdulla, Kamaka Ramadhani, B. Kim Lee Sim, Erika Flannery, Thao Nguyen, Matthew Fishbaugher, Will Betz, Nelly Carmago, Sebastian Mikolajczak, Stefan Kappe, Stephen L. Hoffman, Brandon Sack and Claudia Daubenberger. Intravenous application of irradiation attenuated *Plasmodium falciparum* sporozoites elicits long-lived IgG and IgM invasion inhibitory antibodies in malaria pre-exposed volunteers. Manuscript submitted to *Journal of Infectious Disease*.

Intravenous application of irradiation attenuated *Plasmodium falciparum* sporozoites elicits long-lived IgG and IgM invasion inhibitory antibodies in malaria pre-exposed volunteers

Isabelle Zenklusen[1,2], Said Jongo[4], Salim Abdulla[4], Kamaka Ramadhani[4], B. Kim Lee Sim[5], Erika Flannery[3], Thao Nguyen[3], Matthew Fishbaugher[3], Will Betz[3], Nelly Carmago[3], Sebastian Mikolajczak[3], Stefan Kappe[3,6], Stephen L. Hoffman[5], Brandon Sack[3]* and Claudia Daubenberger[1,2]*

[1]Swiss Tropical and Public Health Institute, Clinical Immunology Unit, 4051 Basel, Switzerland

[2]University of Basel, 4001 Basel, Switzerland

[3]Center for Infectious Disease Research, Seattle, WA 98109, USA

[4]Ifakara Health Institute, Clinical Trial Unit, Bagamoyo, Tanzania

[5]Sanaria Inc., Rockville, MD 20850, USA

[6]University of Washington, Seattle, Department of Global Health, Seattle, WA 98195, USA

*These authors contributed equally to this work

3.1 Abstract

Background

To date, the assessment of vaccine-induced humoral immune responses upon whole sporozoite vaccination focuses largely on antibodies of the IgG isotype. Here, we aimed to investigate if sporozoite binding and invasion inhibitory IgM antibodies are induced following immunization with aseptic, purified, irradiated, non-replicating, metabolically active *Plasmodium falciparum* sporozoites (PfSPZ Vaccine) in malaria pre-exposed volunteers.

Methods

Serum and plasma samples were collected from malaria pre-exposed volunteers immunized by direct venous inoculation (DVI) of PfSPZ Vaccine. Functionality of serum antibodies was assessed by *in vitro* inhibition of sporozoite invasion (ISI) assay. Vaccine-induced IgG and IgM antibodies were determined by enzyme-linked immunosorbent assay (ELISA) against full length circumsporozoite protein (CSP). Plasma from a subset of volunteers was depleted from IgG and IgA antibodies to obtain antibody fractions containing only IgM antibodies and tested in an *in vitr*o ISI assay to determine sporozoite-blocking activity.

Results

Malaria pre-exposed volunteers developed sporozoite-invasion inhibitory antibodies and anti-CSP IgG and IgM antibodies upon DVI-administered PfSPZ vaccination. IgM plasma fractions of three volunteers mediated ISI *in vitro*.

Conclusions

We demonstrate for the first time that sporozoite binding IgM antibodies are induced following repeated PfSPZ vaccination in malaria pre-exposed individuals and that these IgM antibodies can inhibit sporozoite invasion *in vitro*. These findings suggest that the immunological assessment of PfSPZ Vaccine-induced humoral immune responses should include monitoring of parasite specific IgG and IgM antibodies.

Keywords

Malaria, PfSPZ Vaccine, malaria pre-exposed individuals, functional antibodies, IgM, vaccine-induced humoral immunity, ISI, IFA

3.2 Background

Despite the global reduction in malaria incidence and mortality rates between the years 2000 and 2015, malaria remains a major public health concern. In 2016, the World Health Organization (WHO) estimated 212 million new malaria cases globally, of which 429,000 died from the disease, mostly due to *Plasmodium falciparum* (Pf) [1]. Most of these deaths (92%) occurred in the WHO African region with 70% of all deaths reported in children under 5 years of age [1]. The most advanced malaria vaccine candidate, the CSP-based subunit vaccine RTS,S/AS01 (Mosquirix™), showed limited vaccine efficacy of 36.3% against clinical malaria among children aged 5 to 17 months and of 25.9% in young infants 6 to 12 weeks of age in phase 3 clinical trials in several sub-Saharan countries [1, 2]. RTS, S/AS01 mediated protection is short-lived and wanes after the first year of vaccination [2]. This is below the goal of 75% efficacy against clinical malaria set by the WHO Malaria Vaccine Technology Roadmap [1, 3].

Sterile protection against CHMI has been achieved via mosquito bite administration of radiation-attenuated Pf sporozoites (RAS) [4] and by DVI of aseptic, purified, radiation-attenuated, cryopreserved Pf sprozoites (PfSPZ Vaccine) [5]. Administration of fully infectious Pf sporozoites either via mosquito bite or DVI to volunteers taking simultaneously the anti-malarial drug Chloroquine (CVac) has been tested recently with promising results [6–8]. Pf attenuation by genetic modification is under investigation, with no CHMI protection data yet reported [9]. So far, most of these experimental malaria vaccinations followed by CHMI have been performed in volunteers living in non-malaria endemic countries [4–8]. The slow and incremental acquisition of anti-malarial immunity during natural exposure [10, 11] and growing experimental evidence in mouse models suggest that prior exposure of malaria might hamper malaria vaccine-induced protection [12]. Better understanding of type, kinetics and maintenance of malaria-specific immune responses in malaria pre-exposed populations is an indispensable step for successful deployment of the PfSPZ Vaccine [13].

Serum samples used in this study were collected during a phase 1 clinical trial investigating the safety, immunogenicity and protective efficacy of DVI administered PfSPZ Vaccine in Tanzanian adults in Bagamoyo, Tanzania (NCT02132299) (Jongo et al., manuscript submitted). Briefly, two groups of volunteers (n=20) were vaccinated five times each with a dosage of 1.35×10^5 (low-dose) or 2.7×10^5 (high-dose) PfSPZ Vaccine. The first homologous CHMI (CHMI1) using fully infectious NF54 Pf sporozoites was conducted 21

days after last vaccination and was followed by a second homologous CHMI (CHMI2) 140 days later in the subset of volunteers protected after CHMI1 (Jongo et al., manuscript submitted). Here, we aimed i) to determine the *ex vivo* induction of Pf sporozoite invasion inhibitory activity upon PfSPZ vaccination and ii) to investigate if sporozoite-specific IgM antibodies are induced after vaccination and can potentially contribute to protection by preventing sporozoite invasion of hepatocytes *in vitro*. The magnitude and longevity of these vaccine-induced responses were followed for 168 days after last vaccination in a subset of sterile protected volunteers.

3.3 Methods

3.3.1 Ethics statement

All volunteers gave written informed consent before screening. The clinical trial was performed in accordance with Good Clinical Practices. The protocol was approved by the institutional review boards (IRBs) of the Ifakara Health Institute (Ref. No. IHI/IRB/ No: 02-2014), the National Institute for Medical Research Tanzania (NIMR/ HQ/R.8a/Vol.IX/1691) and the Ethikkommission Basel (EKNZ), Basel, Switzerland (reference number 261/13). The protocol was approved by the Tanzania Food and Drug Authority (TFDA) (Ref. No. TFDA 13/CTR/0003) and the trial was registered at Clinical Trials.gov (NCT02132299) and conducted under U.S. FDA IND 14826.

3.3.2 Clinical trial design and study population

Details of the trial procedure and volunteers enrolled are given elsewhere (Jongo et al., manuscript submitted). In summary, healthy male volunteers aged 20 to 30 years were randomized to DVI of 5 doses of normal saline or 1.35 x 10^5 or 2.7 x 10^5 of PfSPZ Vaccine in a double blind clinical trial at the Bagamoyo Clinical Trial Unit (BCTU) of the Ifakara Health Intsitute (IHI) in Bagamoyo, Tanzania between 2014 and 2015. Vaccine efficacy was assessed by CHMI by DVI of 3,200 PfSPZ of PfSPZ Challenge at 3 and 24 weeks, or 24 weeks after the last PfSPZ immunization. The PfSPZ Vaccine proved to be safe and well tolerated in all Tanzanian volunteers. In the low-dose group, 1 of 18 (6%) volunteer was protected against CHMI at 3 weeks and 4 of 20 (20%) volunteers were protected at 3 and 24 weeks in the high-dose group.

3.3.3 Sample collection

Serum samples were collected at screening one week prior to the first immunization (baseline), on the day of each vaccination, followed at weeks 2, 4 and 8 after each immunization. In addition, serum was sampled one week before, and at weeks 2, 4 and 8 after each CHMI. Whole blood was collected in vacutainer tubes with clot activators (Becton Dickinson, 369032), allowed to stand at RT until a clot was formed and subsequently

centrifuged at 2000 g for 10 minutes at 22°C. Afterwards, the serum was collected, aliquoted and stored at -80°C for later antibody immunogenicity assessments.
Plasma was obtained during isolation of peripheral blood mononuclear cells (PBMC) from whole blood using Ficoll density gradient centrifugation and stored at -80°C.

3.3.4 Inhibition of sporozoite invasion assay (ISI)

To determine the capacity of serum antibodies to inhibit sporozoite invasion *in vitro*, a previously described flow cytometry-based assay was performed [9, 14]. Briefly, immortalized HC04 human hepatocyte cells (MRA-975, MR4) were cultured in D10 Media (DMEM, Gibco) supplemented with 10% FBS, 2.5mM glutamine, 1% penicillin/streptomycin and fungizone (Life Technologies) at 37°C in 5% CO2. HC04 cells were split at 90% confluence and plated at 10^5 cells/well in a 96 well plate for the assay. Freshly dissected salivary gland NF54 *P. falciparum* sporozoites [15] were incubated with sera from volunteers at a 1:20 dilution of complete culture media for 15 minutes at 37°C. Sporozoites were then added to HC04 cells in triplicate in 96 well plates in a total volume of 100µL/well. To facilitate sporozoite contact with hepatoma cells, the plate was centrifuged at 400 x g for 3 minutes and afterwards incubated at 37°C for 90 minutes. After incubation, cells were fixed and permeabilized (BD Cytofix/Cytoperm, BD Bioscience) and subsequently stained with an Alexa fluor-647-conjugated anti-CSP monoclonal antibody (clone 2A10). Invasion was analyzed by flow cytometry by first identifying live HC04 cells by forward and side scatter and then monitoring for CSP^+ cells. Percent of inhibition of invasion for each volunteer was determined by normalizing to the CSP cells in triplicate wells containing volunteer matched pre-immune serum or a pooled serum sample from malaria-naïve individuals. Samples were excluded if invasion of cells in untreated wells was < 0.5%. The reported data indicates the average of at least two independent experiments.

3.3.5 CSP enzyme-linked immunosorbent assay (ELISA)

IgG and IgM antibodies were measured against full length Pf CSP protein. Pf CSP was produced in HEK293F cells as previously described [9]. High-binding 96-well plates (Corning) were coated with 0.1 µg Pf CSP/mL in sodium-carbonate/calcium-bicarbonate coating buffer and incubated overnight at 4°C, washed 4 times with 0.05 Tween-20 in PBS (Sigma, Life Technologies), and blocked for 2 hours 15 minutes at RT in dilution/blocking buffer (PBS containing 0.05% Tween-20 and 6% BSA). After washing 4 times, serum

samples were added in dilution/blocking buffer at a dilution of 1/800 for the IgG-CSP ELISA, and at 1/80 for the IgM-CSP ELISA, and incubated for 2 hours at RT. Samples were tested in duplicate. Each independent plate included a standard positive sample, which was used to create an 8-point 2-fold serial dilution series and additional negative controls at dilutions of 1/400 for the IgG-CSP ELISA and 1/80 for the IgM-CSP ELISA. For analysis of IgM antibodies, serial dilutions of fractions were applied as indicated in Figure 4A and ELISA development was performed per manufacturer's protocol (Bethyl Laboratories). After washing, the secondary antibody was applied. For detection of antibodies, a subclass-specific HRP-conjugated anti-human secondary antibody (Life Technologies) was applied at 1/5000 (IgG, IgA) or 1/2000 (IgM). Secondary antibodies were incubated for 2 hours and 15 minutes at RT. After incubation, plates were washed 4 times, developed in SigmaFast OPD (Sigma) for 4 minutes for the IgG-CSP ELISA and for 16 minutes for the IgM-CSP ELISA, and immediately read for absorbance at 450 nm using a Spectramax M2 Molecular Devices Microplate reader. Arbitrary units (AU) were calculated by interpolating values based on the standard curve using nonlinear regression with Prism 6 software and multiplied by the dilution factor. Samples were defined as CSP binding when titers were above a pre-defined cutoff for positivity calculated by the mean of the negative control (pooled serum sample from malaria naïve people) plus 3 standard deviations to the mean. Sample data outside the standard curve range or with coefficient variation (CV) >30% between duplicates values were excluded for analysis. All ELISA values were repeated and are referred to as the mean of two independent runs. Not all volunteers were tested at all the time points due to sample availability.

3.3.6 Generation of IgM antibody fractions

In order to generate antibody fractions containing only IgM antibodies, plasma from a subset of volunteers was first depleted of IgG antibodies by use of protein G columns (GraviTrap Protein G columns, GE Healthcare Life Sciences). This was performed by diluting plasma from immunized volunteers and a pool of pre-immune sera from volunteers 1:2 in binding buffer (GE Healthcare Life Sciences) and applied to protein G column per manufacturer's instructions. Flow-through was collected and columns were washed and eluted using elution buffer (GE Healthcare Life Sciences) per protocol. After column regeneration, this process was repeated for a total of 6 times. IgG recovery in eluate and depletion in flow-through was confirmed via human IgG ELISA (Bethyl Laboratories). IgG flow-through was then buffer-

exchanged into PBS using PD-10 desalting columns and recovery of both IgM and IgA was confirmed via ELISA (Bethyl Laboratories). IgA was then removed from this fraction by application of a calculated 1mg of total IgA to 1mL of PBS-equilibrated Jacalin-sepharose (BioVision, Inc.) and all volumes brought to 12mL in PBS. Samples were incubated with Jacalin-sepharose for 2h at RT with rotation. IgA-depleted fraction ("IgM fraction") was collected by centrifugation at 150 x g for 2 minutes and collection of supernatant. IgA was then eluted using 0.1M melibiose. Depletion of IgA in the IgM fraction and recovery in the eluate was then confirmed by IgA and IgM ELISA. All fractions were then concentrated using 10kD protein concentration filters (Amicon Ultra-15, EMD Millipore) and returned to original input volumes to maintain equivalent dilutions for ISTI analysis. Purity was assessed using total human IgM and IgA ELISAs (Bethyl Laboratories) according to manufacturer's protocol.

3.3.7 Sporozoite immunofluoresence assays (IFA)

Sporozoite IFAs were performed as previously described [9]. Briefly, freshly-dissected Pf sporozoites were fixed in 10% PFA for 10 minutes at RT, washed and air-dried onto 12-well glass microscope slides. Sporozoites were permeabilized and blocked in 3% BSA in PBS with 0.1% Triton-X100. IgM antibody fractions were applied at a 1:100 dilution in 3% BSA in PBS and incubated at RT for 1h. Anti-human IgM conjugated to AlexaFluor-594 (Southern Biotech) was then applied at a 1:6000 dilution and incubated in the dark at RT for 1h. Sporozoites were then stained with AlexaFluor-488-conjugated anti-CSP mAb 2A10 at 2µg/mL in 3% BSA in PBS for 1h at RT followed by DAPI nuclear staining. Sporozoites were visualized using Deltavision microscopy. Images were captured using the same exact exposure conditions in the hIgM/Alexafluor-594 channel to allow comparisons of intensity across samples. Images were modified for clarity with the same exact parameters applied to each sample.

3.3.8 Statistical analysis

Statistical analyses were carried out using R (R Development Core Team (2011), R: A Language and Environment for Statistical Computing. Vienna, Austria: the R Foundation for Statistical Computing. Available online at http://www.R-project.org/.). The R package ggplot2 was used for data visualization (H. Wickham.ggplot2: Elegant Graphics for Data Analysis. Springer Verlag New York, 2009).

3.4 Results

3.4.1 Immunization with PfSPZ Vaccine induces sporozoite inhibitory antibodies

An overview of the vaccination schedule followed by two consecutive homologous CHMIs is given in Supplementary Figure 1.

To explore the inhibitory capacity of PfSPZ Vaccine-induced antibodies, we used a previously described flow cytometry-based inhibition assay of Pf sporozoite invasion of HC04 cells (ISI) [9, 14]. For the low-dose (Figure 1A), serum samples collected at 14 days after 3rd and 5th immunization and 28 days past CHMI1 were assessed and likewise for the high-dose group (Figure 1B) except for two additional time-points at 140 days past CHMI1 and 28 days post-CHMI2 included for immunized protected subjects.

Vaccine-induced changes in serum reactivity were determined by normalizing each time point to the inhibitory activity of serum taken at baseline. After 3rd immunization, immunized volunteers in the low-dose group showed an average inhibition of 53.75 ± 10.81 % (Figure 1A) while immunized volunteers from the high-dose group were inhibited by an average of 52.73 ± 5.14 % (Figure 1B). Two volunteers from the low-dose group and one from the high-dose group showed no ISI activity. After the 5th immunization, all volunteers in both groups developed functional antibodies with an average inhibition of 62.93 ± 6.36 % for the low-dose group and 61.47 ± 3.55 % for the high -group. ISI activity remained unchanged in both groups when compared before and after CHMI1. ISI in CHMI protected and unprotected subjects did not differ significantly at any time point (Figure 1A, B). When followed in the four CHMI1 protected volunteers, ISI activity was sustained until day 140 after CHMI1, with an average inhibition of 75.60 ± 7.89 %. ISI results of serum samples collected from placebo controls are provided in Figure 1C. ISI remained undetectable during PfSPZ vaccinations and increased significantly only after CHMI1 (Figure 1C).

Collectively, these results demonstrate that PfSPZ vaccination of malaria pre-exposed Tanzanian volunteers induced antibodies inhibiting Pf sporozoite invasion *in vitro*. No difference was observed between the low- and high-dose groups and in some volunteers, these inhibitory antibodies were detectable up to 140 days past CHMI1.

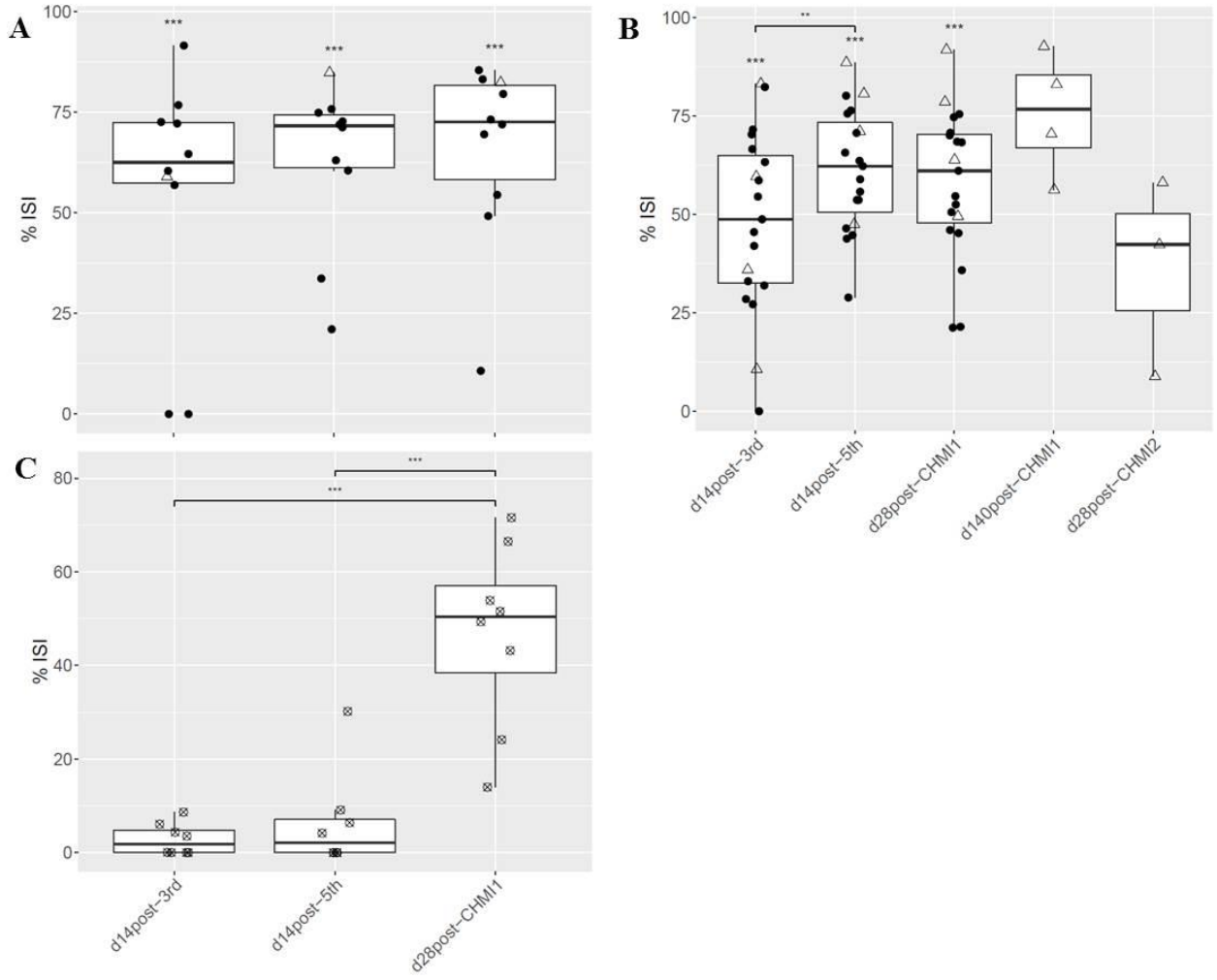

Figure 1 Evaluation of serum from PfSPZ-immunized malaria pre-exposed Tanzanian volunteers for functional inhibition of sporozoite invasion (ISI) *in vitro*. Percentage ISI of HC04 cells infected with Pf sporozoites obtained from post-immunization sera from malaria pre-exposed volunteers immunized with **(A)** 5 x 1.35 x 10^5 PfSPZ Vaccine (n = 10) and **(B)** 5 x 2.7 x 10^5 PfSPZ Vaccine (n = 20). Serum samples at d140post-CHMI1 (n=4) and d28post-CHMI2 (n=3) were only available from protected subjects of the high-dose group. One sample at d14post-5th was missing for the high dose group. Each data point indicates a volunteer's mean value across 2 independent experiments. The middle bar of each box plot represents the median and the whisker maximum length set to 1.5 IQR (interquartile range). Asterisks above box plots indicate a statistically significant difference of the group mean invasion relative to 0% inhibition of invasion, determined by one-sample t-test. Bars with asterisks show statistically significant changes of inhibition of invasion between visits determined by paired t-test. Immunized protected individuals are shown as empty triangles, immunized non-protected volunteers as solid circles and control subjects as crossed circles. **(C)** Percentage ISI from sera collected from control volunteers from low- and high-dose group (n = 8), who received normal saline instead of PfSPZ-immunization at 14 days after the 3rd and 5th immunization. On day 28post-CHMI1 all control volunteers were challenged with 3,200 non-irradiated PfSPZ of PfSPZ Challenge.

3.4.2 PfSPZ vaccination induced anti-CSP IgG and IgM antibodies

The circumsporozoite protein is the major protein on the surface of Pf sporozoites and has been known to be immunodominant [16]. We assessed the IgG and IgM antibody titers specific for full length recombinant CSP [9] using ELISA (Figure 2A, B) at baseline, 14 days past 5th immunization and 140 days post-CHMI1 and 28 days post-CHMI2 for the high-dose group.

We set the positivity cutoff for anti-CSP IgG antibody titers at 10.12 arbitrary units (AU) (Figure 2A). At baseline, four of 23 volunteers showed positive IgG titers (average of 18.89 ± 1.84 AU) with a total group average of 7.94 ± 1.15 AU. The four positive subjects included one volunteer who was protected after CHMI1 and CHMI2. 14 days after the 5th immunization, all vaccinees had developed significantly higher anti-CSP IgG antibodies (average of 68.02 ± 8.63 AU). All placebo controls remained negative with an average of 9.89 ± 0.81 AU. Interestingly, the anti-CSP IgG titers remained unchanged before and after CHMI1 (average of 64.81 ± 9.16 AU for all volunteers). Placebo controls and non-protected vaccinees developed asexual blood stage parasitemia after CHM1. Anti-CSP IgG titers after CHMI1 were not boosted and were remained lower in placebos (29.32 ± 6.87 AU) compared to PfSPZ immunized volunteers (71.91 ± 10.23 AU) (Figure 2A). On follow-up visits at 140 days post-CHMI1 and on 28 days post-CHMI2, the four protected volunteers remained positive for anti-CSP IgG.

The positivity cutoff for anti-CSP IgM antibody titers was set at 9.21 AU. At baseline, CSP-binding IgM antibodies (Figure 2B) were detected in four of 23 volunteers with an average of 12.78 ± 1.83 AU while the total group average was 7.39 ± 0.71 AU. 14 days past 5th immunization, 18 of 23 volunteers showed anti-CSP IgM titers with an average of 89.61 ± 27.30 AU. Three of four placebo controls remained negative at this time point as well as one vaccinee. 28 days post CHMI1, a significant increase in anti-CSP IgM titers (average of 164.30 ± 33.79 AU) in all volunteers which experienced asexual blood stage infections was observed. Interestingly, anti-CSP IgM titers from placebo controls (average: 152.71± 54.50 AU) and non-protected vaccinees (average: 157.88 ± 34.71 AU) did not differ significantly. 28 days post CHMI1. Anti-CSP IgM titers remained unchanged in sterile protected volunteers after CHMI1. One protected volunteer did not develop anti-CSP IgM antibodies during vaccination and after CHMI1 and CHMI2. In serum samples collected 140 days after CHMI1 (average: 134.65 ± 30.93 AU) and 28 days post CHMI2 (average: 168.21 ± 33.99 AU), sustained anti-CSP IgM titers were measured in two of four protected volunteers.

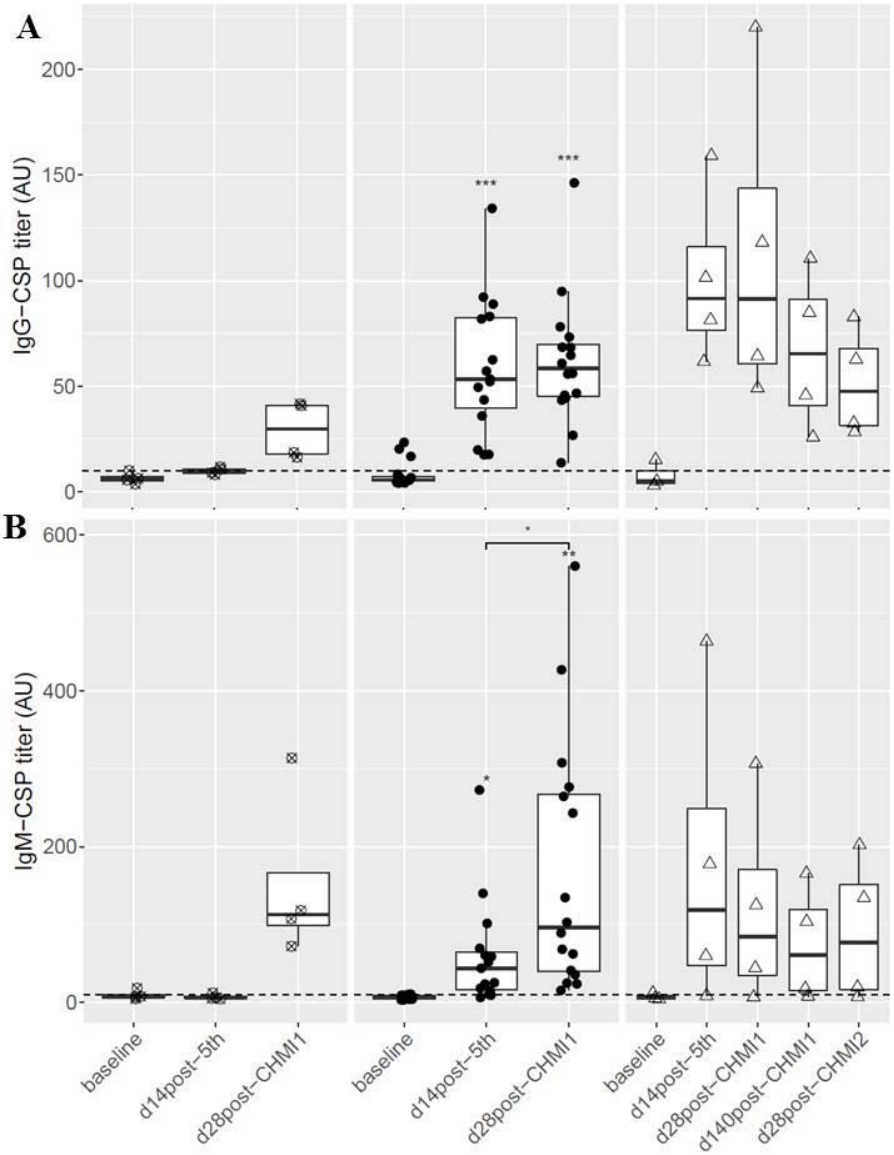

Figure 2 Induction of IgG (A) and IgM antibody (B) responses to full length Pf CSP from malaria pre-exposed volunteers immunized with 5 x 2.7 x 10^5 PfSPZ Vaccine, quantified by ELISA at the time-points: baseline, day 14 post-5th-immunization, day 28 post-CHMI1, day 140 post-CHMI1 and day 28-post-CHMI2. Antibody titers are specified as arbitrary units (AU) with a positivity cutoff shown by a dashed line. Each data point represents the mean of the duplicate ELISA titers for one volunteer. Asterisks indicate statistically significant difference of the mean antibody titer compared to the mean titer measured at the pre-immunization time-point as determined by paired t-test. Bars with asterisks indicate statistically significant difference of the mean antibody titer between visits determined by paired t-test. *$p \leq 0.05$, **$p \leq 0.01$, ***$p \leq 0.001$. Control volunteers are shown as crossed circles (n=4), immunized non-protected volunteers as solid circles (n=16) and immunized protected (n=4) as empty triangles. Serum samples of two volunteers were not available, one at baseline and one at visit of d14post-5th. The two volunteers were not considered for statistical analysis.

Overall these results revealed that malaria pre-exposed Tanzanian adults developed anti-CSP IgG and IgM antibody titers that persisted for more than 6 months after PfSPZ immunization and CHMI. We next tried to correlate level of *in vitro* Pf sporozoite inhibition with anti-CSP IgG and IgM antibody titers from the high-dose group. No significant correlation became apparent between invasion inhibition and anti-CSP IgG (Figure 3A) and IgM titers (Figure 3B).

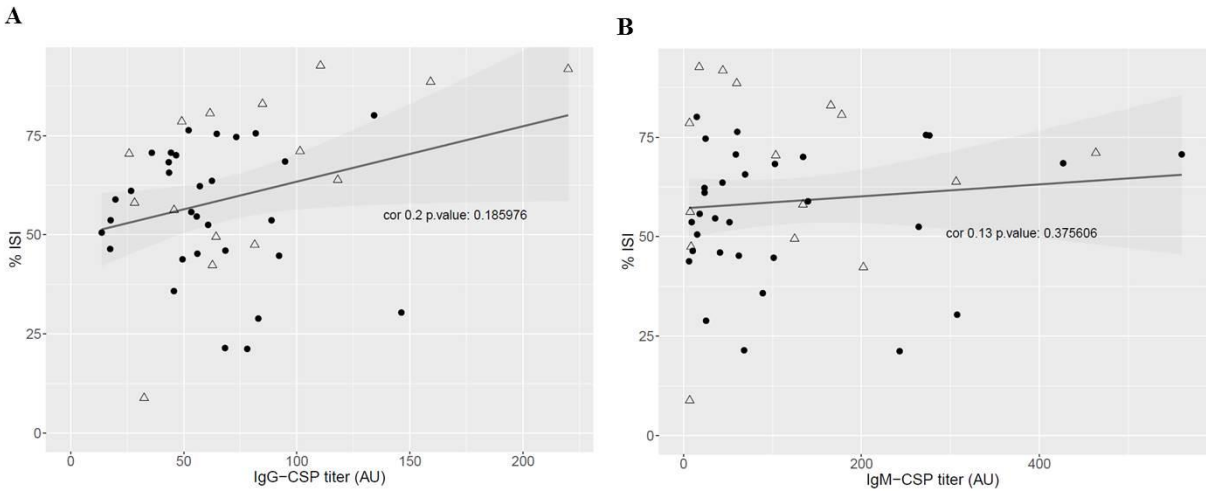

Figure 3 No statistically significant correlation between anti-CSP titers and percentage ISI of HC04 cells assessed from malaria pre-exposed people immunized with 5 x 2.7 x 10^5 PfSPZ Vaccine measured at time-points of baseline, post-immunization and post-CHMI1. (A) Correlation between percentage of ISI and anti-CSP IgG titers and (B) anti-CSP IgM titers determined by Spearman correlation. Immunized non-protected volunteers are shown as solid circles (n = 31) and immunized protected as empty triangles (n = 15).

3.4.3 IgM antibodies contribute to inhibition of sporozoite invasion

Next, we wanted to understand better the potential contribution of vaccine-induced anti-CSP IgM antibodies to *in vitro* sporozoite invasion inhibition. Here, we selected plasma samples collected from five volunteers with high anti-CSP IgM titers 14 days after 5th immunization. Plasma samples were depleted of IgG and IgA antibodies and the IgM enriched fractions were used to test for binding against full length PfCSP in ELISA (Figure 4A) and whole sporozoites in IFA (Figure 4B) and subsequently in ISI assay to determine inhibition of sporozoite invasion *in vitro* (Figure 4C). The resulting fractions after IgG and IgA depletion contained IgM antibodies with higher than 90% purity as measured by total IgM and IgA ELISA and all bound to full length CSP by ELISA (Figure 4A). At a 1:20 dilution in

complete medium the IgM enriched preparation inhibited sporozoite invasion in 3 out of 5 volunteers, ranging between 28 to 43 % (Figure 4C). Before enrichment of IgM fractions, the three ISI positive volunteers had the highest anti-CSP IgM titers with an average AU of 304, while the two ISI negative volunteers had an average of 104 AU. IgM enriched plasma preparations of these three positive volunteers also recognized strongly whole sporozoites in IFA (Figure 4B). IgM fractions from plasma samples of the four high-dose protected volunteers collected 140 days after the first CHMI were tested as well. One volunteer with high anti-CSP IgM titers showed strong binding to purified sporozoites by IFA and showed invasion inhibition at 31% (data not shown).

In summary, PfSPZ Vaccine-induced anti-CSP IgM antibodies in malaria pre-exposed volunteers inhibit *in vitro* sporozoite invasion and persisted in one volunteer for at least 140 days after CHMI1.

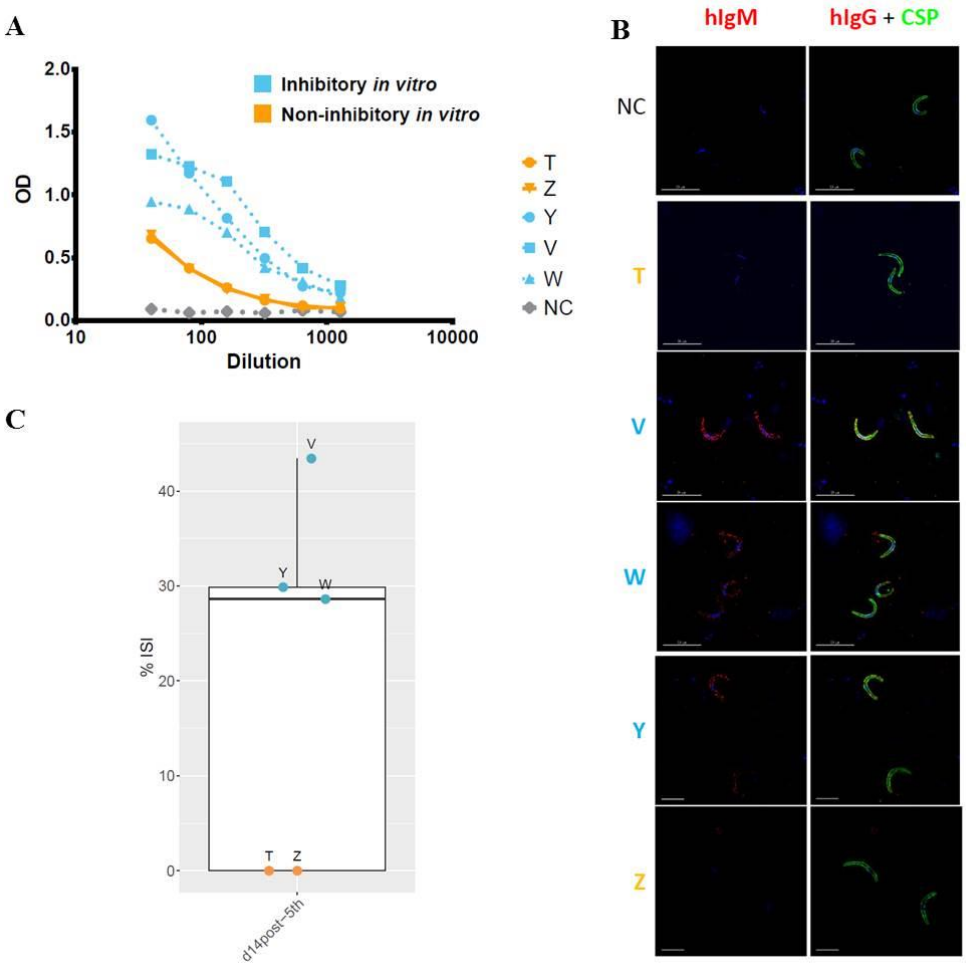

Figure 4 Vacine-induced anti-CSP IgM antibodies bind to whole sporozoites and inhibit sporozoite invasion *in vitro*. Plasma from a subset of volunteers (n=5) collected at 14 days post-5th immunization was depleted of IgG and IgA antibodies to generate IgM antibody fractions. Each individual volunteer is indicated with a different letter (T, V, W, Y, Z). IgM fraction of volunteers which were inhibitory in ISI are indicated in blue while those which were not are in orange. IgM fraction from a pre-immune pool was used as a negative control and is indicated as NC. **A)** IgM fractions were used in ELISA with full length PfCSP at indicated dilutions. Anti-human IgM secondary was used to detect anti-CSP IgM with indicated OD at 405nm. **B)** IgM fractions were applied to fixed, permeabilized whole sporozites and IgM binding detected in IFA by staining with anti-human IgM AlexaFluor594 (red) and anti-CSP monoclonal antibody 2A10 conjugated to AlexaFluor488 (green). Each panel represents an individual volunteer indicated in different letters (n = 5) with each image captured under the same exposure conditions with identical modifications. **C)** IgM fractions were tested in ISI at a ~1:20 dilution from original plasma. Percent ISI as normalized to pre-immune pooled IgM fractions are displayed at time-point 14 days post-5th immunization. Each data point and letter represents a volunteer's mean value across 2 independent experiments. IgM fractions from volunteers W, Y and V showed ISI activity between 28% to 43%.

3.5 Discussion

We demonstrate here that malaria pre-exposed adult volunteers develop antibodies that *ex vivo* inhibit sporozoite invasion following intravenous immunization with PfSPZ Vaccine (Figure 1). At baseline (Supplementary Figure 2) and in placebo controls (Figure 1C), inhibitory antibody activity was not observed strongly supporting the conclusion that we measured PfSPZ Vaccine-induced parasite inhibitory antibodies. Lack of ISI activity at baseline is in concordance with previous field studies demonstrating inefficient acquisition of pre-erythrocytic stage specific humoral immune responses [10, 11]. From our data, the invasion inhibition activity of serum samples does not seem to correlate with PfSPZ Vaccine dosing as similar results were obtained from the low and high-dose group (Figure 1).

CSP is the most immunodominant antigen expressed on the sporozoite surface [16] and therefore we analyzed if anti-CSP IgG and IgM isotypes are detected in serum after PfSPZ vaccination. Two weeks past 5th vaccination, in 17 of 19 immunized volunteers anti-CSP IgM antibodies were observed with all immunized volunteers mounted anti-CSP IgG antibodies (Figure 2A, 2B). Most importantly, we demonstrate that in three volunteers, these anti-CSP IgM antibodies mediate ISI activity in plasma fractions after IgG and IgA depletion. To our knowledge, this is the first demonstration of PfSPZ Vaccine-induced *in vitro* liver cell sporozoite inhibition mediated by enriched IgM preparations. We did not find correlations between anti-CSP IgG or IgM titers and ISI activities (Figure 3A, 3B). One possible explanation could be that antibodies targeting antigens other than CSP are involved in ISI outcomes [17].

Vaccine-induced IgM antibodies have been regarded in the past as short-lived and less affinity-matured compared to IgG antibodies [18]. Therefore, investigation of whole sporozoite vaccine-induced humoral immunity focused on IgG isotypes in malaria-exposed and malaria-naïve populations [5, 9, 19]. Sporozoite binding IgG antibodies have been proposed as correlate of protection in whole irradiation-attenuated sporozoite immunized volunteers [5, 20] and in GAP vaccinated volunteers using passive transfer experiments in FRG mice (Sack et al., npj Vaccines in press).

In RAS immunized mice, IgM antibodies were described as binding to live sporozoites and limiting parasite liver infection by 74% in passive transfer experiments [21]. IgM antibodies cross-reacting with glycoproteins on the sporozoite surface were shown to inhibit parasite infection of hepatocytes *in vivo* and *in vitro* [22]. In the latter example, these antibodies

appeared to function largely through FC-dependent effectors and complement fixation with recruitment of polymorph nuclear cells [22]. Long-lived, somatically hyper-mutated IgM memory B cells can contribute to protection from asexual blood stage infection in mice [23]. Plasma cells secreting IgM antibodies that are somatically hyper-mutated and that reside in the spleen have been detected during vaccination and influenza virus and lymphocytic choriomeningitis virus infections [24].

The PfSPZ Vaccine is given intravenously using exceedingly high sporozoite dosing when compared to natural infection by mosquito bites. It could be assumed that a considerable fraction of injected sporozoites are drained into the spleen and get into contact with macrophages, dendritic cells, neutrophiles and marginal zone (MZ) B cells [25]. MZ B cells are a human B cell subset located in the marginal zones of human spleens [25]. They are defined based on their $IgM^{hi}IgD^{low}CD1c^{+}CD21hiCD23^{-}CD27^{+}$ marker expression [26–28]. MZ B cells have been commonly regarded as front-line sentinels involved in induction of rapid, T cell independent innate-like antibody responses at the host-environmental interface. However, some MZ B cells express somatically mutated V(D)J genes, are dependent on T cell interaction, toll-like receptor co-stimulation and some show past germinal center experience. These B cells could be regarded as memory B cells that have retained IgM and IgD expression [25]. We hypothesize that a subset of MZ B cells could constitute the source of PfSPZ Vaccine-induced long-lived and functionally active anti-CSP IgM antibodies.

Our data suggest that sporozoite binding and invasion inhibitory IgM could contribute to protection against malaria infection. IgM antibodies are excellent in fixing complement which could either eliminate circulating sporozoites by formation of the membrane attack complex leading to parasite lysis, or by C3a formation and recruitment of mononuclear cells (phagocytosis). Complement-mediated lysis has been demonstrated for asexual blood stage merozoite in humans [29, 30]. However, similar evidence is yet lacking for sporozoites but is conceivable as sporozoites could encounter IgM and complement during their journey from the skin to the liver parenchym. It will be interesting to determine if IgM antibodies such as those elicited in our vaccine trial are capable of fixing complement upon sporozoite binding *in vitro*.

3.6 Conclusions

In conclusion, our data show that immunization of malaria pre-exposed volunteers with PfSPZ Vaccine elicits functional, sporozoite invasion inhibitory antibodies. In volunteers that mounted higher titers of anti-CSP IgM antibodies, this sporozoite inhibition could be partially attributed to IgM. Immunological assessment of mode of action of PfSPZ vaccine-induced humoral effector mechanisms should therefore include monitoring of parasite-specific IgG and IgM antibodies. Future studies need to expand on our findings and address if (i) parasite-inhibitory IgM production is related to PfSPZ vaccine delivery route and dosing, (ii) PfSPZ vaccine-induced IgM responses are unique to malaria pre-exposed individuals and (iii) the sporozoite binding IgM antibody repertoire undergoes affinity maturation resulting in improved effector function over repeated vaccinations.

3.7 Abbreviations

AU: Arbitrary units **BCTU:** Bagamoyo Clinical Trial Unit **BSA:** Bovine serum albumin **CHMI:** Controlled human malaria infection **CSP:** Circumsporozoite protein **CV:** Coefficient of variation **CVac:** Chemoprophylaxis Vaccination **DVI:** Direct venous inoculation ELISA: Enzyme-linked immunosorbent assay **EKNZ:** Ethikkommission Basel **FBS:** Fetal bovine serum **HRP:** Horseradish peroxidase **IFA:** Immunofluoresence Assay **IHI:** Ifakara Health Institute **IRBs:** Institutional review boards ISI Inhibition of sporozoite invasion assay **IQR:** Interquartile range **mAB:** Monoclonal antibody **MZ B cells**: Marginal zone B cells **NIMR:** National Institute for Medical Research Tanzania **PBMCs:** Peripheral blood mononuclear cells: **PBS:** Phosphate buffer saline **PFA:** Paraformaldehyde **Pf:** *Plasmodium falciparum* **PfSPZ:** *Plasmodium falciparum* sporozoites **RAS:** Radiation attenuation sporozoites **RT:** Room temperature **TFDA:** Tanzania Food and Drug Authority **WHO:** World Health Organization

3.8 Supplementary Figures

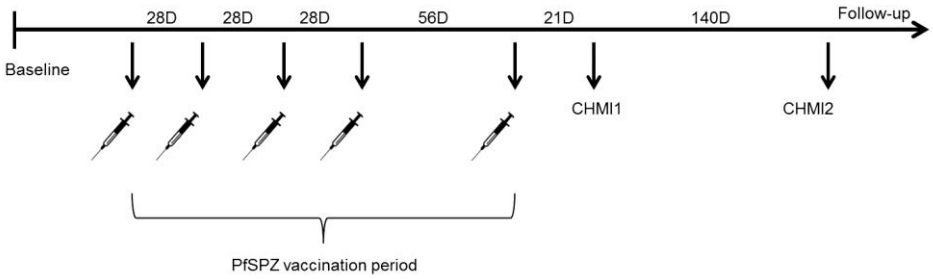

Supplementary Figure 1 Vaccination schedule. Volunteers were immunized with the PfSPZ Vaccine at monthly intervals between the 1st and 4th immunization and 56 days between the 4th and 5th immunization. 21 days after the last immunization, volunteers were challenged for the first time with non-irradiated PfSPZ of PfSPZ challenge (CHMI1). Protected volunteers after the first challenge, were re-challenged (CHMI2) at 140 days post-CHMI1. D indicates the number of days between the vaccination- and CHMI visits.

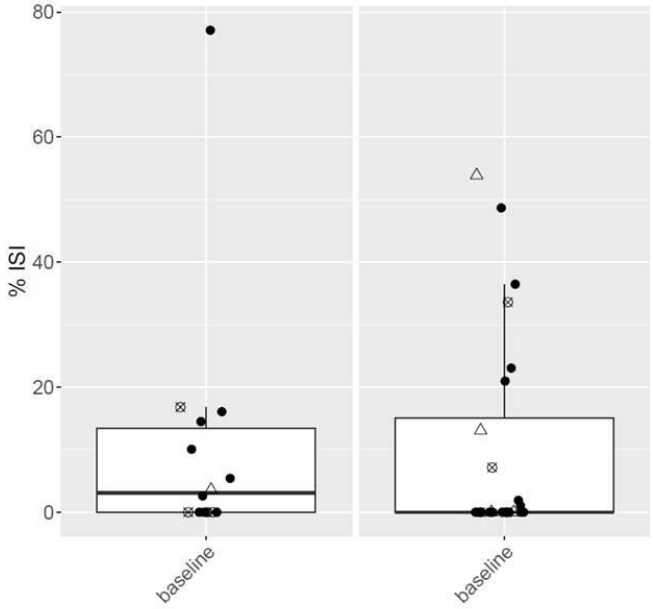

Supplementary Figure 2 No pre-existing inhibitory antibodies in the majority of malaria pre-exposed Tanzanian volunteers prior to immunization with the PfSPZ Vaccine. Percentage ISI of HC04 cells by Pf sporozoites obtained from serum collected from volunteers from the low- and high-dose group measured at baseline visit, before active immunization with the PfSPZ Vaccine. Control volunteers are shown as crossed circles, immunized unprotected as solid circles and immunized protected as empty triangles.

3.9 References

1. World Malaria Report 2016 - 9789241511711-eng.pdf. http://apps.who.int/iris/bitstream/10665/252038/1/9789241511711-eng.pdf?ua=1. Accessed 8 May 2017.

2. Olotu A, Fegan G, Wambua J, Nyangweso G, Leach A, Lievens M, et al. Seven-Year Efficacy of RTS,S/AS01 Malaria Vaccine among Young African Children. N Engl J Med. 2016;374:2519–29.

3. RTS SCTP, Agnandji ST, Lell B, Fernandes JF, Abossolo BP, Methogo BG, et al. A Phase 3 Trial of RTS,S/AS01 Malaria Vaccine in African Infants. N Engl J Med. 2012;367:2284–95.

4. Clyde DF, McCarthy VC, Miller RM, Hornick RB. Specificity of protection of man immunized against sporozoite-induced falciparum malaria. Am J Med Sci. 1973;266:398–403.

5. Seder RA, Chang L-J, Enama ME, Zephir KL, Sarwar UN, Gordon IJ, et al. Protection against malaria by intravenous immunization with a nonreplicating sporozoite vaccine. Science. 2013;341:1359–65.

6. Roestenberg M, McCall M, Hopman J, Wiersma J, Luty AJF, van Gemert GJ, et al. Protection against a malaria challenge by sporozoite inoculation. N Engl J Med. 2009;361:468–77.

7. Roestenberg M, Teirlinck AC, McCall MBB, Teelen K, Makamdop KN, Wiersma J, et al. Long-term protection against malaria after experimental sporozoite inoculation: an open-label follow-up study. Lancet Lond Engl. 2011;377:1770–6.

8. Mordmüller B, Surat G, Lagler H, Chakravarty S, Ishizuka AS, Lalremruata A, et al. Sterile protection against human malaria by chemoattenuated PfSPZ vaccine. Nature. 2017;542:445–9.

9. Kublin JG, Mikolajczak SA, Sack BK, Fishbaugher ME, Seilie A, Shelton L, et al. Complete attenuation of genetically engineered Plasmodium falciparum sporozoites in human subjects. Sci Transl Med. 2017;9:eaad9099.

10. Portugal S, Pierce SK, Crompton PD. Young lives lost as B cells falter: what we are learning about antibody responses in malaria. J Immunol Baltim Md 1950. 2013;190:3039–46.

11. Ryg-Cornejo V, Ly A, Hansen DS. Immunological processes underlying the slow acquisition of humoral immunity to malaria. Parasitology. 2016;143:199–207.

12. Keitany GJ, Kim KS, Krishnamurty AT, Hondowicz BD, Hahn WO, Dambrauskas N, et al. Blood Stage Malaria Disrupts Humoral Immunity to the Pre-erythrocytic Stage Circumsporozoite Protein. Cell Rep. 2016;17:3193–205.

13. Greenwood B. Progress with the PfSPZ Vaccine for malaria. Lancet Infect Dis. 2017;17:463–4.

14. Kaushansky A, Rezakhani N, Mann H, Kappe SHI. Development of a quantitative flow cytometry-based assay to assess infection by Plasmodium falciparum sporozoites. Mol Biochem Parasitol. 2012;183:100–3.

15. Kennedy M, Fishbaugher ME, Vaughan AM, Patrapuvich R, Boonhok R, Yimamnuaychok N, et al. A rapid and scalable density gradient purification method for Plasmodium sporozoites. Malar J. 2012;11:421.

16. Plassmeyer ML, Reiter K, Shimp RL, Kotova S, Smith PD, Hurt DE, et al. Structure of the Plasmodium falciparum circumsporozoite protein, a leading malaria vaccine candidate. J Biol Chem. 2009;284:26951–63.

17. Trieu A, Kayala MA, Burk C, Molina DM, Freilich DA, Richie TL, et al. Sterile protective immunity to malaria is associated with a panel of novel P. falciparum antigens. Mol Cell Proteomics MCP. 2011;10:M111.007948.

18. Seifert M, Przekopowitz M, Taudien S, Lollies A, Ronge V, Drees B, et al. Functional capacities of human IgM memory B cells in early inflammatory responses and secondary germinal center reactions. Proc Natl Acad Sci U S A. 2015;112:E546-555.

19. Sissoko MS, Healy SA, Katile A, Omaswa F, Zaidi I, Gabriel EE, et al. Safety and efficacy of PfSPZ Vaccine against Plasmodium falciparum via direct venous inoculation in healthy malaria-exposed adults in Mali: a randomised, double-blind phase 1 trial. Lancet Infect Dis. 2017;0. doi:10.1016/S1473-3099(17)30104-4.

20. Ishizuka AS, Lyke KE, DeZure A, Berry AA, Richie TL, Mendoza FH, et al. Protection against malaria at 1 year and immune correlates following PfSPZ vaccination. Nat Med. 2016;22:614–23.

21. Kumar KA, Sano G, Boscardin S, Nussenzweig RS, Nussenzweig MC, Zavala F, et al. The circumsporozoite protein is an immunodominant protective antigen in irradiated sporozoites. Nature. 2006;444:937–40.

22. Yilmaz B, Portugal S, Tran TM, Gozzelino R, Ramos S, Gomes J, et al. Gut microbiota elicits a protective immune response against malaria transmission. Cell. 2014;159:1277–89.

23. Krishnamurty AT, Thouvenel CD, Portugal S, Keitany GJ, Kim KS, Holder A, et al. Somatically Hypermutated Plasmodium-Specific IgM(+) Memory B Cells Are Rapid, Plastic, Early Responders upon Malaria Rechallenge. Immunity. 2016;45:402–14.

24. Bohannon C, Powers R, Satyabhama L, Cui A, Tipton C, Michaeli M, et al. Long-lived antigen-induced IgM plasma cells demonstrate somatic mutations and contribute to long-term protection. Nat Commun. 2016;7. doi:10.1038/ncomms11826.

25. Cerutti A, Cols M, Puga I. Marginal zone B cells: virtues of innatelike antibody-producing lymphocytes. Nat Rev Immunol. 2013;13:118–32.

26. Martin F, Kearney JF. Marginal-zone B cells. Nat Rev Immunol. 2002;2:323–35.

27. Weill J-C, Weller S, Reynaud C-A. Human marginal zone B cells. Annu Rev Immunol. 2009;27:267–85.

28. Pillai S, Cariappa A. The follicular versus marginal zone B lymphocyte cell fate decision. Nat Rev Immunol. 2009;9:767–77.

29. Sack BK, Keitany GJ, Vaughan AM, Miller JL, Wang R, Kappe SHI. Mechanisms of stage-transcending protection following immunization of mice with late liver stage-arresting genetically attenuated malaria parasites. PLoS Pathog. 2015;11:e1004855.

30. Boyle MJ, Reiling L, Feng G, Langer C, Osier FH, Aspeling-Jones H, et al. Human antibodies fix complement to inhibit Plasmodium falciparum invasion of erythrocytes and are associated with protection against malaria. Immunity. 2015;42:580–90.

Chapter 4

CSP-specific human monoclonal antibodies inhibiting *Plasmodium falciparum* liver stage infection target a distinct sequence at the N-terminus

Isabelle Zenklusen[*], Joshua Tan[*], Brandon Sack[*], Luca Piccoli, Sonia Barbieri, Chiara Silacci Fregni, Said Jongo, Salim Abdulla, Stefan Kappe, Stephen L. Hoffman, Claudia Daubenberger[*] and Antonio Lanzavecchia[*]. CSP-specific human monoclonal antibodies inhibiting *Plasmodium falciparum* liver stage infection target a distinct sequence at the N-terminus. *Working manuscript*.

CSP-specific human monoclonal antibodies inhibiting *Plasmodium falciparum* liver stage infection target a distinct sequence at the N-terminus

Isabelle Zenklusen[3,4]*, Joshua Tan[1,2]*, Brandon Sack[5]*, Luca Piccoli[1], Sonia Barbieri[1], Chiara Silacci Fregni[1], Said Jongo[6], Salim Abdulla[6], Stefan Kappe[5,8], Stephen L. Hoffman[7], Claudia Daubenberger[3,4*] and Antonio Lanzavecchia[1*]

[1]Institute for Research in Biomedicine, Università della Svizzera Italiana, Via Vincenzo Vela 6, 6500 Bellinzona, Switzerland

[2]University of Oxford, John Radcliffe Hospital, Radcliffe Department of Medicine, Headington, Oxford, OX3 9DU, UK

[3]Swiss Tropical and Public Health Institute, Clinical Immunology Unit, CH 4051 Basel, Switzerland

[4]University of Basel, 4001 Basel, Switzerland

[5]Center for Infectious Disease Research, Seattle, WA 98109, USA

[6]Ifakara Health Institute, Clinical Trial Unit, Bagamoyo, Tanzania

[7]Sanaria Inc., Rockville, MD 20850, USA

[8]University of Washington, Department of Global Health Seattle, WA 98195, USA

*These authors contributed equally to this work

4.1 Abstract

The immunization with radiation-attenuated whole *Plasmodium falciparum* (Pf) sporozoites mediates sterilizing immunity in malaria-naïve volunteers, but the protective role of antibodies induced by this vaccination approach remains to be elucidated. To investigate this, we isolated a panel of monoclonal antibodies from individuals living in malaria-endemic Tanzania, who received active immunization with whole, radiation-attenuated sporozoites (Sanaria® PfSPZ Vaccine), and who were subsequently found to be protected against homologous sporozoite challenge. Using an antigen-agnostic approach to identify any antibodies that can bind to the surface of intact sporozoites, we found that all of the isolated antibodies targeted the circumsporozoite protein, confirming its known immunodominance. Characterization of these antibodies using epitope mapping and *in vitro* and *in vivo* functional assays revealed a few antibodies with distinct binding properties that were very potent in reducing liver burden in an *in vivo* human-liver chimeric mouse model of Pf sporozoite invasion. Overall, these findings identified and characterized human monoclonal antibodies that show potent inhibition of sporozoite invasion in an *in vivo* model and reveal an epitope that is not in the current leading malaria vaccine canidate of RTS, S but that appears to be a target of antibodies in protected individuals immunized with the PfSPZ Vaccine.

4.2 Introduction

Malaria is a mosquito-borne disease caused by *Plasmodium* parasites. In 2016, the World Health Organization (WHO) estimated approximately 212 million malaria cases and 429,000 malaria-related deaths globally [1]. The life cycle of *Plasmodium falciparum* (*P. falciparum*) is complex and starts with the injection of sporozoites by infected mosquito in the skin, which then progress through the blood circulation to the liver, where the sporozoites begin to traverse and infect hepatocytes [2]. Inside the hepatocyte, the sporozoites start to replicate and further develop into merozoites, which are released in the blood initiating the development of disease-causing asexual blood-stage parasites [2]. There is currently no protective malaria vaccine available [3]. The most clinically advanced malaria vaccine candidate, the circumsporozoite (CSP) protein-based RTS, S subunit vaccine, showed only partial and short-term efficacy in malaria-endemic populations [4]. To date, the only experimental vaccination approach which has ever achieved complete sterile protection in humans is the immunization with whole-attenuated sporozoites [5–9]. Immunologic correlates of protection against pre-erythrocytic stage infection in humans remain to be investigated [10, 11]. Findings from animal studies in mice and non-human primates (NHPs) suggest that sterile protection relies on a combination of cellular and humoral immune responses. Hepatic alpha beta CD8+ T cells that secrete interferon-γ upon recognition of infected liver cells result in killing of the parasite inside the hepatocytes. Antibodies bind and block sporozoites in the skin and inhibit their traversal and inhibition in the liver [4, 9, 10, 12–14]. It has been demonstrated that immunization with whole-attenuated sporozoites can induce functional antibodies that inhibit sporozoite invasion *in vitro* and in *in vivo* models in mice [11, 15–17]. Nonetheless, contribution to protection in vaccinated humans is unclear and antigens recognized by sporozoite inhibiting antibodies are incompletely known [18]. To better understand the repertoire and targets of sporozoite binding antibodies in humans inoculated intravenously with high numbers of purified sporozoites, we have isolated a panel of sporozoite-specific human monoclonal antibodies in this study. The donors were residing in a malaria-endemic area of Tanzania and received active immunization of 5 doses of 1.35×10^5 or 2.7×10^5 aseptic, purified, radiation-attenuated, whole *P. falciparum* sporozoites (PfSPZ Vaccine). Three weeks and after last vaccination, these volunteers underwent homologous controlled human malaria infection (CHMI) and were found to be sterile protected (Jongo et al.,

manuscript submitted). We characterized the biological function of these antibodies by using *in vitro* and *in vivo* sporozoite infection models of Pf in human liver cells [16].

4.3 Results

4.3.1 Serological screen of IgG and IgM antibodies against whole sporozoites

We developed a flow cytometry-based screening assay that allows detection of serum antibodies binding to whole intact sporozoites in vaccinees and placebo controls. IgG and IgM titers against whole sporozoites were measured at time-points before immunization (baseline), two weeks after last vaccination (2w post-vaccination) and 4 and 20 weeks after homologous CHMI Challenge (Supplementary Figure 1). The results of immunized donors showed that IgG and IgM titers are low at baseline and increase significantly after vaccination. There is no boost of IgG and IgM antibodies induced at 4 weeks after CHMI compared to titers measured at 2 weeks after last vaccination (Supplementary Figure 1). Antibody titers, especially IgG, of immunized volunteers measured at 20 weeks after CHMI, remain sustained above baseline level. No clear differences between protected and non-protected volunteers were observed. In contrast, antibody titers of placebo controls were low at all time-points, except for titers measured at 4 weeks after challenge, where titers increased. In conclusion, these results indicate that immunization with the PfSPZ Vaccine boosts sporozoite-specific IgG and IgM antibodies in Tanzanian adults after vaccination and IgG and IgM antibody titers remain sustained above background levels at 20 weeks after CHMI. Furthermore, there was no boost in the antibody responses observed in the vaccine recipients 4 weeks after challenge compared to the titers measured 2 weeks after the vaccination.

4.3.2 Isolation of anti-sporozoite monoclonal antibodies

Next, we immortalized IgG^+ memory B cells [19] from five CHMI protected donors (U, G, V, H and W). IgG^+ memory B cells were isolated from PBMC, sorted by flow cytometry and subsequently immortalized with Epstein-Barr virus and a TLR agonist using established protocols [19, 20] (Figure 1). Two weeks after immortalization, B cell supernatants from immortalized IgG^+ memory cells were screened for their capacity to bind intact sporozoites by flow cytometry. Positive B cell clones were selected for isolation of mRNA, sequencing of heavy and light chain variable regions (VH and VL), and recombinant IgG^+ monoclonal

antibody production [21]. Staining of whole intact sporozoites of a subset of produced recombinant IgG^+ monoclonal antibodies (mABs) by flow cytometry are shown in Supplementary Figure 2. Using this approach, we have isolated a panel of sporozoite-specific IgG^+ mABs from five Tanzanian donors who have been immunized with the PfSPZ Vaccine and were protected against homologous CHMI.

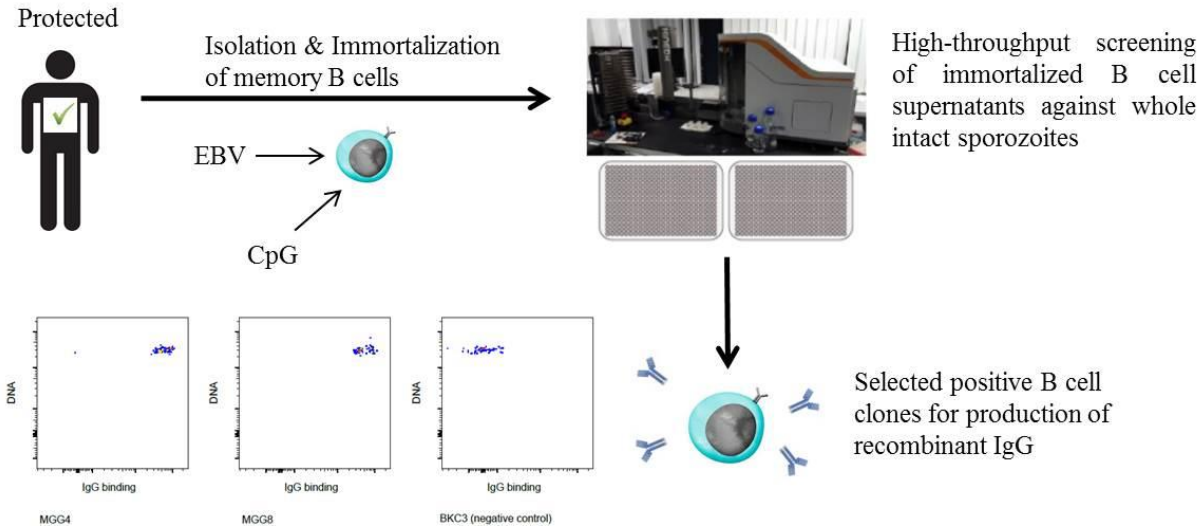

Figure 1 Workflow of sporozoite-specific monoclonal antibody isolation from protected PfSPZ Vaccine-immunized Tanzanian donors using a high-throughput screening system.

4.3.3 All monoclonal antibodies target the circumsporozoite protein

After successful production of IgG^+ mABs, we wanted to test if the mABs target the *P. falciparum* circumsporozoite protein (PfCSP). PfCSP is the predominant sporozoite surface antigen [22]. Therefore an enzyme-linked immunosorbent assay (ELISA) against full length recombinant PfCSP protein was performed (data not shown). A schematic representation of the full length PfCSP protein is given in Figure 3A. The ELISA results revealed that all isolated monoclonal antibodies target the PfCSP protein.

4.3.4 *In vitro* sporozoite-blocking activity of monoclonal antibodies

To assess the functional capacity of the anti-CSP mABs in relation to inhibition of sporozoite infection of human hepatocytes (HC-04 cells) *in vitro*, a flow cytometry-based inhibition of sporozoite traversal and invasion assay (ISTI) was performed [17, 23]. Each anti-CSP

antibody was mixed with *P. falciparum* sporozoites in the presence of FITC-dextran and then used for infection of HC-04 cells. Monoclonal antibody 2A10 served as positive control in our ISTI assays [23]. This antibody targets the NANP repeats of CSP and is known to inhibit sporozoite invasion and traversal at approximately 80% and 50%, respectively. Traversed HC-04 cells, wounded by sporozoite invasion and egress and therefore allowing dextran uptake, were identified as dextran-positive cells. Sporozoite invasion of HC-04 cells was monitored by gating CSP- positive hepatocytes using a fluorescently-conjugated anti-CSP mAb [17, 23].

ISTI activity of a panel of anti-CSP antibodies from donors G, H, U and V were tested and are presented in Figure 2A. All anti-CSP antibodies showed ISTI activity with mAB MGG4, MGH1, MGH2 and MGH3 displaying the strongest sporozoite inhibition in both assays (Figure 2A).

4.3.5 *In vivo* functional activity of anti-CSP monoclonal antibodies

To investigate the *in vivo* blocking activity of the monoclonal antibodies, MGG4, MGG8, MGG3, MGH1, MGH2 and MGH3, we used a human liver-chimeric mouse model (FRG huHep) in combination with luciferase-expressing *P. falciparum* sporozoites [16, 24, 25]. FRG huHep mice consist of engrafted human hepatocytes and lack mouse B cells, T cells and natural killer cells. This mouse model has proven to allow complete liver-stage development of *P. falciparum* parasites and to distinguish in vivo antibody function [25]. Our collection of mABs were passively transferred into four FRG mice per antibody at a concentration of 150µg/mouse. *P. falciparum* liver stage burden of mice was measured by an *in vivo* imaging system at the peak of liver burden six days after mosquito-bite challenge with malaria parasites [16, 26]. The anti-CSP repeat monoclonal antibody 2A10 was used as a positive control and as a negative control non-specific IgG was used. Reduction of the liver stage burden induced by anti-CSP mAB is summarized in Figure 2B. Out of the six antibodies tested, mAB MGG4, MGH2 and MGG3 showed the strongest reduction of liver burden to less than 6% (Figure 2B).

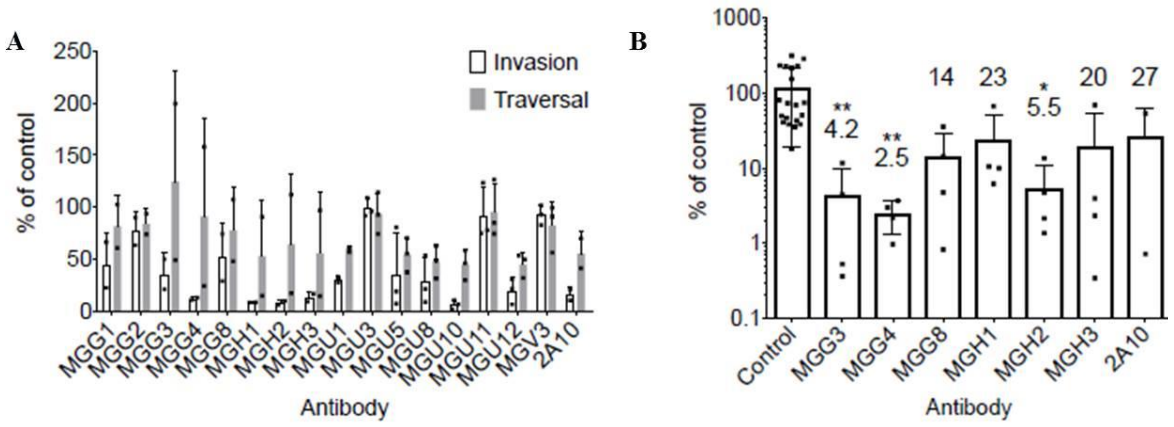

Figure 2 Functional assessment of sporozoite-blocking activity of isolated anti-CSP monoclonal antibodies. A) Anti-CSP monoclonal antibodies isolated from four protected immunized donors (G, H, U, V) were evaluated for *in vitro* inhibition of sporozoite traversal and invasion (ISTI) of HC04 hepatocytes. The ISTI activity of each anti-CSP antibody was normalized to a negative control of non-specific human IgG. Percent of inhibition of invasion are indicated in empty bars and percent of inhibition of traversal are shown in gray bars. The anti-CSP repeat antibody 2A10 was used as a positive control. **B)** Anti-CSP antibodies MGG3, MGG4, MGG8, MGH1, MGH2 and MGH3 were selected for passive transfer into FRG huHep mice to assess *in vivo* reduction of liver-stage Pf parasites. Liver-stage burden was assessed by bioluminescent imaging six days after mosquito bite challenge with infected luciferase-expressing *P. falciparum* sporozoites. Each data point in the graph represents one mouse. The y-axis shows the parasite liver burden as a percent of the average of control mice given non-specific IgG. Each anti-CSP antibody tested is indicated on the x-axis. Anti-CSP antibodies MGG4, MGH2 and MGG3 reduced liver burden to less than 6%.

4.3.6 Potent parasite inhibitory monoclonal antibodies target a distinct peptide at the N-terminal end and the NANP repeat, which is not included in the RTS, S vaccine

To identify further the target structure of our collection of mABs, we performed ELISA with three synthetic peptides representing different parts of CSP and full length recombinant CSP protein (Figure 3A). Peptide 22-110 encompasses the N-terminal region and Region I of CSP, Peptide NANP10 consists of 10 consecutive NANP repeat sequences and the 18-mer peptide with the sequence KQPADGNPDPNANPNKNN covers the junction between the N-terminal end and the NANP repeat region of PfCSP. The ELISA results demonstrated that all mABs bound to full length CSP. Monoclonal antibodies MGG4, MGH2 and MGG3, which were

most potent in the *in vivo* model, showed strong binding to the 18-mer peptide and the NANP repeats (Figure 3B).

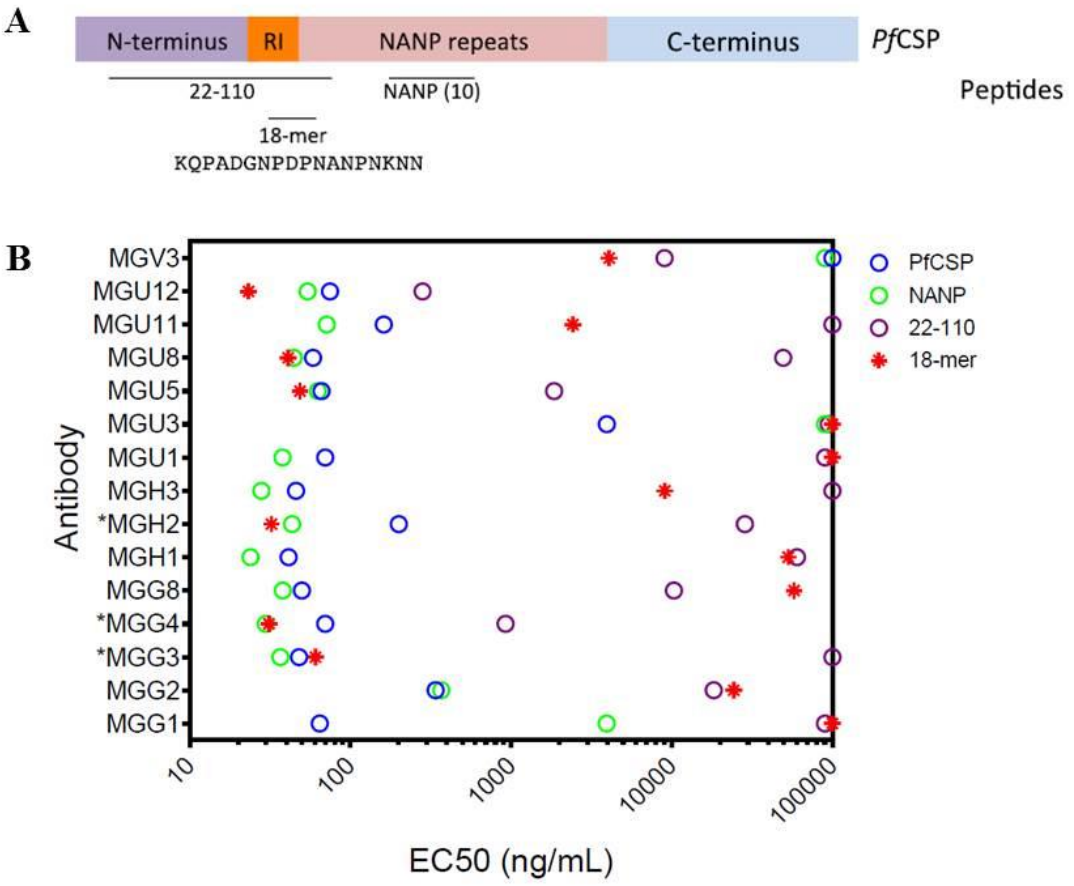

Figure 3: The most potent anti-CSP antibodies show strong binding to the 18-mer peptide. **A)** Schematic representation of the PfCSP protein showing the different peptides used in the ELISA screen of the monoclonal antibodies. **B)** EC50 values of different monolconal antibodies from 4 donors (G, H, U, V) to full length PfCSP and to peptides shown in different symbols on the legend to the right of the plot. The monoclonal antibodies that were most potent in the *in vivo* model, MGG3, MGG4 and MGH2 are marked by black asterisks and show strong binding to the 18-mer peptide (KQPADGNPDPNANPNKNN) and the NANP repeats.

4.4 Discussion

We have isolated a panel of sporozoite binding mABs from five Tanzanian adults who were immunized with aseptic, purified, radiation-attenuated, whole *P. falciparum* sporozoites (Sanaria® PfSPZ Vaccine) and showed sterile protection against homologous challenge three weeks post last vaccination. All mABs target the PfCSP protein, the major surface antigen expressed on sporozoites. Strikingly, the anti-CSP monoclonal antibodies which were most potent in reducing the liver stage burden *in vivo* (Figure 2B) showed strong binding to an 18-mer peptide sequence (KQPADGNPDPNANPNKNN) located at the junction between the N-terminal end and the NANP repeat region (Figure 3B). Interestingly, this peptide is not included in the most advanced malaria subunit vaccine, RTS, S vaccine, which consists of a fusion protein of hepatitis B and 16 NANP repeats and the entire C-terminus [27]. The N-terminus of PfCSP has been described as functionally relevant in the process of sporozoite attachment and invasion into liver cells [22, 27–29]. Moreover, the 18-mer peptide also includes three amino acids of the highly conserved region I (RI) (Figure 3A), which has been reported to contain the CSP cleavage site essential for rapid CSP processing shown to be critical for sporozoite entry into hepatocytes [22, 29]. Our functional data strongly suggest that antibodies targeting a region between a CSP-N-terminal peptide (KQPADGNPDPNANPNKNN) and NANP could be highly potent in blocking sporozoite infection. Previous studies in mice have shown that immunization with peptides located at the PfCSP N-terminus can induce invasion-inhibiting antibodies [30]. In field studies conducted in children living in malaria-endemic regions of Tanzania, a correlation between the presence of antibodies targeting the PfCSP N-terminus with protection from clinical malaria was observed [31]. Our approach of studying vaccine-induced sporozoite binding humoral immunity at the single cell level from Tanzanian donors has the power to identify rare B cell clones that produce highly effective parasite inhibitory antibodies.

Taken together, we developed for the first time PfCSP-specific mABs from African donors, who received active immunization of the PfSPZ Vaccine. The mAbs with strongest parasite growth inhibition in a humanized mouse model target a distinct peptide located at the N-terminal end of PfCSP and the first NANP repeat. The target recognized by these mABs might support a second generation of PfCSP subunit vaccines against the most deadly malaria species [20].

4.5 Acknowledgements

We thank Sanaria Inc. for providing *P. falciparum* sporozoites (PfSPZ). This work was supported by a grant from the Swiss Vaccine Research Institute and the Swiss Tropical and Public Health Institute.

4.6 Contributors

J.T & I.Z performed experiments involving flow cytometry based screening against whole intact sporozoites, J.T and L.P characterized antibodies and performed CSP ELISA, J.T, I.Z & B.S analyzed the data, D.J performed cell sorting, C.S.F performed B cell immortalization; I.Z & S.J managed and provided clinical sample collection and information, S.B produced antibodies, B.S & I.Z performed functional assays, I.Z wrote this current manuscript and J.T & CDA reviewed it. A.L and CDA provided supervision of the whole project.

4.7 Material and Methods

4.7.1 Clinical trial and donors

All samples used in this study were collected from malaria pre-exposed volunteers during a clinical phase I trial on the safety, immunogenicity and protective efficacy of the Sanaria® PfSPZ Vaccine in Bagamoyo, Tanzania between 2014 and 2015. The protocol was approved by the Tanzanian Food and Drug Authority (TFDA) (Ref. No TFDA 13/CTR/0003) and the trial was registered at Clinical Trial.gov (NCT02132299) and conducted under U.S. FDA IND 14826. Detailed information on the study procedures and the volunteers enrolled are described elsewhere (Jongo et al., manuscript submitted). Briefly, healthy male volunteers aged 20 to 30 years were randomized to direct venous inoculation of 5 doses of normal saline or 1.35×10^5 or 2.7×10^5 of the Sanaria® PfSPZ Vaccine. Vaccine efficacy was evaluated by homologous controlled human malaria infection (CHMI) by direct venous inoculation of 3,200 infectious *P. falciparum* sporozoites at 3 and 24 weeks after the last immunization. The PfSPZ Vaccine proved to be safe and well tolerated in all Tanzanian volunteers. In the low-dose group,1 of 18 (6%) volunteer was protected against CHMI at 3 weeks and in the high-

dose group, 4 of 20 (20%) volunteers were protected at 3 and 24 weeks after the last vaccination.

4.7.2 Sample collection and preparation

For serum preparation, whole blood was collected in vacutainer tubes containing clot activators (Becton, Dickison, 369032) and kept at RT until a clot was formed. Then the tube was centrifuged at 2000g for 10 minutes at 22°C and the serum fraction was collected in cryogenic vials and stored at -80°C.

Peripheral blood mononuclear cells (PBMCs) were isolated from whole blood by Ficoll density gradient centrifugation. Whole blood was collected with a syringe containing EDTA-Na_2 as anti-coagulant and subsequently diluted with the same volume of 1 X PBS in order to facilitate the separation process. The anti-coagulated blood was poured into LeucosepTM tubes (227 789 or 227 290) prefilled with Ficoll Paque separation medium (Ficoll Paque Premium GE17-5442-03) and centrifuged at 800 x g for 15 minutes at RT (20-22°C) with acceleration and brake set to 0. After centrifugation, the layer of PBMCs was collected and transferred to a separate tube containing wash buffer (1X PBS/2% FCS). The PBMC fraction was washed twice at 250 x g for 10 minutes at RT (20-22°C). After washing, the PBMC cell pellet was resuspended in freezing medium (10%DMSO/90%FCS) and stored in Mr. Frosties at -80°C overnight and on the day after transferred to liquid nitrogen for long-term storage.

4.7.3 Evaluation of serum IgG and IgM antibodies against whole intact sporozoites by flow cytometry

Binding of IgG and IgM serum antibodies to intact sporozoites was analyzed by flow cytometry. Aseptic, purified, cryopreserved PfSPZ from Sanaria were labeled with 6.7× SYBR Green I (ThermoFisher Scientific) and incubated with each of the serum samples at a 12-point 2-fold serial dilution (6000PfSPZ per sample) for 20 minutes at RT. The PfSPZ were washed twice by centrifugation at 4,000 rpm for 5 minutes, split into two, and then stained with 2.5 µg/mL of Alexa Fluor 647-conjugated goat anti-human IgG or Alexa Fluor 647-conjugated goat anti-human IgM (Jackson ImmunoResearch) for 1 h at 4°C. After incubation, the sporozoites were washed twice and the samples were analyzed by flow cytometry. The PfSPZ were gated based on high SYBR Green I and low forward scatter, and binding of IgG

or IgM antibodies was calculated based on the mean fluorescence intensity (MFI) of the PfSPZ in the Alexa Fluor 647 channel.

4.7.4 B cell immortalization and isolation of monoclonal antibodies

IgG^+ memory B cells were isolated from PBMCs by flow cytometry-based cell sorting. The sorted memory B cells were used for immortalization with Epstein-Barr virus (EBV) in the presence of CpG-DNA (2.5 µg ml-1) and irradiated feeder cells, as previously described [19]. Two weeks after immortalization, culture supernatants were screened for their capacity to stain to the surface of whole intact sporozoites using a high-throughput flow cytometer. PfSPZ were thawed and stained with 6.7 x SYBR Green I (ThermoFisher Scientific) and incubated with the B cell supernatants for 30 minutes at RT. To detect IgG-antibody binding to whole sporozoites, 2.5 µg/mL of Alexa Fluor 647-conjugated goat anti-human IgG was added and incubated for 1 hour at 4°C.

4.7.5 Sequence analysis of antibody cDNA and production of recombinant antibodies

Antibody sequences were obtained by amplifying cDNA using primers specific for IgG heavy or light chains. Antibody heavy and light chains were cloned into human IgG expression vectors and expressed by transient transfection of Expi293F Cells using polyethylenimine (PEI).

4.7.6 ELISA with full length CSP and CSP peptides

All recombinant monoclonal antibodies were measured in an ELISA against full length recombinant CSP (rCSP) and peptides 22-110, NANP(10) and 18-mer peptide. High-binding surface 96-well plates (Costar 3690) were coated with 1µg full length rCSP and 22-110 peptide/mL or 2µg NANP(10)/ml in PBS and incubated overnight at 4°C. Plates were washed 4 times before blocking with PBS/1%BSA for 1 hour at RT. Plates were washed twice before purified recombinant monoclonal antibodies were applied to the coated wells in a 1:3 serial dilution and incubated for 1 hour at RT. Afterwards, plates were washed 4 times and the substrate was added, developed and plates were read at 30 minutes and 1 hour.

4.7.7 *In vitro* assay of inhibition of sporozoite traversal and invasion (ISTI)

A previously described inhibition of sporozoite traversal and invasion assay (ISTI) [17, 23] was used to assess the *in vitro* sporozoite blocking activity of the monoclonal antibodies. In brief, freshly dissected salivary gland NF54 *P. falciparum* sporozoites were incubated together with each monoclonal antibody at a concentration of 10µg/ml in DMEM medium supplemented with 10%FBS, 2.5mM glutamine, penicillin/streptomycin, fungizone and 10mg/mL FITC dextran for 15 minutes at 37°C. Afterwards the sporozoite-antibody mixture was added to HC-04 cells at an MOI of 0.3:1 (30,000 sporozoites: 100,000 HC-04 cells) in triplicate in a 96 well plate in a total volume of 100µl/ml. The plate was centrifuged at 400 x g for 3 minutes to enhance interaction of sporozoites with HC-04 cells and then incubated for 90 minutes at 37°C. After incubation was completed, cells were fixed, permeabilized (BD Cytofix/Cytoperm, BD Bioscience) and stained with an Alexa fluor-647-conjugated anti-CSP monoclonal antibody (clone 2A10). Sporozoite invasion (CSP^+) and traversal ($dextran^+$) of HC-04 cells was analyzed by flow cytometry by first gating live HC-04 cells by forward and side scatter and then gating for CSP^+ and $dextran^+$ cells. Percent of inhibition of invasion and traversal for each monoclonal antibody was determined by normalizing it to a negative control consisting of non-specific human IgG at 10µg/ml. Triplicate samples which had a coefficient of variation (CV) > 30% were rejected for data analysis. The reported data shows the average of three independent experiments.

4.7.8 *In vivo* functional assay in FRG humanized mice (huHep)

To assess the sporozoite blocking activity of the monoclonal antibodies *in vivo*, a previously described human liver-chimeric mouse model (FRG huHep) was used in combination with luciferase expressing *P. falciparum* sporozoites (Sack et al, manuscript submitted) [16, 24, 25]. Each monoclonal antibody was injected intraperitoneally into FRG huHep mice at a concentration of 150µg/mouse and 24 hours later, the mice were challenged by the bites of 50 mosquitoes infected with luciferase-expressing *P. falciparum* sporozoites [24]. Six days post-challenge, the liver-stage burden was determined by measuring the luciferase activity in anesthetized mice through imaging of whole bodies with an in vivo imaging system (IVIS) [26]. Percent of mock (% of mock) parasite liver burden was calculated by dividing the total flux (pixels per second) of each individual mouse by the average of mice receiving non-specific IgG.

4.8 Supplementary Material

4.8.1 Figure Legends

Supplementary Figure 1: IgG and IgM antibody titers to whole intact sporozoites obtained from serum samples of Tanzanian adults who received active immunization with the PfSPZ Vaccine. Antibody titers against whole intact sporozoites were quantified by flow cytometry at time-points before vaccination (baseline), 2 weeks after last vaccination (2w post-vaccination), 4 and 20 weeks after the first CHMI challenge. IgM antibody titers are shown in red and IgG antibody titers in black. The y-axis indicates the antibody binding to sporozoites expressed by the median fluorescence intensity (MFI) and the serum dilution is shown on the x-axis. Donor U, G, V and H were protected against CHMI at 3 and 24 weeks. Placebo controls were injected with normal saline instead of PfSPZ Vaccination and challenged with PfSPZ Challenge at 3 and 24 weeks. Antibody titers of protected donor W are not shown.

Supplementary Figure 2: Staining of whole sporozoites with recombinant IgG^+ monoclonal antibodies by flow cytometry: Flow plots showing the binding of a subset of recombinant IgG^+ monoclonal antibodies to whole sporozoites. The SYBR-green stained DNA of the sporozoites is shown on the vertical axis versus the IgG binding of the mABs on the horizontal axis. BKC3 (last plot) is an antibody of irrelevant specificity and was used as a negative control.

4.8.2 Supplementary Figures

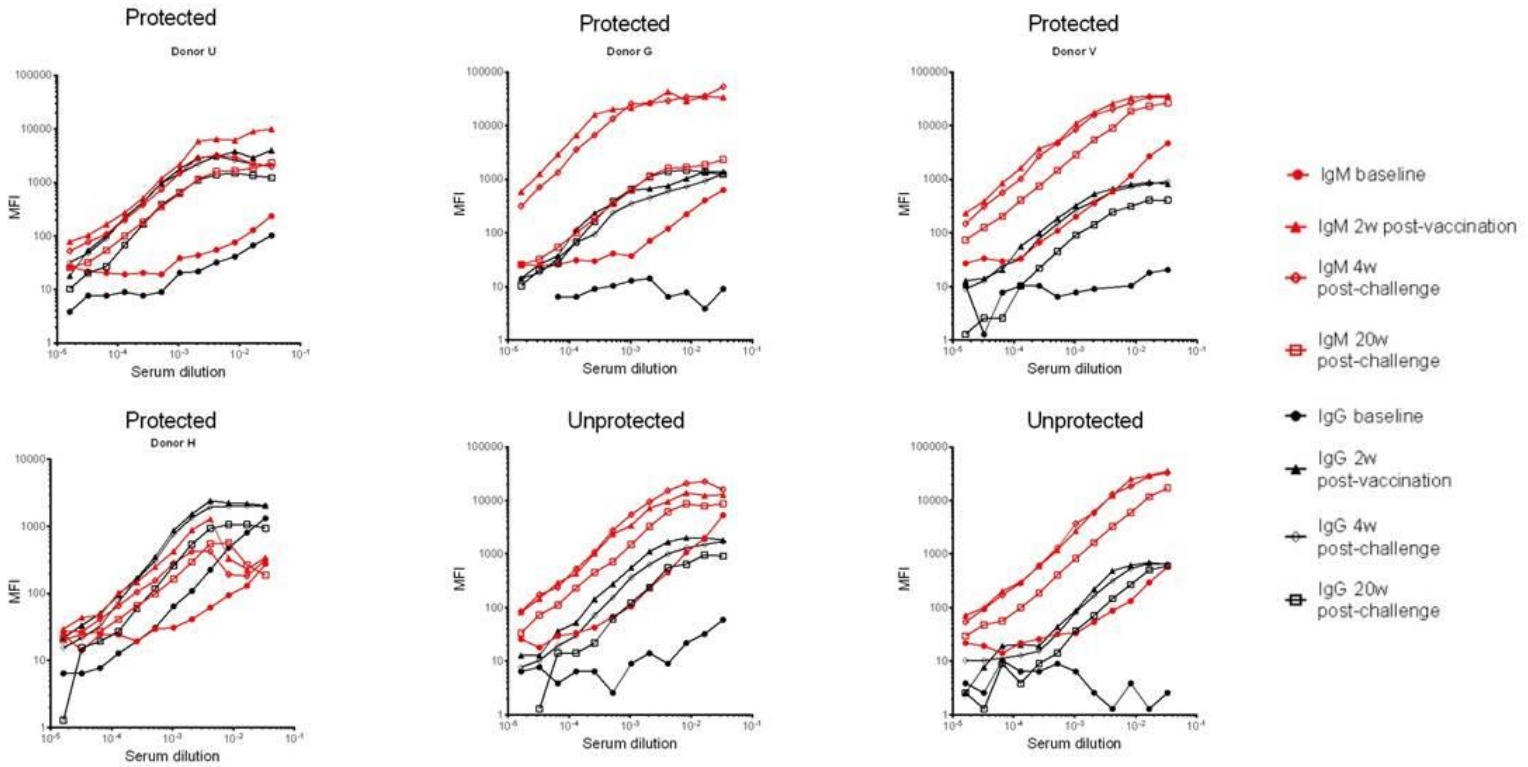

Supplementary Figure S1-1

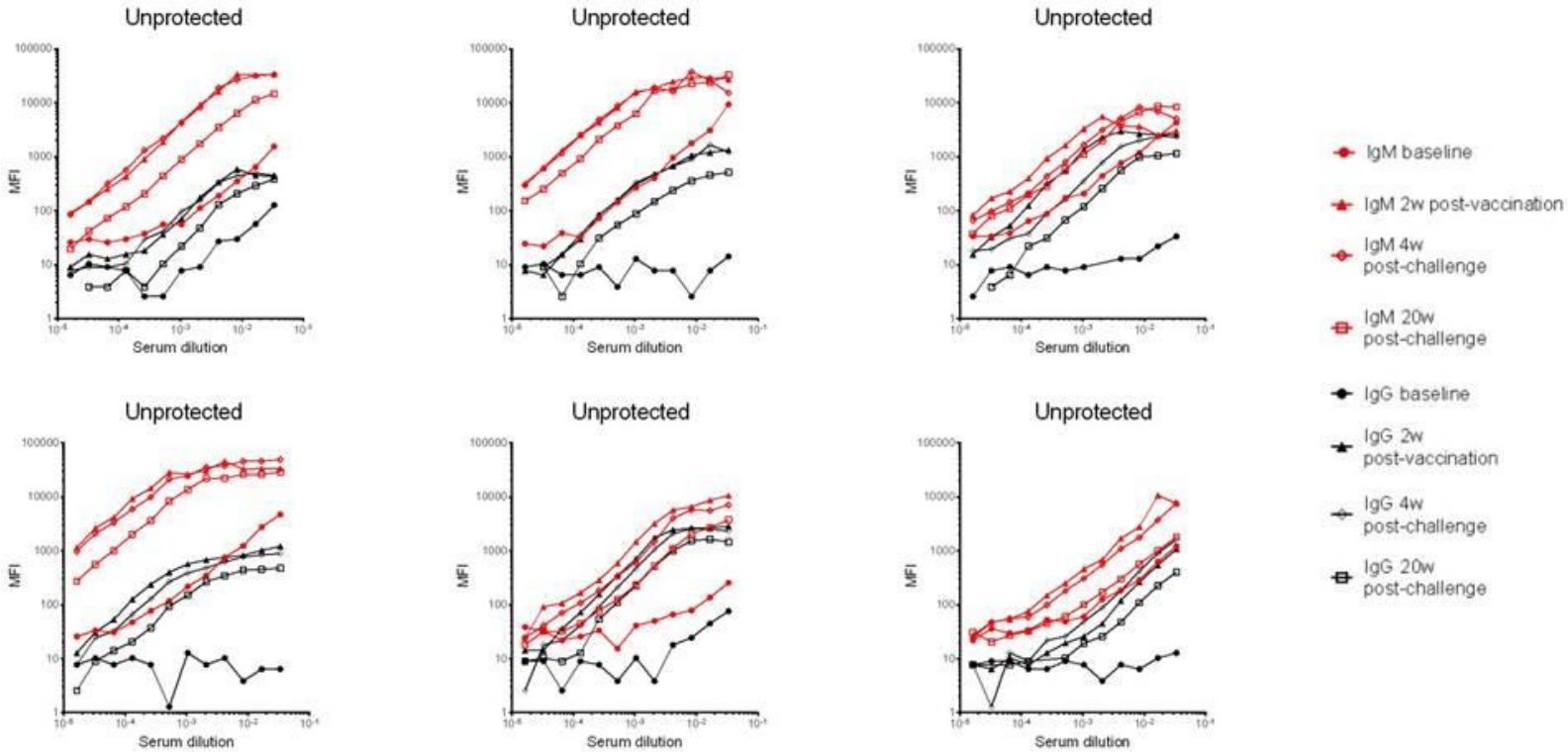

Supplementary Figure S1-2

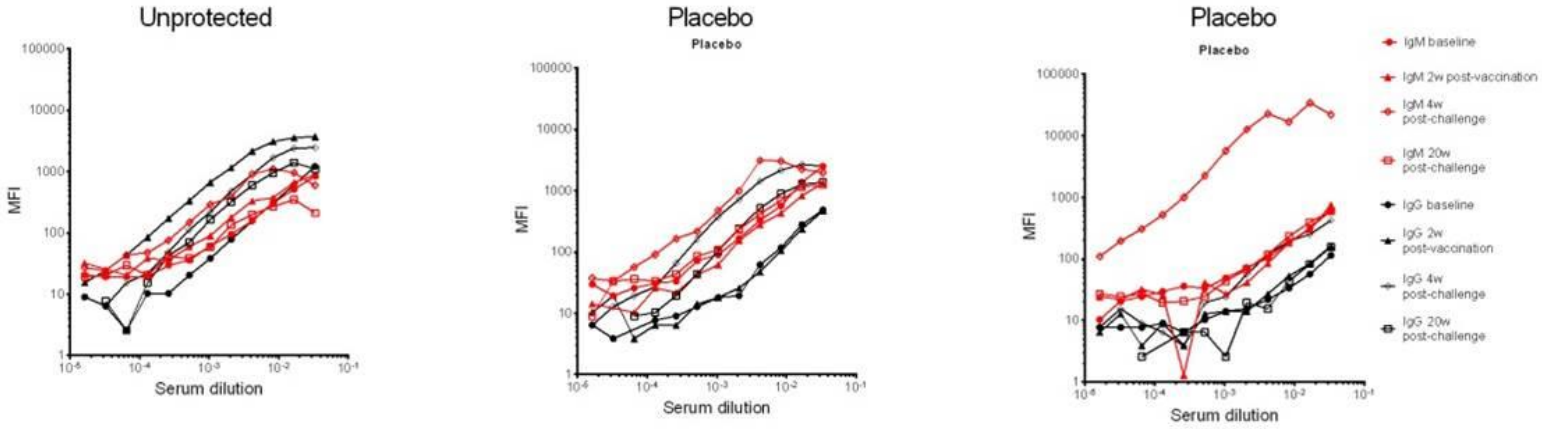

Supplementary Figure S1-3

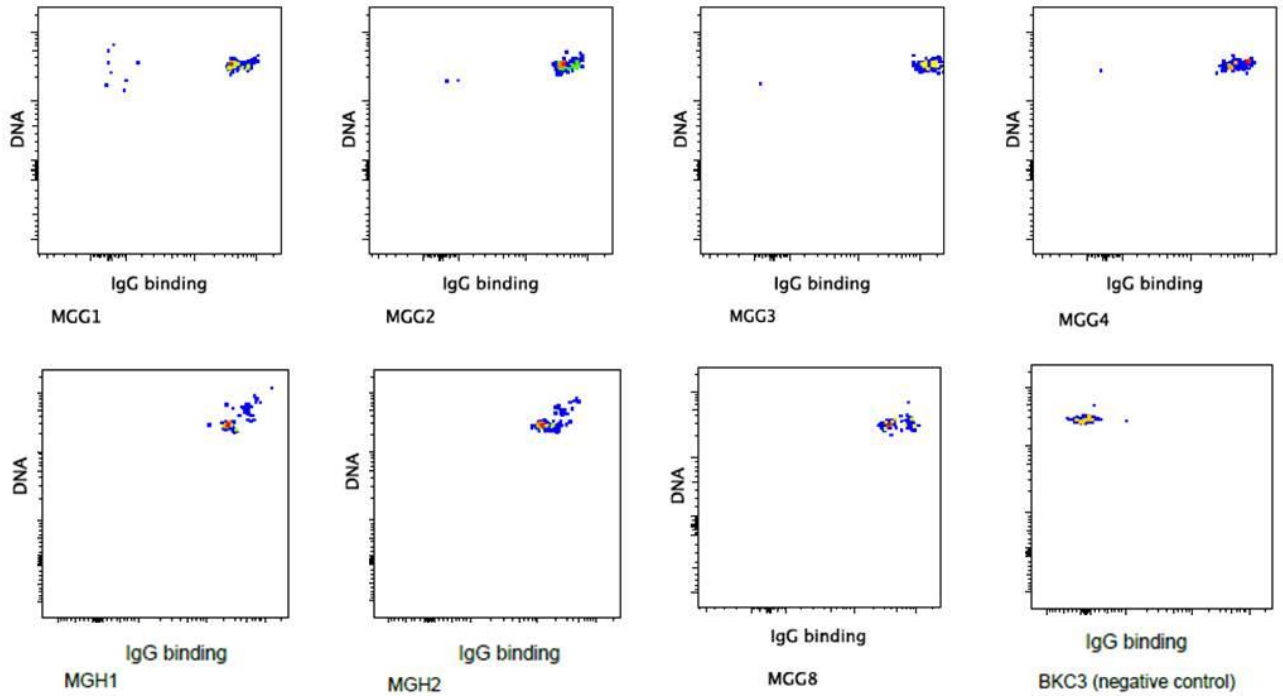

Supplementary Figure S2

4.9 References

1. World Malaria Report 2016 - 9789241511711-eng.pdf. http://apps.who.int/iris/bitstream/10665/252038/1/9789241511711-eng.pdf?ua=1. Accessed 8 May 2017.

2. Sturm A, Amino R, van de Sand C, Regen T, Retzlaff S, Rennenberg A, et al. Manipulation of host hepatocytes by the malaria parasite for delivery into liver sinusoids. Science. 2006;313:1287–90.

3. Who. World malaria report 2015. [S.l.]: World Health Organization; 2016.

4. Epstein JE, Tewari K, Lyke KE, Sim BKL, Billingsley PF, Laurens MB, et al. Live attenuated malaria vaccine designed to protect through hepatic CD8+ T cell immunity. Science. 2011;334:475–80.

5. Clyde DF, McCarthy VC, Miller RM, Hornick RB. Specificity of protection of man immunized against sporozoite-induced falciparum malaria. Am J Med Sci. 1973;266:398–403.

6. Mordmüller B, Surat G, Lagler H, Chakravarty S, Ishizuka AS, Lalremruata A, et al. Sterile protection against human malaria by chemoattenuated PfSPZ vaccine. Nature. 2017;542:445–9.

7. Roestenberg M, McCall M, Hopman J, Wiersma J, Luty AJF, van Gemert GJ, et al. Protection against a malaria challenge by sporozoite inoculation. N Engl J Med. 2009;361:468–77.

8. Roestenberg M, Teirlinck AC, McCall MBB, Teelen K, Makamdop KN, Wiersma J, et al. Long-term protection against malaria after experimental sporozoite inoculation: an open-label follow-up study. Lancet Lond Engl. 2011;377:1770–6.

9. Seder RA, Chang L-J, Enama ME, Zephir KL, Sarwar UN, Gordon IJ, et al. Protection against malaria by intravenous immunization with a nonreplicating sporozoite vaccine. Science. 2013;341:1359–65.

10. Ishizuka AS, Lyke KE, DeZure A, Berry AA, Richie TL, Mendoza FH, et al. Protection against malaria at 1 year and immune correlates following PfSPZ vaccination. Nat Med. 2016;22:614–23.

11. Sissoko MS, Healy SA, Katile A, Omaswa F, Zaidi I, Gabriel EE, et al. Safety and efficacy of PfSPZ Vaccine against Plasmodium falciparum via direct venous inoculation in healthy malaria-exposed adults in Mali: a randomised, double-blind phase 1 trial. Lancet Infect Dis. 2017;0. doi:10.1016/S1473-3099(17)30104-4.

12. Schofield L, Villaquiran J, Ferreira A, Schellekens H, Nussenzweig R, Nussenzweig V. Gamma interferon, CD8+ T cells and antibodies required for immunity to malaria sporozoites. Nature. 1987;330:664–6.

13. Weiss WR, Sedegah M, Beaudoin RL, Miller LH, Good MF. CD8+ T cells (cytotoxic/suppressors) are required for protection in mice immunized with malaria sporozoites. Proc Natl Acad Sci U S A. 1988;85:573–6.

14. Crompton PD, Moebius J, Portugal S, Waisberg M, Hart G, Garver LS, et al. Malaria Immunity in Man and Mosquito: Insights into Unsolved Mysteries of a Deadly Infectious Disease*. Annu Rev Immunol. 2014;32:157–87.

15. Behet MC, Foquet L, van Gemert G-J, Bijker EM, Meuleman P, Leroux-Roels G, et al. Sporozoite immunization of human volunteers under chemoprophylaxis induces functional antibodies against pre-erythrocytic stages of Plasmodium falciparum. Malar J. 2014;13:136.

16. Sack BK, Miller JL, Vaughan AM, Douglass A, Kaushansky A, Mikolajczak S, et al. Model for In Vivo Assessment of Humoral Protection against Malaria Sporozoite Challenge by Passive Transfer of Monoclonal Antibodies and Immune Serum. Infect Immun. 2014;82:808–17.

17. Kublin JG, Mikolajczak SA, Sack BK, Fishbaugher ME, Seilie A, Shelton L, et al. Complete attenuation of genetically engineered Plasmodium falciparum sporozoites in human subjects. Sci Transl Med. 2017;9:eaad9099.

18. Dups JN, Pepper M, Cockburn IA. Antibody and B cell responses to Plasmodium sporozoites. Front Microbiol. 2014;5. doi:10.3389/fmicb.2014.00625.

19. Traggiai E, Becker S, Subbarao K, Kolesnikova L, Uematsu Y, Gismondo MR, et al. An efficient method to make human monoclonal antibodies from memory B cells: potent neutralization of SARS coronavirus. Nat Med. 2004;10:871–5.

20. Corti D, Lanzavecchia A. Efficient Methods To Isolate Human Monoclonal Antibodies from Memory B Cells and Plasma Cells. Microbiol Spectr. 2014;2.

21. Tiller T, Meffre E, Yurasov S, Tsuiji M, Nussenzweig MC, Wardemann H. Efficient generation of monoclonal antibodies from single human B cells by single cell RT-PCR and expression vector cloning. J Immunol Methods. 2008;329:112–24.

22. Coppi A, Natarajan R, Pradel G, Bennett BL, James ER, Roggero MA, et al. The malaria circumsporozoite protein has two functional domains, each with distinct roles as sporozoites journey from mosquito to mammalian host. J Exp Med. 2011;208:341–56.

23. Kaushansky A, Rezakhani N, Mann H, Kappe SHI. Development of a quantitative flow cytometry-based assay to assess infection by Plasmodium falciparum sporozoites. Mol Biochem Parasitol. 2012;183:100–3.

24. Vaughan AM, Mikolajczak SA, Camargo N, Lakshmanan V, Kennedy M, Lindner SE, et al. A transgenic Plasmodium falciparum NF54 strain that expresses GFP-luciferase throughout the parasite life cycle. Mol Biochem Parasitol. 2012;186:143–7.

25. Vaughan AM, Mikolajczak SA, Wilson EM, Grompe M, Kaushansky A, Camargo N, et al. Complete Plasmodium falciparum liver-stage development in liver-chimeric mice. J Clin Invest. 2012;122:3618–28.

26. Miller JL, Murray S, Vaughan AM, Harupa A, Sack B, Baldwin M, et al. Quantitative bioluminescent imaging of pre-erythrocytic malaria parasite infection using luciferase-expressing Plasmodium yoelii. PloS One. 2013;8:e60820.

27. Plassmeyer ML, Reiter K, Shimp RL, Kotova S, Smith PD, Hurt DE, et al. Structure of the Plasmodium falciparum circumsporozoite protein, a leading malaria vaccine candidate. J Biol Chem. 2009;284:26951–63.

28. Rathore D, Sacci JB, de la Vega P, McCutchan TF. Binding and invasion of liver cells by Plasmodium falciparum sporozoites. Essential involvement of the amino terminus of circumsporozoite protein. J Biol Chem. 2002;277:7092–8.

29. Coppi A, Pinzon-Ortiz C, Hutter C, Sinnis P. The Plasmodium circumsporozoite protein is proteolytically processed during cell invasion. J Exp Med. 2005;201:27–33.

30. Rathore D, Nagarkatti R, Jani D, Chattopadhyay R, Vega P de la, Kumar S, et al. An Immunologically Cryptic Epitope of Plasmodium falciparum Circumsporozoite Protein Facilitates Liver Cell Recognition and Induces Protective Antibodies That Block Liver Cell Invasion. J Biol Chem. 2005;280:20524–9.

31. Bongfen SE, Ntsama PM, Offner S, Smith T, Felger I, Tanner M, et al. The N-terminal domain of Plasmodium falciparum circumsporozoite protein represents a target of protective immunity. Vaccine. 2009;27:328–35.

Chapter 5

General Discussion and Conclusion

In *Chapter 2* we demonstrated that direct venous inoculation of PfSPZ Vaccine following two homologous CHMI studies in Tanzanian adults was safe and well tolerated. This was the first study using CHMI as an assessment tool for malaria vaccine efficacy in Africa and the results demonstrated the potential to introduce it into malaria-endemic settings. This is of great value since experimental human challenge infection models can accelerate clinical malaria vaccine development through rapid screening of candidate malaria vaccines and providing preliminary information on efficacy compared to more costly and time consuming field trials [100]. Immunogenicity and protective efficacy were significantly lower in the Tanzanian vaccine recipients when compared to malaria-naïve people from the U.S., who received the same vaccination regimen [29]. Lower antibody and T cells responses compared to malaria-naïve vaccine recipients were also seen in volunteers of a study in Mali, at which the safety and efficacy of the PfSPZ Vaccine was tested in similar immunization regimens as in the Tanzanian trial, but here, vaccine efficacy was assessed through natural field exposure to *P. falciparum* parasites [99]. Such population-based differences in response to vaccination have been described in other vaccines against BCG, hepatitis B, tetanus, diphtheria, pertussis, measles, influenza, oral cholera vaccine and yellow fever [114–116], all of which performed less well in populations from developing countries compared to populations living in industrialized countries [117]. The immunogenetics behind these variations in immune responses to vaccines observed in different human populations remain largely unknown [118]. Antigenic variation of *P. falciparum*, immunoregulation due to lifelong exposure (summarized in section 1.2.3) to the parasite and sub-optimal immunization regimen could have an influence on the poor immunogenicity seen in the malaria pre-exposed individuals of the studies in Tanzania and Mali [99]. It is hypothesized that higher individual doses of the PfSPZ Vaccine might be required in these main target populations to achieve high-level protection lasting for at least six months [99]. Studies testing this hypothesis are currently ongoing in Africa, the U.S. and Europe [99]. Furthermore, it could be possible that previous or frequent exposure to blood stage parasites diminish humoral immune responses to pre-erythrocytic stage parasites in malaria pre-exposed people. This finding has been recently reported from studies in mice where CSP-specific humoral memory formation was found to be impaired after blood stage infection [119]. Other factors possibly affecting vaccine-induced immune responses differing between human populations could be differences in genetic background environment, diet, gut microbiota, co-infections or an activated immune microenvironment as described in Ugandan volunteers who participated in a yellow fever vaccine study [114, 116]. In the latter study, the vaccine-induced immune responses of a

licensed, live attenuated yellow fever vaccine were compared between volunteers residing in Entebbe, Uganda, and volunteers living in Lausanne, Switzerland. The study revealed that the vaccine-induced CD8+ T cell and B cell responses were significantly lower in the Ugandan volunteers as a result of high frequencies of exhausted and activated NK cells, differentiated T and B lymphocytes and pro-inflammatory monocytes measured before vaccination. This immune activation negatively correlated with the vaccine-induced neutralizing antibody titers and was probably associated to higher exposure frequency to infectious diseases in Entebbe compared to Lausanne [116]. Higher immune activation status at baseline could also be present in the Tanzanian volunteers compared to U.S. resident volunteers enrolled into the PfSPZ vaccination studies. To confirm this hypothesis, similar immunological measurements between the two cohorts would need to be conducted.

To gain a better understanding of potential immunological correlates against malaria induced in malaria-endemic populations after PfSPZ vaccination, measures of vaccine-induced immune responses need to be greatly expanded. This could be done at a single-cell level as described in *Chapter 4*, whereby B cell clones producing highly effective anti-parasite inhibitory antibodies are identified from the total memory B cell pool of immunized donors protected after CHMI [107]. Approaches including antibody repertoire sequencing [120], analysis of immune cells, cytokines and whole-genome tanscriptomics might also support the identification of correlates or markers of protection [121].

In conclusion, the manuscript in *Chapter 2* demonstrates that the immunization regimen of the PfSPZ Vaccine tested in volunteers of malaria-endemic Tanzania needs further optimization if the target of an efficacious vaccine > 75 % efficacy, lasting for at least six months is to be met. More research is required to understand the immunological mechanisms underlying the insufficient protective efficacy and immunogenicity observed in malaria-endemic target populations. Despite low protective efficacy, the trial did show protection in a few volunteers and consequently there are valuable samples available to study potential immune correlates of host protection. Overall, these results also highlight the importance of conducting early stage malaria vaccine trials in the relevant target population e.g. in sub-Saharan Africa, and the potential of CHMI as an assessment tool to measure vaccine efficacy.

In *Chapter 3*, we reported for the first time that anti-sporozoite IgM antibodies are induced in malaria pre-exposed Tanzanian adults after immunization with PfSPZ Vaccine, and most importantly that these IgM antibodies can mediate inhibition of sporozoite infection *in vitro*. To our knowledge this is the first demonstration of anti-sporozoite IgM antibody function reported in humans. So far, little has been published about the functional relevance of IgM antibodies in human malaria infection [56]. "Natural" or "non-immune" IgM antibodies, which are the first antibodies produced during a primary antibody response, are polyreactive and of low antigen-binding affinity [122]. They have been reported to bind to the surface of *P. falciparum*-infected erythrocytes and thereby contribute to RBC rosetting, as well to syndromes of severe malaria, such as placental malaria [123–126]. In contrast, *Plasmodium*-specific or "immune" IgM antibodies proved to be protective against murine asexual blood stage parasites of *P. chabaudi* [127]. Furthermore, elevated levels of IgM antibodies specific for α-Gal, a glycoprotein expressed on the surface of *Plasmodium* sporozoites and of the human gut pathobiont *E. coli,* were detected in children with no *P. falciparum* infection versus children who became infected with *P. falciparum* during a 6-month malaria season [128]. In the same study, anti-α-Gal IgM antibodies inhibited parasite infection of hepatocytes *in vivo* and in *vitro*. In addition, *Arama et al*., 2015, reported a protein microarray study of profiling in total 1087 *P. falciparum* antigens and demonstrated that plasma samples collected from the Fulani ethnic showed higher breadth and magnitude of IgM antibody responses towards *Plasmodium* antigens compared to the Dogon ethnic group, who live in the same geographic area in Mali [56]. The Fulani and Dogon groups differ in their resistance against clinical malaria with the Fulani having a higher resistance. These findings could further support a potential protective role of malaria specific IgM antibodies during human malaria infection.

To date, vaccine-induced IgM antibody responses have not been investigated in great detail during experimental malaria vaccine trials [27, 29, 32, 99]. This is not surprising, since IgM antibodies are traditionally believed to be short-lived and not affinity-matured and thereby do not contribute to memory and long-term immunity like antibodies of the switched isotype [129, 130]. It is commonly accepted that humoral immune memory is formed during a primary antibody response to foreign antigens. During this process, antigen-activated naïve B cells receive stimulating signals from T helper cells, which results in the proliferation of the activated B cells [131]. The majority of the proliferating cells differentiates into short-lived, mostly IgM, antibody-secreting plasmablasts, which act as a first line of defense while some B cell clones begin to form germinal center (GC) reactions through the interaction with

follicular helper T cells and dendritic cells in secondary lymphoid organs [132]. Germinal center B cells undergo T cell-dependent class-switching and somatic hypermutation (SHM) in their variable regions, which results in the generation of long lived-memory B cells (MBCs) and long-lived plasma cells (LLPCs) producing high-affinity antibodies of switched isotype [133, 134]. Upon re-challenge with the same antigen, these classical memory B cells become re-activated and rapidly begin to proliferate and differentiate into either plasmablasts that secrete high-affinity antibodies or re-enter germinal center reactions to undergo further affinity maturation [58]. In recent years, this view of humoral memory has been scrutinized in various studies with growing evidence demonstrating the existence of a higher diversity of the memory B cell (MBC) subset including germinal-center-independent memory B cells [135–137], T cell-independent MBCs [138–140] and unswitched, somatically hypermutated IgM memory B cells [58, 141, 142] as well long-lived antigen-induced IgM plasma cells with somatic mutations [143]. In malaria, such phenotypically distinct MBC populations have been identified in murine malaria infection models, where somatically hypermutated, high-affinity *Plasmodium*-specific IgM MBCs targeting asexual blood stage parasites dominated the early response upon malaria re-infection [144]. In the same study, switched and unswitched *Plasmodium*-specific MBCs were also detected in PBMCs from malaria pre-exposed Malian subjects. Nevertheless, these findings so far describe asexual blood-stage-specific MBCs, since B cell tetramers specific for MSP1 were used for tracking *Plasmodium*-specific B cells [144]. Referring to our results of the PfCSP-specific IgM antibodies induced in malaria pre-exposed volunteers after PfSPZ vaccination, the cellular source of these antibodies remains to be investigated.

One limitation of our study *in Chapter 3* was the low number of samples tested on day 140 after the first CHMI. A sample size of two out of four does not allow for meaningful statistical analyses of the proportion of volunteers generating such vaccine-induced CSP-binding IgM antibodies up to 140 days post-CHMI1. Results presented in *Chapter 4* (Supplementary Figure 1) clearly demonstrate elevated and sustained serum IgM antibody titers binding to whole sporozoites when measured by flow cytometry on day 140 post-CHMI1. With their pentameric structure, IgM antibodies can bind to antigens with higher affinity compared to other immunoglobulins, allowing them to efficiently neutralize and agglutinate pathogens [145, 146]. In addition, IgM antibodies can activate the classical complement cascade with 1000-fold increased binding affinity than IgG [147]. Moreover, long-term production protective IgM antibodies have also been described under natural conditions against viral (Influenza, West Nile virus) and intracellular bacterial infections

[129, 138, 148–152]. There are many childhood vaccines that induced low but persistent protective IgM antibodies against infection [153–156]. Furthermore, sustained and long-term IgM production was also found in human volunteers in a phase I clinical trial of a *Francisella tularensis* vaccine [157] as well after immunization with the HIV envelope glycoprotein gp120 [158]. Overall, our data suggest that IgG and IgM antibody responses should both be assessed in future malaria vaccine trials.

Taken together, the manuscript in *Chapter 3* demonstrated that malaria pre-exposed individuals induce PfCSP-specific IgM antibodies following intravenous inoculation of 2.7 x 10^5 purified sporozoites. It can be assumed that a large portion of these intravenously applied sporozoites are reaching the marginal zone of the spleen, an organ with important function in host defense against blood-borne pathogens and which receives large amounts of blood of about 5 % from the general circulation [159]. In these splenic marginal zones, so called marginal zone B cells (MZ B cells) are present in order to capture incoming antigens with the help of B cell-helper neutrophils, macrophages and DCs and subsequently differentiate into plasmasblasts producing large amounts of IgM or antibodies of switched isotype [160]. With the release of IL-21 from B cell helper-neutrophils, human MZ B cell undergo SHM and class switch recombination (CSR) [160]. B cells identical to splenic MZ B cells have been identified in human peripheral blood, suggesting that these cells recirculate [161, 162]. It could be possible that splenic MZ B cells are the source of the induced PfCSP-IgM antibodies observed in our study from *Chapter 3*.

In *Chapter 4* we reported for the first time the successful isolation and establishment of PfCSP-specific human monoclonal antibodies (mABs) from Tanzanian adults who received PfSPZ Vaccine and were protected against homologous CHMI three weeks past last vaccination. To our knowledge, this is the first time sporozoite-specific human mAbs were generated from African donors living in malaria-endemic regions. We found that the mAbs with the strongest capacity to inhibit parasite growth *in vitro* and *in vivo* target a distinct peptide located at the junction between the N-terminus and the first NANP repeat of the CS protein (KQPADGNPDPNANPNKNN). The N-terminus of PfCSP is known to be critical for sporozoite attachment and invasion of hepatocytes, and antibodies targeting this part of PfCSP were associated with protection from clinical malaria in children living in malaria-endemic regions [163, 164]. However, the latter study tested serum samples in an ELISA against several PfCSP N-terminal peptides differing in length. ELISA measures the presence of the total antibody response in serum, but does not dissect the response at the clonal B cell

level. In contrast, our study investigated the efficacy of specific antibodies produced by single B cell clones from protected donors and identified the most inhibitory antibodies as those able to bind to a narrow region between the N-terminus and the repeat region of PfCSP.

Overall, our data presented in *Chapter 4* suggest that we have identified a promising epitope that appears to be a target of antibodies in individuals protected from malaria. However, the key question, whether this epitope when delivered as synthetic peptide in combination with a strong adjuvant is immunogenic and induces protective humoral immunity in humans, remains to be investigated. This could be analyzed further through direct testing of one of the highly effective mAbs in humans, e.g. via passive transfer experiments followed by controlled human malaria infection. Production of GMP conform mAB that could be tested in humans requires a long process of extensive pre-clinical safety studies evaluating immunotoxicity, pharmacokinetics and pharmacodynamics of mAbs, which may take several years before entering human clinical trials [165, 166]. Foremost, based on our current findings, the next critical step is to test if the epitope is immunogenic in mice and to test the functional capacity of the induced antibodies to block sporozoite invasion *in vitro* and *in vi*vo similar to the experiments described in *Chapter 4*. Structural analysis of epitope – antibody interactions are currently carried out in collaboration with Ian Wilson (unpublished data).

Chapter 6

Outlook

Clinical trials on the safety and efficacy of the PfSPZ Vaccine are ongoing in Africa, the U.S. and Europe and new studies are planned. All of these studies are testing higher doses and fewer immunizations of the PfSPZ Vaccine than used in the BSPZV1 study described in *Chapter 2*. The aim is to finally arrive at an effective dosing and vaccination regimen for malaria-endemic populations to achieve high-level protection. These studies include follow-up trials in Equatorial Guinea, Mali, Tanzania, Burkina Faso and Kenya in adult volunteers but also in adolescents, children and infants (Tanzania and Kenya). All of these trials are testing the safety, tolerability and protective efficacy of 3 dose regimens of 4.5×10^5, 9×10^5 and 1.8×10^6 radiation-attenuated PfSPZ. Besides of increasing the doses of radiation-attenuated PfSPZ Vaccine, it will also be important to investigate if improved immunogenicity and protective efficacy in malaria pre-exposed populations can be achieved through other whole sporozoite vaccination approaches using chemoprophylaxis vaccination (CVac) or genetically attenuated parasites (GAP). In CVac, the Sanaria PfSPZ are administered as non-irradiated sporozoites under anti-malaria drug coverage [30]. This vaccination approach conferred sterile protection (100%) against homologous CHMI in malaria-naïve volunteers in Germany when administered at 3 doses of 5.12×10^4 non-irradiated PfSPZ at 28-day intervals under choloroquine chemoprophylaxis coverage [167]. In contrast to radiation-attenuated PfSPZ used in the PfSPZ Vaccine, the non-attenuated PfSPZ in CVac develop into mature liver stages and give rise to schizonts that are released as merozoites into the blood, where the parasites are killed by the antimalarial-drug chloroquine. CVac exposes the immune system to an increased breath and quantity of malaria antigens compared to radiation-attenuated PfSPZ [30]. To induce complete protection, CVac requires approximately 20-fold fewer PfSPZ than immunization with radiation-attenuated PfSPZ (PfSPZ Vaccine), but is limited by the need of continuous taking of anti-malarial drugs during immunization [31]. The CVac approach is currently tested in malaria-endemic adults in Equatorial Guinea using a dosage of 1×10^5 PfSPZ in each vaccination (unpublished data). Alternatively, GAPs are attenuated via genetic engineering of *P. falciparum* through targeted deletions of genes that are essential to complete pre-erythrocytic infection and transition into blood-stage parasites [32]. As a result, homogeneous populations of parasites with a defined attenuation phenotype can be generated and used for immunization. This has the advantage of preventing over-attenuation and batch-to-batch variation [32]. Recently, *Kublin* et al., reported complete attenuation of genetically-attenuated *P. falciparum* sporozoites from a first-in-human phase 1 safety and immunogenicity trial in malaria-naïve people from the U.S. [32]. Another promising GAP malaria vaccine candidate [168] is currently tested in humans in the

Netherlands (unpublished data) and it will be interesting to explore the efficacy of GAP malaria vaccine candidates in malaria-endemic target populations.

Based on our findings in *Chapter 3*, the next important step will be to confirm the functional capacity of sporozoite-inhibiting IgM antibodies *in vivo* in mice studies. This can be done with the same human liver-chimeric mouse model as described in *Chapter 4*, except of passively transferring monoclonal antibodies into FRG-mice, IgM-purified sera will be used for the the passive transfer. Alternatively, generation and testing of sporozoite binding IgM human monoclonal antibodies from African donors as described in *Chapter 4* could support this research. Furthermore, it will be interesting to investigate if the IgM antibodies elicited by the PfSPZ Vaccine are capable of fixing complement upon sporozoite binding *in vitro*. It would be important to compare our findings with serum samples collected from malaria-naïve volunteers who have been immunized with the same dosing and regimen to see if induction of sporozoite-specific IgM antibodies after PfSPZ immunization is restricted to individuals residing in malaria-endemic areas. In order to get a better understanding of the cellular source of these sporozoite –specific IgM antibodies, one could use the PBMC samples collected at the same time-points and sort for plasmablasts and MBCs using specific markers for MZ B cells by flow cytometry. MZ B cells are defined based on their $IgM^{hi}IgD^{low}CD1c^{+}CD21^{hi}CD23^{-}CD27^{+}$ marker expression [169–171]. Future studies should also address if the sporozoite binding IgM antibody repertoire undergoes affinity maturation resulting in improved effector function upon repeated vaccinations.

Considering our findings in *Chapter 4*, the next step would be to test whether the target epitope of the highly functional antibodies is immunogenic in mice. Therefore, BALB/C mice could be immunized with the peptide conjugated to a carrier protein such as KLH. Afterwards, the serum will be collected to analyze the induced IgG and IgM antibody responses against the 18-mer peptide by ELISA and against whole sporozoites by our newly developed flow cytometry screening assay. If the epitope is immunogenic in mice, the next step will be to collect sera from the immunized mice and test for functional antibodies capable of inhibiting sporozoite development *in vitro* (ISTI). In parallel, production of mouse monoclonal antibodies targeting the 18-mer peptide could be tested similarly *in vitro* and *in vivo*. In addition, resolution of a crystal structure of a highly functional human mAb with its corresponding target peptide could provide insight into antibody affinity maturation steps and peptide structure essential for providing functionally highly active humoral immunity. Three-

dimensional structural analysis of antibody-epitope specificity through high-resolution X-ray crystallography is necessary in order to understand the mechanism of immune recognition and for the rational design of synthetic vaccines [172].

Chapter 7

References

1. World Malaria Report 2016 - 9789241511711-eng.pdf. http://apps.who.int/iris/bitstream/10665/252038/1/9789241511711-eng.pdf?ua=1. Accessed 8 May 2017.

2. Bhatt S, Weiss DJ, Cameron E, Bisanzio D, Mappin B, Dalrymple U, et al. The effect of malaria control on Plasmodium falciparum in Africa between 2000 and 2015. Nature. 2015;526:207–11.

3. Aly ASI, Vaughan AM, Kappe SHI. Malaria Parasite Development in the Mosquito and Infection of the Mammalian Host. Annu Rev Microbiol. 2009;63:195.

4. Naing C, Whittaker MA, Nyunt Wai V, Mak JW. Is Plasmodium vivax Malaria a Severe Malaria?: A Systematic Review and Meta-Analysis. PLoS Negl Trop Dis. 2014;8. doi:10.1371/journal.pntd.0003071.

5. Singh B, Daneshvar C. Human Infections and Detection of Plasmodium knowlesi. Clin Microbiol Rev. 2013;26:165–84.

6. Ahmed MA, Cox-Singh J. Plasmodium knowlesi – an emerging pathogen. ISBT Sci Ser. 2015;10:134–40.

7. Gueirard P, Tavares J, Thiberge S, Bernex F, Ishino T, Milon G, et al. Development of the malaria parasite in the skin of the mammalian host. Proc Natl Acad Sci U S A. 2010;107:18640–5.

8. Tavares J, Formaglio P, Thiberge S, Mordelet E, Van Rooijen N, Medvinsky A, et al. Role of host cell traversal by the malaria sporozoite during liver infection. J Exp Med. 2013;210:905–15.

9. Crompton PD, Moebius J, Portugal S, Waisberg M, Hart G, Garver LS, et al. Malaria immunity in man and mosquito: insights into unsolved mysteries of a deadly infectious disease. Annu Rev Immunol. 2014;32:157–87.

10. Sturm A, Amino R, van de Sand C, Regen T, Retzlaff S, Rennenberg A, et al. Manipulation of host hepatocytes by the malaria parasite for delivery into liver sinusoids. Science. 2006;313:1287–90.

11. Miller LH, Baruch DI, Marsh K, Doumbo OK. The pathogenic basis of malaria. Nature. 2002;415:673–9.

12. Bannister LH, Hopkins JM, Fowler RE, Krishna S, Mitchell GH. A Brief Illustrated Guide to the Ultrastructure of Plasmodium falciparum Asexual Blood Stages. Parasitol Today. 2000;16:427–33.

13. Cowman AF, Healer J, Marapana D, Marsh K. Malaria: Biology and Disease. Cell. 2016;167:610–24.

14. Schofield L, Grau GE. Immunological processes in malaria pathogenesis. Nat Rev Immunol. 2005;5:722–35.

15. Roth JM, Korevaar DA, Leeflang MMG, Mens PF. Molecular malaria diagnostics: A systematic review and meta-analysis. Crit Rev Clin Lab Sci. 2015.

http://www.tandfonline.com/doi/full/10.3109/10408363.2015.1084991. Accessed 18 May 2017.

16. Tietje K, Hawkins K, Clerk C, Ebels K, McGray S, Crudder C, et al. The essential role of infection-detection technologies for malaria elimination and eradication. Trends Parasitol. 2014;30:259–66.

17. Bousema T, Okell L, Felger I, Drakeley C. Asymptomatic malaria infections: detectability, transmissibility and public health relevance. Nat Rev Microbiol. 2014;12:833–40.

18. Murray CK, Gasser RA, Magill AJ, Miller RS. Update on Rapid Diagnostic Testing for Malaria. Clin Microbiol Rev. 2008;21:97–110.

19. Moody A. Rapid diagnostic tests for malaria parasites. Clin Microbiol Rev. 2002;15:66–78.

20. Lengeler C. Insecticide-treated bed nets and curtains for preventing malaria. Cochrane Database Syst Rev. 2004;:CD000363.

21. Eisele TP, Larsen D, Steketee RW. Protective efficacy of interventions for preventing malaria mortality in children in Plasmodium falciparum endemic areas. Int J Epidemiol. 2010;39 Suppl 1:i88-101.

22. Bijker EM, Sauerwein RW. Enhancement of naturally acquired immunity against malaria by drug use. J Med Microbiol. 2012;61 Pt 7:904–10.

23. Schellenberg D, Menendez C, Aponte JJ, Kahigwa E, Tanner M, Mshinda H, et al. Intermittent preventive antimalarial treatment for Tanzanian infants: follow-up to age 2 years of a randomised, placebo-controlled trial. The Lancet. 2005;365:1481–3.

24. Brentlinger PE, Dgedge M, Correia MAC, Rojas AJB, Saúte F, Gimbel-Sherr KH, et al. Intermittent preventive treatment of malaria during pregnancy in central Mozambique. Bull World Health Organ. 2007;85:873–9.

25. Sicuri E, Bardají A, Nhampossa T, Maixenchs M, Nhacolo A, Nhalungo D, et al. Cost-Effectiveness of Intermittent Preventive Treatment of Malaria in Pregnancy in Southern Mozambique. PLOS ONE. 2010;5:e13407.

26. WHO | Insecticide resistance. WHO. http://www.who.int/malaria/areas/vector_control/insecticide_resistance/en/. Accessed 19 May 2017.

27. RTS SCTP, Agnandji ST, Lell B, Fernandes JF, Abossolo BP, Methogo BG, et al. A Phase 3 Trial of RTS,S/AS01 Malaria Vaccine in African Infants. N Engl J Med. 2012;367:2284–95.

28. Clyde DF, Most H, McCarthy VC, Vanderberg JP. Immunization of man against sporozite-induced falciparum malaria. Am J Med Sci. 1973;266:169–77.

29. Seder RA, Chang L-J, Enama ME, Zephir KL, Sarwar UN, Gordon IJ, et al. Protection against malaria by intravenous immunization with a nonreplicating sporozoite vaccine. Science. 2013;341:1359–65.

30. Roestenberg M, Teirlinck AC, McCall MBB, Teelen K, Makamdop KN, Wiersma J, et al. Long-term protection against malaria after experimental sporozoite inoculation: an open-label follow-up study. Lancet Lond Engl. 2011;377:1770–6.

31. Roestenberg M, McCall M, Hopman J, Wiersma J, Luty AJF, van Gemert GJ, et al. Protection against a malaria challenge by sporozoite inoculation. N Engl J Med. 2009;361:468–77.

32. Kublin JG, Mikolajczak SA, Sack BK, Fishbaugher ME, Seilie A, Shelton L, et al. Complete attenuation of genetically engineered Plasmodium falciparum sporozoites in human subjects. Sci Transl Med. 2017;9:eaad9099.

33. Riley EM, Stewart VA. Immune mechanisms in malaria: new insights in vaccine development. Nat Med. 2013;19:168–78.

34. Tran TM, Li S, Doumbo S, Doumtabe D, Huang C-Y, Dia S, et al. An intensive longitudinal cohort study of Malian children and adults reveals no evidence of acquired immunity to Plasmodium falciparum infection. Clin Infect Dis Off Publ Infect Dis Soc Am. 2013;57:40–7.

35. Nussenzweig RS, Vanderberg J, Most H, Orton C. Protective immunity produced by the injection of x-irradiated sporozoites of plasmodium berghei. Nature. 1967;216:160–2.

36. Vaughan AM, Wang R, Kappe SHI. Genetically engineered, attenuated whole-cell vaccine approaches for malaria. Hum Vaccin. 2010;6:107–13.

37. Hoffman SL, Goh LML, Luke TC, Schneider I, Le TP, Doolan DL, et al. Protection of humans against malaria by immunization with radiation-attenuated Plasmodium falciparum sporozoites. J Infect Dis. 2002;185:1155–64.

38. Cohen S, McGREGOR IA, Carrington S. Gamma-Globulin and Acquired Immunity to Human Malaria. Nature. 1961;192:733–7.

39. Blackman MJ, Heidrich HG, Donachie S, McBride JS, Holder AA. A single fragment of a malaria merozoite surface protein remains on the parasite during red cell invasion and is the target of invasion-inhibiting antibodies. J Exp Med. 1990;172:379–82.

40. Persson KEM, Fowkes FJI, McCallum FJ, Gicheru N, Reiling L, Richards JS, et al. Erythrocyte-binding antigens of Plasmodium falciparum are targets of human inhibitory antibodies and function to evade naturally acquired immunity. J Immunol Baltim Md 1950. 2013;191:785.

41. Hill DL, Eriksson EM, Suen CSNLW, Chiu CY, Ryg-Cornejo V, Robinson LJ, et al. Opsonising Antibodies to P. falciparum Merozoites Associated with Immunity to Clinical Malaria. PLOS ONE. 2013;8:e74627.

42. Osier FH, Feng G, Boyle MJ, Langer C, Zhou J, Richards JS, et al. Opsonic phagocytosis of Plasmodium falciparum merozoites: mechanism in human immunity and a correlate of protection against malaria. BMC Med. 2014;12:108.

43. Bouharoun-Tayoun H, Oeuvray C, Lunel F, Druilhe P. Mechanisms underlying the monocyte-mediated antibody-dependent killing of Plasmodium falciparum asexual blood stages. J Exp Med. 1995;182:409–18.

44. Boyle MJ, Reiling L, Feng G, Langer C, Osier FH, Aspeling-Jones H, et al. Human antibodies fix complement to inhibit Plasmodium falciparum invasion of erythrocytes and are associated with protection against malaria. Immunity. 2015;42:580–90.

45. Beeson JG, Mann EJ, Elliott SR, Lema VM, Tadesse E, Molyneux ME, et al. Antibodies to Variant Surface Antigens of Plasmodium falciparum-Infected Erythrocytes and Adhesion Inhibitory Antibodies Are Associated with Placental Malaria and Have Overlapping and Distinct Targets. J Infect Dis. 2004;189:540.

46. Saul A. Mosquito stage, transmission blocking vaccines for malaria. Curr Opin Infect Dis. 2007;20:476–81.

47. Takala SL, Plowe CV. Genetic diversity and malaria vaccine design, testing, and efficacy: Preventing and overcoming "vaccine resistant malaria." Parasite Immunol. 2009;31:560.

48. Niederwieser I, Felger I, Beck HP. Limited polymorphism in Plasmodium falciparum sexual-stage antigens. Am J Trop Med Hyg. 2001;64:9–11.

49. Mackinnon MJ, Marsh K. The selection landscape of malaria parasites. Science. 2010;328:866–71.

50. Gupta S, Snow RW, Donnelly CA, Marsh K, Newbold C. Immunity to non-cerebral severe malaria is acquired after one or two infections. Nat Med. 1999;5:340–3.

51. Sidjanski S, Vanderberg JP. Delayed migration of Plasmodium sporozoites from the mosquito bite site to the blood. Am J Trop Med Hyg. 1997;57:426–9.

52. Gilson PR, Crabb BS. Morphology and kinetics of the three distinct phases of red blood cell invasion by Plasmodium falciparum merozoites. Int J Parasitol. 2009;39:91–6.

53. Doolan DL, Dobano C, Baird JK. Acquired Immunity to Malaria. Clin Microbiol Rev. 2009;22:13–36.

54. Sauerwein RW. Clinical malaria vaccine development. Immunol Lett. 2009;122:115–7.

55. Langhorne J, Ndungu FM, Sponaas A-M, Marsh K. Immunity to malaria: more questions than answers. Nat Immunol. 2008;9:725–32.

56. Arama C, Skinner J, Doumtabe D, Portugal S, Tran TM, Jain A, et al. Genetic Resistance to Malaria Is Associated With Greater Enhancement of Immunoglobulin (Ig)M Than IgG Responses to a Broad Array of Plasmodium falciparum Antigens. Open Forum Infect Dis. 2015;2. doi:10.1093/ofid/ofv118.

57. Tangye SG, Tarlinton DM. Memory B cells: effectors of long-lived immune responses. Eur J Immunol. 2009;39:2065–75.

58. Dogan I, Bertocci B, Vilmont V, Delbos F, Mégret J, Storck S, et al. Multiple layers of B cell memory with different effector functions. Nat Immunol. 2009;10:1292–9.

59. Manz RA, Thiel A, Radbruch A. Lifetime of plasma cells in the bone marrow. Nature. 1997;388:133–4.

60. Slifka MK, Antia R, Whitmire JK, Ahmed R. Humoral immunity due to long-lived plasma cells. Immunity. 1998;8:363–72.

61. Maple PA, Jones CS, Wall EC, Vyseb A, Edmunds WJ, Andrews NJ, et al. Immunity to diphtheria and tetanus in England and Wales. Vaccine. 2000;19:167–73.

62. Hammarlund E, Lewis MW, Hansen SG, Strelow LI, Nelson JA, Sexton GJ, et al. Duration of antiviral immunity after smallpox vaccination. Nat Med. 2003;9:1131–7.

63. Amanna IJ, Carlson NE, Slifka MK. Duration of humoral immunity to common viral and vaccine antigens. N Engl J Med. 2007;357:1903–15.

64. Ryg-Cornejo V, Ly A, Hansen DS. Immunological processes underlying the slow acquisition of humoral immunity to malaria. Parasitology. 2016;143:199–207.

65. Scholzen A, Sauerwein RW. How malaria modulates memory: activation and dysregulation of B cells in Plasmodium infection. Trends Parasitol. 2013;29:252–62.

66. Migot F, Chougnet C, Henzel D, Dubois B, Jambou R, Fievet N, et al. Anti-malaria antibody-producing B cell frequencies in adults after a Plasmodium falciparum outbreak in Madagascar. Clin Exp Immunol. 1995;102:529–34.

67. Wipasa J, Suphavilai C, Okell LC, Cook J, Corran PH, Thaikla K, et al. Long-lived antibody and B Cell memory responses to the human malaria parasites, Plasmodium falciparum and Plasmodium vivax. PLoS Pathog. 2010;6:e1000770.

68. Nogaro SI, Hafalla JC, Walther B, Remarque EJ, Tetteh KKA, Conway DJ, et al. The breadth, but not the magnitude, of circulating memory B cell responses to P. falciparum increases with age/exposure in an area of low transmission. PloS One. 2011;6:e25582.

69. Clark EH, Silva CJ, Weiss GE, Li S, Padilla C, Crompton PD, et al. Plasmodium falciparum malaria in the Peruvian Amazon, a region of low transmission, is associated with immunologic memory. Infect Immun. 2012;80:1583–92.

70. Weiss GE, Clark EH, Li S, Traore B, Kayentao K, Ongoiba A, et al. A Positive Correlation between Atypical Memory B Cells and Plasmodium falciparum Transmission Intensity in Cross-Sectional Studies in Peru and Mali. PLoS ONE. 2011;6. doi:10.1371/journal.pone.0015983.

71. Muellenbeck MF, Ueberheide B, Amulic B, Epp A, Fenyo D, Busse CE, et al. Atypical and classical memory B cells produce Plasmodium falciparum neutralizing antibodies. J Exp Med. 2013;210:389–99.

72. Portugal S, Tipton CM, Sohn H, Kone Y, Wang J, Li S, et al. Malaria-associated atypical memory B cells exhibit markedly reduced B cell receptor signaling and effector function. eLife. 2015;4:e07218.

73. Donati D, Zhang LP, Chen Q, Chêne A, Flick K, Nyström M, et al. Identification of a Polyclonal B-Cell Activator in Plasmodium falciparum. Infect Immun. 2004;72:5412–8.

74. Donati D, Mok B, Chêne A, Xu H, Thangarajh M, Glas R, et al. Increased B cell survival and preferential activation of the memory compartment by a malaria polyclonal B cell activator. J Immunol Baltim Md 1950. 2006;177:3035–44.

75. Simone O, Bejarano MT, Pierce SK, Antonaci S, Wahlgren M, Troye-Blomberg M, et al. TLRs innate immunereceptors and Plasmodium falciparum erythrocyte membrane protein 1 (PfEMP1) CIDR1α-driven human polyclonal B-cell activation. Acta Trop. 2011;119:144–50.

76. Nduati E, Gwela A, Karanja H, Mugyenyi C, Langhorne J, Marsh K, et al. The plasma concentration of the B cell activating factor is increased in children with acute malaria. J Infect Dis. 2011;204:962–70.

77. Rickert RC, Jellusova J, Miletic AV. Signaling by the tumor necrosis factor receptor superfamily in B-cell biology and disease. Immunol Rev. 2011;244:115–33.

78. Craxton A, Magaletti D, Ryan EJ, Clark EA. Macrophage- and dendritic cell--dependent regulation of human B-cell proliferation requires the TNF family ligand BAFF. Blood. 2003;101:4464–71.

79. Nardelli B, Belvedere O, Roschke V, Moore PA, Olsen HS, Migone TS, et al. Synthesis and release of B-lymphocyte stimulator from myeloid cells. Blood. 2001;97:198–204.

80. Muehlenbachs A, Fried M, Lachowitzer J, Mutabingwa TK, Duffy PE. Genome-wide expression analysis of placental malaria reveals features of lymphoid neogenesis during chronic infection. J Immunol Baltim Md 1950. 2007;179:557–65.

81. Portugal S, Pierce SK, Crompton PD. Young lives lost as B cells falter: what we are learning about antibody responses in malaria. J Immunol Baltim Md 1950. 2013;190:3039–46.

82. Butler NS, Moebius J, Pewe LL, Traore B, Doumbo OK, Tygrett LT, et al. Therapeutic blockade of PD-L1 and LAG-3 rapidly clears established blood-stage Plasmodium infection. Nat Immunol. 2011;13:188–95.

83. Illingworth J, Butler NS, Roetynck S, Mwacharo J, Pierce SK, Bejon P, et al. Chronic exposure to Plasmodium falciparum is associated with phenotypic evidence of B and T cell exhaustion. J Immunol Baltim Md 1950. 2013;190:1038–47.

84. Zander RA, Obeng-Adjei N, Guthmiller JJ, Kulu DI, Li J, Ongoiba A, et al. PD-1 Co-inhibitory and OX40 Co-stimulatory Crosstalk Regulates Helper T Cell Differentiation and Anti-Plasmodium Humoral Immunity. Cell Host Microbe. 2015;17:628–41.

85. Urban BC, Hien TT, Day NP, Phu NH, Roberts R, Pongponratn E, et al. Fatal Plasmodium falciparum Malaria Causes Specific Patterns of Splenic Architectural Disorganization. Infect Immun. 2005;73:1986–94.

86. Stevenson MM, Kraal G. Histological changes in the spleen and liver of C57BL/6 and A/J mice during Plasmodium chabaudi AS infection. Exp Mol Pathol. 1989;51:80–95.

87. Achtman AH, Khan M, MacLennan ICM, Langhorne J. Plasmodium chabaudi chabaudi infection in mice induces strong B cell responses and striking but temporary changes in splenic cell distribution. J Immunol Baltim Md 1950. 2003;171:317–24.

88. Beattie L, Engwerda CR, Wykes M, Good MF. CD8+ T lymphocyte-mediated loss of marginal metallophilic macrophages following infection with Plasmodium chabaudi chabaudi AS. J Immunol Baltim Md 1950. 2006;177:2518–26.

89. Tran TM, Portugal S, Draper SJ, Crompton PD. Malaria Vaccines: Moving Forward After Encouraging First Steps. Curr Trop Med Rep. 2015;2:1–3.

90. Efficacy and safety of RTS,S/AS01 malaria vaccine with or without a booster dose in infants and children in Africa: final results of a phase 3, individually randomised, controlled trial. The Lancet. 2015;386:31–45.

91. Crompton PD, Pierce SK, Miller LH. Advances and challenges in malaria vaccine development. J Clin Invest. 2010;120:4168–78.

92. World Health Organization. Malaria vaccine: WHO position paper, January 2016 - Recommendations. Vaccine. 2017.

93. WHO | Malaria vaccine technology roadmap. WHO. http://www.who.int/immunization/topics/malaria/vaccine_roadmap/en/. Accessed 30 Jun 2017.

94. Khan SM, Janse CJ, Kappe SHI, Mikolajczak SA. Genetic engineering of attenuated malaria parasites for vaccination. Curr Opin Biotechnol. 2012;23:908–16.

95. Hoffman SL, Billingsley PF, James E, Richman A, Loyevsky M, Li T, et al. Development of a metabolically active, non-replicating sporozoite vaccine to prevent Plasmodium falciparum malaria. Hum Vaccin. 2010;6:97–106.

96. Yoshida N, Nussenzweig RS, Potocnjak P, Nussenzweig V, Aikawa M. Hybridoma produces protective antibodies directed against the sporozoite stage of malaria parasite. Science. 1980;207:71–3.

97. Epstein JE, Tewari K, Lyke KE, Sim BKL, Billingsley PF, Laurens MB, et al. Live Attenuated Malaria Vaccine Designed to Protect Through Hepatic CD8+ T Cell Immunity. Science. 2011;334:475–80.

98. Nganou-Makamdop K, Ploemen I, Behet M, Van Gemert G-J, Hermsen C, Roestenberg M, et al. Reduced Plasmodium berghei sporozoite liver load associates with low protective efficacy after intradermal immunization. Parasite Immunol. 2012;34:562–9.

99. Sissoko MS, Healy SA, Katile A, Omaswa F, Zaidi I, Gabriel EE, et al. Safety and efficacy of PfSPZ Vaccine against Plasmodium falciparum via direct venous inoculation in healthy malaria-exposed adults in Mali: a randomised, double-blind phase 1 trial. Lancet Infect Dis. 2017;0. doi:10.1016/S1473-3099(17)30104-4.

100. Sauerwein RW, Roestenberg M, Moorthy VS. Experimental human challenge infections can accelerate clinical malaria vaccine development. Nat Rev Immunol. 2011;11:57–64.

101. Engwerda CR, Minigo G, Amante FH, McCarthy JS. Experimentally induced blood stage malaria infection as a tool for clinical research. Trends Parasitol. 2012;28:515–21.

102. James SP. Some general Results of a Study of induced Malaria in England. Trans R Soc Trop Med Hyg. 1931;24. https://www.cabdirect.org/cabdirect/abstract/19311000328. Accessed 5 Jul 2017.

103. Roestenberg M, Bijker EM, Sim BKL, Billingsley PF, James ER, Bastiaens GJH, et al. Controlled Human Malaria Infections by Intradermal Injection of Cryopreserved Plasmodium falciparum Sporozoites. Am J Trop Med Hyg. 2013;88:5–13.

104. Shekalaghe S, Rutaihwa M, Billingsley PF, Chemba M, Daubenberger CA, James ER, et al. Controlled human malaria infection of Tanzanians by intradermal injection of aseptic, purified, cryopreserved Plasmodium falciparum sporozoites. Am J Trop Med Hyg. 2014;91:471–80.

105. Mordmüller B, Supan C, Sim KL, Gómez-Pérez GP, Ospina Salazar CL, Held J, et al. Direct venous inoculation of Plasmodium falciparum sporozoites for controlled human malaria infection: a dose-finding trial in two centres. Malar J. 2015;14:117.

106. Breedveld FC. Therapeutic monoclonal antibodies. Lancet Lond Engl. 2000;355:735–40.

107. Corti D, Lanzavecchia A. Efficient Methods To Isolate Human Monoclonal Antibodies from Memory B Cells and Plasma Cells. Microbiol Spectr. 2014;2.

108. Riglar DT, Richard D, Wilson DW, Boyle MJ, Dekiwadia C, Turnbull L, et al. Super-resolution dissection of coordinated events during malaria parasite invasion of the human erythrocyte. Cell Host Microbe. 2011;9:9–20.

109. Cowman AF, Berry D, Baum J. The cellular and molecular basis for malaria parasite invasion of the human red blood cell. J Cell Biol. 2012;198:961–71.

110. Barfod L, Dobrilovic T, Magistrado P, Khunrae P, Viwami F, Bruun J, et al. Chondroitin Sulfate A-Adhering Plasmodium falciparum-Infected Erythrocytes Express Functionally Important Antibody Epitopes Shared by Multiple Variants. J Immunol Baltim Md 1950. 2010;185:7553–61.

111. Barfod L, Bernasconi NL, Dahlbäck M, Jarrossay D, Andersen PH, Salanti A, et al. Human pregnancy-associated malaria-specific B cells target polymorphic, conformational epitopes in VAR2CSA. Mol Microbiol. 2007;63:335–47.

112. Soerli J, Barfod L, Lavstsen T, Bernasconi NL, Lanzavecchia A, Hviid L. Human monoclonal IgG selection of Plasmodium falciparum for the expression of placental malaria-specific variant surface antigens. Parasite Immunol. 2009;31:341–6.

113. Stubbs J, Olugbile S, Saidou B, Simpore J, Corradin G, Lanzavecchia A. Strain-transcending Fc-dependent killing of Plasmodium falciparum by merozoite surface protein 2 allele-specific human antibodies. Infect Immun. 2011;79:1143–52.

114. Kollmann TR. Variation between Populations in the Innate Immune Response to Vaccine Adjuvants. Front Immunol. 2013;4. doi:10.3389/fimmu.2013.00081.

115. Levine MM. Immunogenicity and efficacy of oral vaccines in developing countries: lessons from a live cholera vaccine. BMC Biol. 2010;8:129.

116. Muyanja E, Ssemaganda A, Ngauv P, Cubas R, Perrin H, Srinivasan D, et al. Immune activation alters cellular and humoral responses to yellow fever 17D vaccine. J Clin Invest. 2014;124:3147–58.

117. Clemens J, Jodar L. Introducing new vaccines into developing countries: obstacles, opportunities and complexities. Nat Med. 2005;11 4 Suppl:S12-15.

118. Poland GA, Ovsyannikova IG, Jacobson RM. Vaccine immunogenetics: bedside to bench to population. Vaccine. 2008;26:6183–8.

119. Keitany GJ, Kim KS, Krishnamurty AT, Hondowicz BD, Hahn WO, Dambrauskas N, et al. Blood Stage Malaria Disrupts Humoral Immunity to the Pre-erythrocytic Stage Circumsporozoite Protein. Cell Rep. 2016;17:3193–205.

120. Wendel BS, He C, Qu M, Wu D, Hernandez SM, Ma K-Y, et al. Accurate immune repertoire sequencing reveals malaria infection driven antibody lineage diversification in young children. Nat Commun. 2017;8:531.

121. Plotkin SA. Correlates of Protection Induced by Vaccination. Clin Vaccine Immunol CVI. 2010;17:1055–65.

122. Boes M. Role of natural and immune IgM antibodies in immune responses. Mol Immunol. 2000;37:1141–9.

123. Clough B, Atilola FA, Black J, Pasvol G. Plasmodium falciparum: the importance of IgM in the rosetting of parasite-infected erythrocytes. Exp Parasitol. 1998;89:129–32.

124. Ghumra A, Semblat J-P, McIntosh RS, Raza A, Rasmussen IB, Braathen R, et al. Identification of residues in the Cμ4 domain of polymeric IgM essential for interaction with P. falciparum erythrocyte membrane protein 1 (PfEMP1). J Immunol Baltim Md 1950. 2008;181:1988–2000.

125. Rowe JA, Shafi J, Kai OK, Marsh K, Raza A. Nonimmune IgM, but not IgG binds to the surface of Plasmodium falciparum-infected erythrocytes and correlates with rosetting and severe malaria. Am J Trop Med Hyg. 2002;66:692–9.

126. Scholander C, Treutiger CJ, Hultenby K, Wahlgren M. Novel fibrillar structure confers adhesive property to malaria-infected erythrocytes. Nat Med. 1996;2:204–8.

127. Couper KN, Phillips RS, Brombacher F, Alexander J. Parasite-specific IgM plays a significant role in the protective immune response to asexual erythrocytic stage Plasmodium chabaudi AS infection. Parasite Immunol. 2005;27:171–80.

128. Yilmaz B, Portugal S, Tran TM, Gozzelino R, Ramos S, Gomes J, et al. Gut microbiota elicits a protective immune response against malaria transmission. Cell. 2014;159:1277–89.

129. Racine R, McLaughlin M, Jones DD, Wittmer ST, MacNamara KC, Woodland DL, et al. IgM production by bone marrow plasmablasts contributes to long-term protection against intracellular bacterial infection. J Immunol Baltim Md 1950. 2011;186:1011–21.

130. Seifert M, Przekopowitz M, Taudien S, Lollies A, Ronge V, Drees B, et al. Functional capacities of human IgM memory B cells in early inflammatory responses and secondary germinal center reactions. Proc Natl Acad Sci U S A. 2015;112:E546-555.

131. McHeyzer-Williams LJ, McHeyzer-Williams MG. Antigen-specific memory B cell development. Annu Rev Immunol. 2005;23:487–513.

132. MacLennan IC. Germinal centers. Annu Rev Immunol. 1994;12:117–39.

133. Tarlinton DM. Evolution in miniature: selection, survival and distribution of antigen reactive cells in the germinal centre. Immunol Cell Biol. 2008;86:133–8.

134. Maul RW, Gearhart PJ. AID and somatic hypermutation. Adv Immunol. 2010;105:159–91.

135. Anderson SM, Tomayko MM, Ahuja A, Haberman AM, Shlomchik MJ. New markers for murine memory B cells that define mutated and unmutated subsets. J Exp Med. 2007;204:2103–14.

136. Taylor JJ, Pape KA, Jenkins MK. A germinal center-independent pathway generates unswitched memory B cells early in the primary response. J Exp Med. 2012;209:597–606.

137. Kaji T, Ishige A, Hikida M, Taka J, Hijikata A, Kubo M, et al. Distinct cellular pathways select germline-encoded and somatically mutated antibodies into immunological memory. J Exp Med. 2012;209:2079–97.

138. Alugupalli KR, Leong JM, Woodland RT, Muramatsu M, Honjo T, Gerstein RM. B1b lymphocytes confer T cell-independent long-lasting immunity. Immunity. 2004;21:379–90.

139. Obukhanych TV, Nussenzweig MC. T-independent type II immune responses generate memory B cells. J Exp Med. 2006;203:305–10.

140. Yang Y, Ghosn EEB, Cole LE, Obukhanych TV, Sadate-Ngatchou P, Vogel SN, et al. Antigen-specific memory in B-1a and its relationship to natural immunity. Proc Natl Acad Sci U S A. 2012;109:5388–93.

141. Klein U, Küppers R, Rajewsky K. Evidence for a large compartment of IgM-expressing memory B cells in humans. Blood. 1997;89:1288–98.

142. Pape KA, Taylor JJ, Maul RW, Gearhart PJ, Jenkins MK. Different B cell populations mediate early and late memory during an endogenous immune response. Science. 2011;331:1203–7.

143. Bohannon C, Powers R, Satyabhama L, Cui A, Tipton C, Michaeli M, et al. Long-lived antigen-induced IgM plasma cells demonstrate somatic mutations and contribute to long-term protection. Nat Commun. 2016;7. doi:10.1038/ncomms11826.

144. Krishnamurty AT, Thouvenel CD, Portugal S, Keitany GJ, Kim KS, Holder A, et al. Somatically Hypermutated Plasmodium-Specific IgM(+) Memory B Cells Are Rapid, Plastic, Early Responders upon Malaria Rechallenge. Immunity. 2016;45:402–14.

145. Bendtzen K, Hansen MB, Ross C, Svenson M. High-avidity autoantibodies to cytokines. Immunol Today. 1998;19:209–11.

146. Notkins AL. Polyreactivity of antibody molecules. Trends Immunol. 2004;25:174–9.

147. Cooper NR. The classical complement pathway: activation and regulation of the first complement component. Adv Immunol. 1985;37:151–216.

148. Haas KM, Poe JC, Steeber DA, Tedder TF. B-1a and B-1b cells exhibit distinct developmental requirements and have unique functional roles in innate and adaptive immunity to S. pneumoniae. Immunity. 2005;23:7–18.

149. Diamond MS, Sitati EM, Friend LD, Higgs S, Shrestha B, Engle M. A critical role for induced IgM in the protection against West Nile virus infection. J Exp Med. 2003;198:1853–62.

150. Throsby M, van den Brink E, Jongeneelen M, Poon LLM, Alard P, Cornelissen L, et al. Heterosubtypic neutralizing monoclonal antibodies cross-protective against H5N1 and H1N1 recovered from human IgM+ memory B cells. PloS One. 2008;3:e3942.

151. Skountzou I, Satyabhama L, Stavropoulou A, Ashraf Z, Esser ES, Vassilieva E, et al. Influenza virus-specific neutralizing IgM antibodies persist for a lifetime. Clin Vaccine Immunol CVI. 2014;21:1481–9.

152. Harada Y, Muramatsu M, Shibata T, Honjo T, Kuroda K. Unmutated immunoglobulin M can protect mice from death by influenza virus infection. J Exp Med. 2003;197:1779–85.

153. Vauloup-Fellous C, Grangeot-Keros L. Humoral immune response after primary rubella virus infection and after vaccination. Clin Vaccine Immunol CVI. 2007;14:644–7.

154. Clutterbuck EA, Oh S, Hamaluba M, Westcar S, Beverley PCL, Pollard AJ. Serotype-specific and age-dependent generation of pneumococcal polysaccharide-specific memory B-cell and antibody responses to immunization with a pneumococcal conjugate vaccine. Clin Vaccine Immunol CVI. 2008;15:182–93.

155. Helfand RF, Gary HE, Atkinson WL, Nordin JD, Keyserling HL, Bellini WJ. Decline of Measles-Specific Immunoglobulin M Antibodies after Primary Measles, Mumps, and Rubella Vaccination. Clin Diagn Lab Immunol. 1998;5:135–8.

156. Baxendale HE, Johnson M, Stephens RCM, Yuste J, Klein N, Brown JS, et al. Natural human antibodies to pneumococcus have distinctive molecular characteristics and protect against pneumococcal disease. Clin Exp Immunol. 2008;151:51–60.

157. El Sahly HM, Atmar RL, Patel SM, Wells JM, Cate T, Ho M, et al. Safety, reactogenicity and immunogenicity of Francisella tularensis live vaccine strain in humans. Vaccine. 2009;27:4905–11.

158. Sheppard NC, Bates AC, Sattentau QJ. A functional human IgM response to HIV-1 Env after immunization with NYVAC HIV C. AIDS Lond Engl. 2007;21:524–7.

159. Mebius RE, Kraal G. Structure and function of the spleen. Nat Rev Immunol. 2005;5:606–16.

160. Cerutti A, Cols M, Puga I. Marginal zone B cells: virtues of innatelike antibody-producing lymphocytes. Nat Rev Immunol. 2013;13:118–32.

161. Berkowska MA, Driessen GJA, Bikos V, Grosserichter-Wagener C, Stamatopoulos K, Cerutti A, et al. Human memory B cells originate from three distinct germinal center-dependent and -independent maturation pathways. Blood. 2011;118:2150–8.

162. Weller S, Braun MC, Tan BK, Rosenwald A, Cordier C, Conley ME, et al. Human blood IgM "memory" B cells are circulating splenic marginal zone B cells harboring a prediversified immunoglobulin repertoire. Blood. 2004;104:3647–54.

163. Rathore D, Sacci JB, de la Vega P, McCutchan TF. Binding and invasion of liver cells by Plasmodium falciparum sporozoites. Essential involvement of the amino terminus of circumsporozoite protein. J Biol Chem. 2002;277:7092–8.

164. Bongfen SE, Ntsama PM, Offner S, Smith T, Felger I, Tanner M, et al. The N-terminal domain of Plasmodium falciparum circumsporozoite protein represents a target of protective immunity. Vaccine. 2009;27:328–35.

165. Brennan FR, Morton LD, Spindeldreher S, Kiessling A, Allenspach R, Hey A, et al. Safety and immunotoxicity assessment of immunomodulatory monoclonal antibodies. mAbs. 2010;2:233–55.

166. Chapman K, Pullen N, Graham M, Ragan I. Preclinical safety testing of monoclonal antibodies: the significance of species relevance. Nat Rev Drug Discov. 2007;6:120–6.

167. Mordmüller B, Surat G, Lagler H, Chakravarty S, Ishizuka AS, Lalremruata A, et al. Sterile protection against human malaria by chemoattenuated PfSPZ vaccine. Nature. 2017;542:445–9.

168. van Schaijk BCL, Ploemen IHJ, Annoura T, Vos MW, Foquet L, van Gemert G-J, et al. A genetically attenuated malaria vaccine candidate based on P. falciparum b9/slarp gene-deficient sporozoites. eLife. 2014;3.

169. Martin F, Kearney JF. Marginal-zone B cells. Nat Rev Immunol. 2002;2:323–35.

170. Weill J-C, Weller S, Reynaud C-A. Human marginal zone B cells. Annu Rev Immunol. 2009;27:267–85.

171. Pillai S, Cariappa A. The follicular versus marginal zone B lymphocyte cell fate decision. Nat Rev Immunol. 2009;9:767–77.

172. Afonin PV, Fokin AV, Tsygannik IN, Mikhailova IY, Onoprienko LV, Mikhaleva II, et al. Crystal structure of an anti-interleukin-2 monoclonal antibody Fab complexed with an antigenic nonapeptide. Protein Sci Publ Protein Soc. 2001;10:1514–21.

Appendix

A: Public antibodies to malaria antigens generated by two *LAIR1* insertion modalities

LETTER

doi:10.1038/nature23670

Public antibodies to malaria antigens generated by two *LAIR1* insertion modalities

Kathrin Pieper[1]*, Joshua Tan[1,2]*, Luca Piccoli[1]*, Mathilde Foglierini[1,3], Sonia Barbieri[1], Yiwei Chen[1,4], Chiara Silacci-Fregni[1], Tobias Wolf[1,4], David Jarrossay[1], Marica Anderle[1], Abdirahman Abdi[5], Francis M. Ndungu[5], Ogobara K. Doumbo[6], Boubacar Traore[6], Tuan M. Tran[7], Said Jongo[8], Isabelle Zenklusen[9,10], Peter D. Crompton[11], Claudia Daubenberger[9,10], Peter C. Bull[12], Federica Sallusto[1,4] & Antonio Lanzavecchia[1,4]

In two previously described donors, the extracellular domain of LAIR1, a collagen-binding inhibitory receptor encoded on chromosome 19 (ref. 1), was inserted between the V and DJ segments of an antibody. This insertion generated, through somatic mutations, broadly reactive antibodies against RIFINs, a type of variant antigen expressed on the surface of *Plasmodium falciparum*-infected erythrocytes[2]. To investigate how frequently such antibodies are produced in response to malaria infection, we screened plasma from two large cohorts of individuals living in malaria-endemic regions. Here we report that 5–10% of malaria-exposed individuals, but none of the European blood donors tested, have high levels of LAIR1-containing antibodies that dominate the response to infected erythrocytes without conferring enhanced protection against febrile malaria. By analysing the antibody-producing B cell clones at the protein, cDNA and gDNA levels, we characterized additional *LAIR1* insertions between the V and DJ segments and discovered a second insertion modality whereby the *LAIR1* exon encoding the extracellular domain and flanking intronic sequences are inserted into the switch region. By exon shuffling, this mechanism leads to the production of bispecific antibodies in which the LAIR1 domain is precisely positioned at the elbow between the VH and CH1 domains. Additionally, in one donor the genomic DNA encoding the VH and CH1 domains was deleted, leading to the production of a camel-like LAIR1-containing antibody. Sequencing of the switch regions of memory B cells from European blood donors revealed frequent templated inserts originating from transcribed genes that, in rare cases, comprised exons with orientations and frames compatible with expression. These results reveal different modalities of *LAIR1* insertion that lead to public and dominant antibodies against infected erythrocytes and suggest that insertion of templated DNA represents an additional mechanism of antibody diversification that can be selected in the immune response against pathogens and exploited for B cell engineering.

LAIR1-containing antibodies were initially isolated from two Kenyan donors who were selected from a large cohort of more than 500 individuals for their capacity to produce broadly reactive antibodies to *P. falciparum*-infected erythrocytes[2]. To establish the prevalence of LAIR1-containing antibodies in malaria-exposed individuals, we screened plasma samples from two large cohorts in Tanzania[3] and Mali[4]. To identify LAIR1-containing antibodies irrespective of their specificity for parasite isolates, we developed a two-determinant immunoassay using beads coated with anti-LAIR1 or control antibodies.

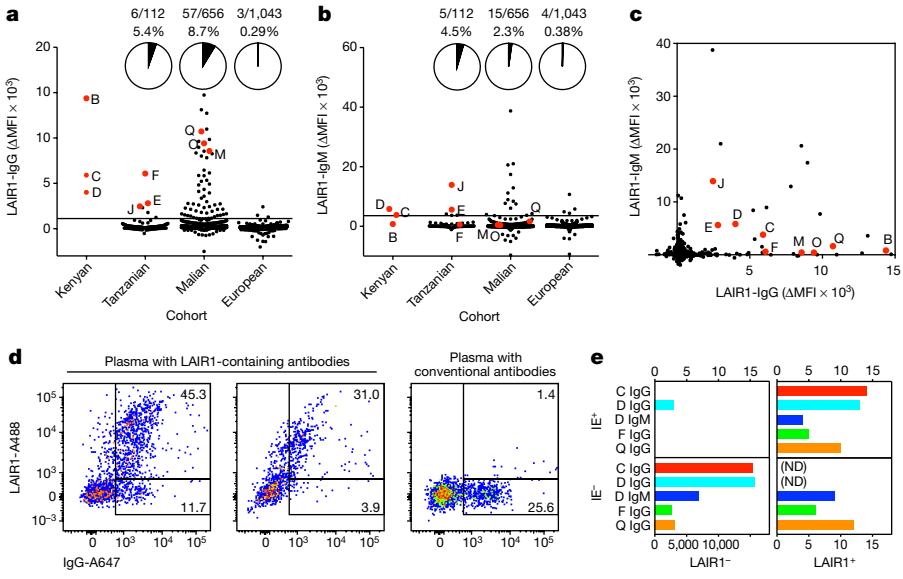

Figure 1 | Prevalence and dominance of LAIR1-containing antibodies in malaria-endemic regions. a, **b**, Prevalence of LAIR1-containing IgG and IgM in African individuals living in malaria-endemic regions and in European blood donors. Donors from whom LAIR1-containing antibodies were isolated are highlighted in red. **c**, Comparison between LAIR1-containing IgG and IgM values. MFI, median fluorescence intensity. Data points with a ΔMFI value below −2,000 are not shown. **d**, Staining of infected erythrocytes by LAIR1-containing IgG and conventional IgG from three representative donors. **e**, Dominance of LAIR1-containing B cell clones among memory B cells specific for infected erythrocytes. Monoclonal antibodies isolated from immortalized memory B cells were classified according to their ability to bind to infected erythrocytes and the presence of a *LAIR1* insert. Bars show number of IgG or IgM monoclonal antibodies isolated from each donor. For gating strategy, see Supplementary Fig. 1. ND, not determined.

[1]Institute for Research in Biomedicine, Università della Svizzera Italiana, Via Vincenzo Vela 6, 6500 Bellinzona, Switzerland. [2]Nuffield Department of Clinical Medicine, University of Oxford, John Radcliffe Hospital, Headington, Oxford OX3 9DU, UK. [3]Swiss Institute of Bioinformatics (SIB), 1015 Lausanne, Switzerland. [4]Institute for Microbiology, ETH Zurich, Wolfgang-Pauli-Strasse 10, 8093 Zurich, Switzerland. [5]KEMRI-Wellcome Trust Research Programme, CGMRC, PO Box 230, 80108 Kilifi, Kenya. [6]Malaria Research and Training Centre, University of Sciences, Technique, and Technology of Bamako, 91094 Bamako, Mali. [7]Division of Infectious Diseases, Department of Medicine, Indiana University School of Medicine, 46202 Indianapolis, Indiana, USA. [8]Ifakara Health Institute, Bagamoyo Clinical Trial Unit, P.O. Box 74, Bagamoyo, Tanzania. [9]Swiss Tropical and Public Health Institute, Clinical Immunology Unit, 4002 Basel, Switzerland. [10]University of Basel, Petersplatz 1, 4003 Basel, Switzerland. [11]Laboratory of Immunogenetics, National Institute of Allergy and Infectious Diseases, National Institutes of Health, Rockville, Maryland 20852, USA. [12]Department of Pathology, University of Cambridge, Cambridge CB2 1QP, UK.
*These authors contributed equally to this work.

Six out of 112 Tanzanian donors (5.4%) and 57 out of 656 Malian donors (8.7%) had detectable levels of LAIR1-containing IgG (Fig. 1a). In addition, 2–4% of African donors had LAIR1-containing IgM, with no or variable levels of LAIR1-containing IgG (Fig. 1b, c). By contrast, only 3 and 4 out of 1,043 European blood donors showed a low positive result in the assays for LAIR1-containing IgG and IgM, respectively. The presence of LAIR1-containing antibodies was confirmed by the isolation of 52 immortalized B cell clones from seven East and West African donors (Extended Data Table 1 and Supplementary Table 1), whereas we were not able to isolate LAIR1-containing monoclonal antibodies from four European donors that showed serum reactivity. The finding that 5–10% of individuals living in malaria-endemic regions produce LAIR1-containing antibodies is suggestive of a public antibody response.

To investigate the contribution of LAIR1-containing antibodies to the response to infected erythrocytes, we dissected this response at the polyclonal and monoclonal levels. Staining of infected erythrocytes with plasma from selected individuals with LAIR1-containing antibodies revealed that most infected erythrocytes were recognized by the LAIR1-containing antibodies, whereas only a minority of infected erythrocytes was recognized by conventional IgG (Fig. 1d). Furthermore, when immortalized memory B cell clones from four donors were analysed for reactivity to infected erythrocytes and for the presence of LAIR1, all of the infected erythrocyte-recognizing monoclonal antibodies from three donors and most of such antibodies from the fourth donor contained the *LAIR1* insert (Fig. 1e). These findings suggest that, in certain individuals, circulating antibody and memory B cell responses are dominated by LAIR1-containing antibodies, a finding that may be explained both by the breadth of these antibodies' reactivities and by clonal expansion of the B cells that produce these antibodies.

To investigate the nature of the *LAIR1* insertion, we sequenced cDNA and gDNA from B cell clones isolated from different individuals. As reported for the first two Kenyan donors[2], the B cell clones isolated from four Malian and Tanzanian donors (E, F, O and Q) contained an insertion of the *LAIR1* exon with flanking intronic sequences between the V and DJ segments, positioning the LAIR1 domain in the CDR3 loop (Fig. 2a and Extended Data Fig. 1). The size of the insert and the partial splicing of the upstream intronic region differed between donors, but were identical in the sister clones isolated from each individual, indicating that in each donor the LAIR1-containing antibody response is monoclonal.

Strikingly, B cell clones from three additional donors showed a different insertion modality (Fig. 2b–d). The cDNA of clones isolated from donors M (Malian) and J (Tanzanian) contained only the *LAIR1* exon, which was precisely located between the JH and CH1 domains. In both cases, gDNA analysis revealed that a DNA fragment comprising the *LAIR1* exon flanked by intronic sequences was inserted into the switch-μ region (Extended Data Fig. 2) and, by alternative splicing, gave rise to two mRNA variants with or without the *LAIR1* insert. This was confirmed by the production of antibodies with or without LAIR1 in similar proportions by a single B cell clone (Fig. 2e). Another example of *LAIR1* insertion into the switch region was observed in donor B (Kenyan), from whom we isolated a B cell clone (MGB47) producing a truncated LAIR1-containing IgG3 heavy chain without an attached light chain (Fig. 2f, g). In this clone, the gDNA carried multiple deletions that removed most of the VDJ and the entire CH1 region, leading to the production of a camel-like antibody[5] (Fig. 2d). Together, these findings highlight a new modality of exon insertion in the switch region that can add an extra domain to an antibody.

The two insertion modalities result in the production of antibodies with non-conventional structures in which an additional domain is inserted into the CDR3 region or into the elbow between VH and CH1 (Fig. 3a). To investigate the effect of the insert position on antibody specificity, we designed different constructs in which unmutated LAIR1, mutated LAIR1 or other Ig-like domains were inserted into

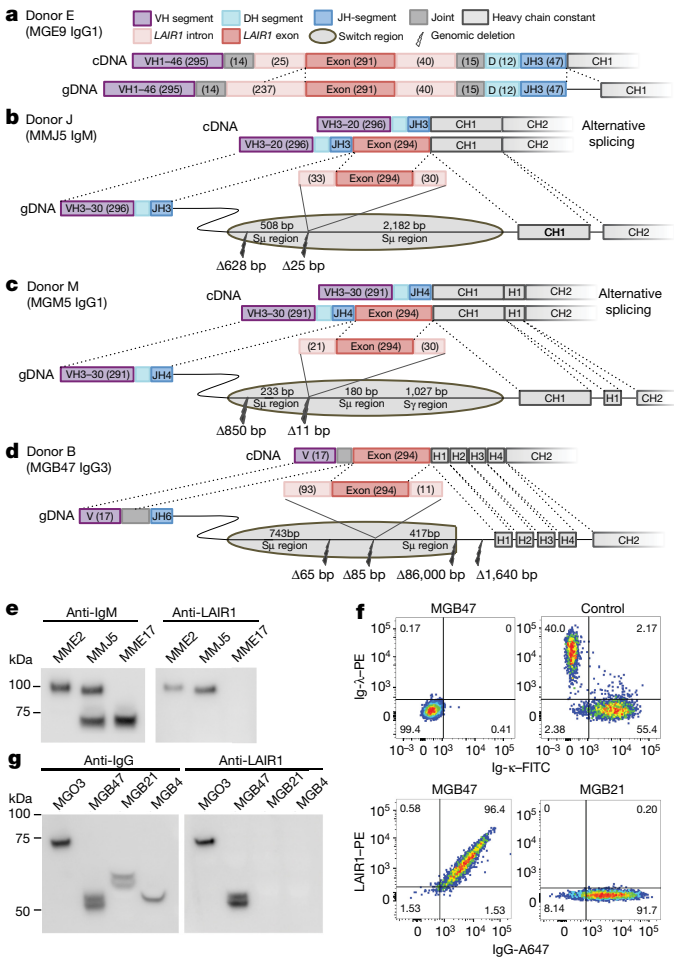

Figure 2 | LAIR1-containing antibodies produced by two insertion modalities. a–d, cDNA and gDNA organization in representative B cell clones from different donors. Donors E and J are Tanzanian, donor M is Malian and donor B is Kenyan. **e**, Western blot analysis of culture supernatants of B cell clones with *LAIR1* insertion in the VDJ (MME2, donor E) or in the switch region (MMJ5, donor J) or a conventional antibody (MME17) ($n = 4$). **f**, Surface staining of clone MGB47 showing co-expression of LAIR1 and IgG and lack of light chain ($n = 3$). A positive control and a LAIR1-negative clone (MGB21) are shown for comparison. For gating strategy, see Supplementary Fig. 1. **g**, Western blot analysis of culture supernatant of the camel-like clone MGB47 ($n = 4$). Also shown are supernatants from clones MGO3 (*LAIR1* insertion in VDJ region), MGB21 (IgG3 control) and MGB4 (IgG1 control). For gel source data, see Supplementary Fig. 2.

the CDR3 or elbow regions of an antibody of known specificity that was used as a scaffold (Fig. 3b). Antibody constructs carrying LAIR1 stained infected erythrocytes and were recognized by an anti-LAIR1 antibody, independent of the position of LAIR1 in the scaffold. While insertion of LAIR1 into the CDR3 region of an antibody specific for granulocyte–macrophage colony-stimulating factor (GM-CSF)[6] abolished binding to GM-CSF, insertion of LAIR1, programmed cell death-1 (PD-1), or signalling lymphocytic activation molecule family member (SLAM) Ig-like domains into the elbow region did not affect binding to GM-CSF. This indicates that the VH–CH1 elbow is permissive for insertions of different domains without affecting the original antibody specificity and may therefore be suitable for the generation of bispecific antibodies.

To analyse the role of somatic mutations, we aligned and compared the LAIR1 sequences of 52 antibodies (Extended Data Fig. 3 and Extended Data Table 1). *LAIR1* inserts between the V and DJ segments carried several amino acid substitutions clustering at hot spots around

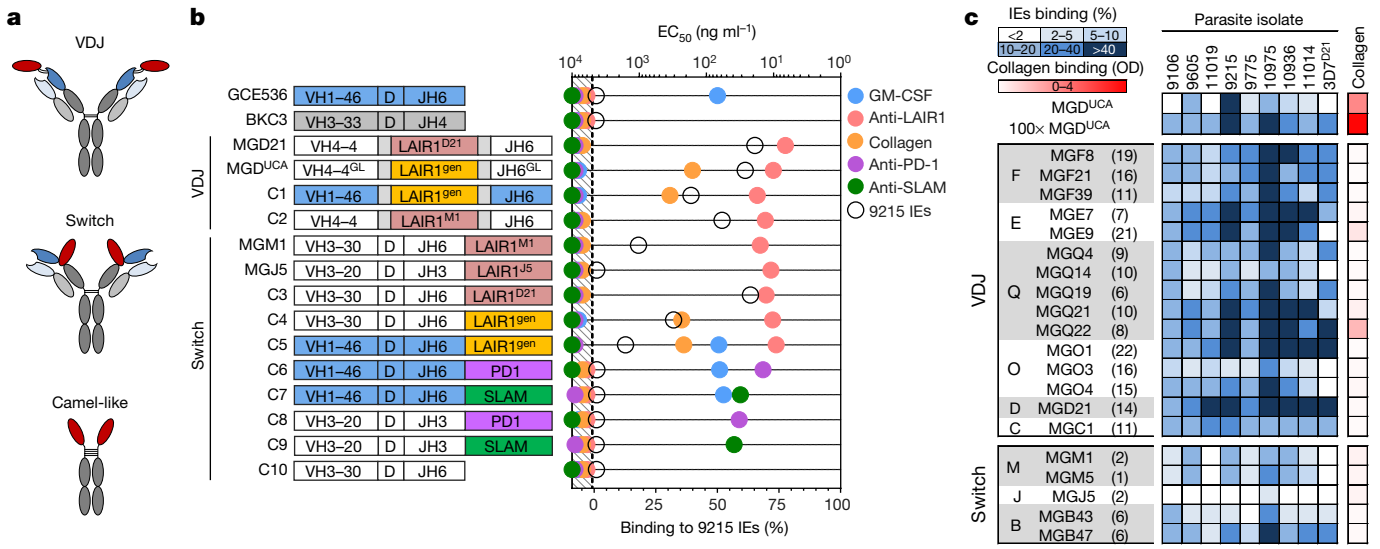

Figure 3 | The influence of insert position and somatic mutations on antibody specificity. a, Schematic representation of LAIR1-containing antibodies produced by different insertion modalities. **b**, Scheme of constructs (C1–C10) containing LAIR1 or other Ig-like domains in different positions that were tested for binding to a set of antigens or anti-domain antibodies by enzyme-linked immunosorbent assay (ELISA) or flow cytometry. The construct domains and their binding values to the cognate ligands are colour coded as depicted in the figure. The V and J segments that do not contribute to any binding are not coloured. BKC3 (grey) is a negative control. $LAIR1^{D21}$, $LAIR1^{M1}$ and $LAIR1^{J5}$ are the exons from MGD21, MGM1 and MGJ5 antibodies, respectively. $LAIR1^{gen}$ is the unmutated genomic sequence of LAIR1 encoded on chromosome 19. MGD^{UCA}, unmutated common ancestor of donor D antibodies; GL, germline; IEs, infected erythrocytes. Data are from one experiment out of two. EC_{50}, half-maximum effective concentration. **c**, Binding of LAIR1-containing antibodies to erythrocytes infected with nine parasite isolates and to human collagen ($n = 1$). Values refer to binding at a concentration of 1 μg ml^{-1}. The MGD^{UCA} was also tested at 100 μg ml^{-1}. The number of amino acid substitutions is shown in brackets next to the antibody names. OD, optical density.

positions 67, 77 and 102 that determined distinct patterns of reactivity with parasite isolates, as well as loss of collagen binding (Fig. 3c). By contrast, LAIR1 inserted into the switch region carried only a few substitutions, which were, however, sufficient to abolish collagen binding. In particular, the camel-like antibody MGB47, which had the highest level of amino acid substitutions among those with inserts in the switch region, showed considerable breadth, staining eight out of the nine parasites tested. Notably, unmutated LAIR1 bound to a few isolates when tested at 1 μg ml^{-1} and to all parasites when tested at a 100-fold higher concentration (Fig. 3c). We conclude that the unmutated LAIR1 domain binds with low affinity to most parasite isolates and that mutations can increase affinity and modify the spectrum of cross-reactivity. Furthermore, the finding that collagen binding is lost even in cases where the somatic mutation mechanism is less effective, as in the case of insertions into the switch region, suggests that there is strong pressure to 'redeem' this B cell receptor from autoreactivity[7].

The insertion of an extra exon into the switch region represents a new modality of antibody diversification, analogous to exon shuffling[8,9], that has the potential to generate a panoply of bispecific antibodies. To investigate how generally and how frequently templated DNA sequences are inserted into the switch region, we isolated gDNA from switched memory B cells of European blood donors, amplified the switch regions and sequenced them using the Illumina platform (Extended Data Fig. 4). Using a bioinformatics pipeline, we identified templated inserts at a frequency of approximately one in more than 1,000 B cells, with the length of the inserts ranging from below 100 to over 1,000 nucleotides (Fig. 4a, Extended Data Fig. 5 and Supplementary Tables 2–4). Switch region inserts could also be detected using long-read MinION sequencing of intact amplicons, which provided a suitable platform for insert identification, in spite of its high error rate[10]. Using MinION, we confirmed the identity of several inserts using biological replicates and estimated a higher frequency of templated inserts, in the region of one in a few hundred switched memory B cells (Fig. 4a and Extended Data Fig. 6). By contrast, no insert was detected in the switch region of naive B cells (Fig. 4c). Most of the inserts were derived from genic regions from all chromosomes and in particular from genes expressed in B cells, such as *PAX5* and *EBF1* (Fig. 4b, e, f and Extended Data Fig. 7). The genic inserts, which account for 75% of all inserts, were derived from introns and exons, and in some cases comprised an entire exon with preserved splice sites (Fig. 4d). A fraction of the latter had the correct frame and orientation for the potential expression of an extra protein sequence in the immunoglobulin elbow (Extended Data Fig. 8). Together, the above findings indicate that templated inserts derived from transcribed genes are found frequently in the switch regions of memory B cells.

We have shown that LAIR1-containing antibodies are produced by two insertion modalities and have a prevalence of 5–10% of individuals exposed to malaria infection, suggesting that they may contribute to acquired immunity to blood-stage parasites. However, in spite of their breadth and opsonizing activity[2], the presence of LAIR1-containing antibodies did not confer improved protection against febrile malaria (Extended Data Fig. 9), a finding that may be explained by the fact that the LAIR1-containing antibodies recognize only a fraction of cultured parasites and may allow the selection of escape mutants. A thorough investigation of the role of the LAIR1-containing antibodies *in vivo* will require the isolation of autologous parasites from the individuals who possess these antibodies.

It is unusual that, in all cases observed so far, the LAIR1-containing antibodies are produced by a single expanded B cell clone that dominates the antibody response to infected erythrocytes in these individuals. The finding that unmutated LAIR1 has the inherent ability to bind to infected erythrocytes explains how the insertion of this domain results in the generation of public antibodies with a common specificity. Furthermore, the fact that this domain binds to all parasite isolates tested, albeit with low affinity, suggests a mechanism for the extraordinary clonal expansion and selection of mutated antibody variants with improved affinity and breadth by repeated infections with different *P. falciparum* parasites. These findings illustrate, in a biologically relevant system, the power of clonal selection driven by both antigen binding and loss of self-reactivity. Furthermore, the binding of infected erythrocytes to LAIR1 suggests the possibility that the parasite might target this inhibitory receptor to modulate the host immune response.

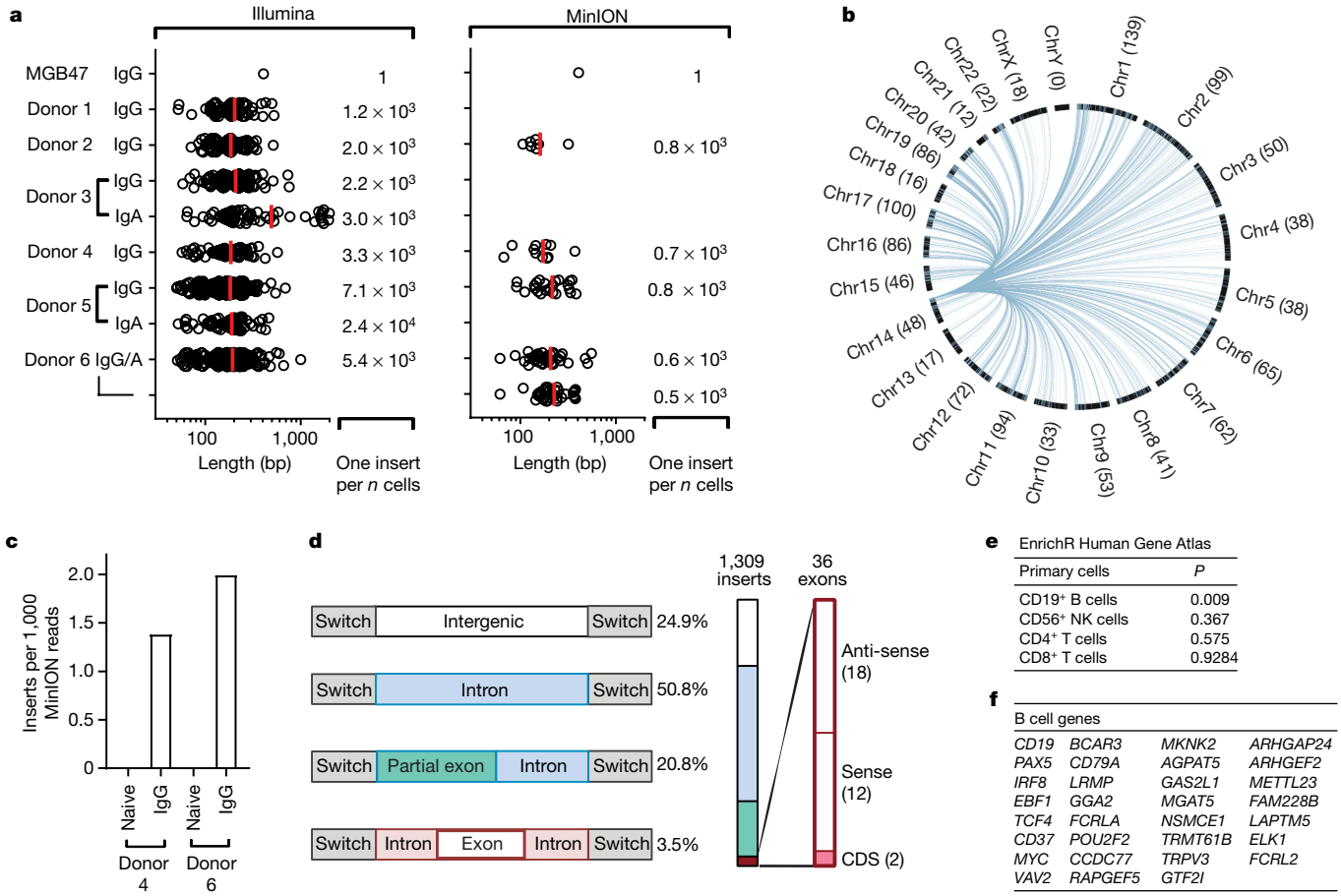

Figure 4 | Frequent occurrence of templated inserts in the switch region. a, Inserts in the switch region were detected by amplification and Illumina MiSeq sequencing (left) of six polyclonal samples of primary B cells from European donors and of the MGB47 monoclonal cell line as a control. Biological replicates were analysed with MinION technology (right). Shown are the size distribution of all detected inserts and the estimated number of B cells that need to be analysed to detect one insert. For each technology, two independent experiments with 2–3 donors were performed. Red lines show mean values. **b**, Circos plot showing the origin of the inserts from different chromosomes. **c**, Insert frequencies in switch-μ (Sμ) regions of naive B cells and in μ–γ joint regions of IgG memory B cells. **d**, Frequency of intergenic and different types of genic inserts. The red bar shows the number of exon-containing inserts with preserved splice sites in anti-sense and sense orientation. Inserts with the correct orientation and frame of the coding sequence (CDS) are highlighted in pink. **e**, EnrichR analysis on the Human Gene Atlas reveals significant enrichment for B cell-associated genes. **f**, List of B cell-specific genes donating inserts.

The insertion of *LAIR1* into the switch region, resulting in the expression of a new domain in the elbow between the VH and CH1 domains, represents a new and possibly general example of protein engineering by exon shuffling[8,9], as suggested by the frequent occurrence of templated inserts. Although insertions in the CDR3 loop result in monospecific antibodies, insertions in the switch region do not affect the specificity of the original antibody but rather add a second specificity that is found in approximately half of the antibodies produced by alternative splicing. We are not aware of deliberate attempts to engineer the antibody elbow, and in this context, nature has shown considerable ingenuity by taking advantage of the exon shuffling principle.

It has been reported that, in mice, chronic *Plasmodium chabaudi* infection promotes genomic instability that leads to chromosomal translocations involving the switch region[11]. Although we cannot exclude the possibility that the *LAIR1* insertions in the switch region observed in African donors may have been promoted by malaria infection, the frequent templated insertions found in European blood donors would be consistent with a general mechanism that does not necessarily rely on malaria infection. Nevertheless, the data suggest that it is the exposure to the malaria parasite that selects the rare B cells with a *LAIR1* insertion in the VDJ or switch region. Finally, it remains to be established whether chromosomal translocations and templated insertions share a common mechanism.

The finding of templated inserts in the switch region of switched memory B cells, but not naive B cells, suggests that the insertions occur in germinal centres as a consequence of unconventional repair of activation-induced cytidine deaminase (AID)-induced double-strand DNA breaks. Similarly, repair of recombination activating gene (RAG)-induced double-strand breaks during B cell development in the bone marrow may give rise to insertions in the CDR3 region. Our finding that switch region inserts are derived from transcribed genes suggests the involvement of nascent RNA as an insert template, and recent publications have shown that both nascent[12,13] and foreign RNA[14,15] can be used to repair double-strand DNA breaks. Furthermore, multiple templated inserts from transcribed genes have been observed in engineered double-strand breaks in a human cell line and mouse pro-B cells[14,16]. However, we cannot exclude the possibility that accessible DNA is a primary substrate. The possibility of inducing naive human B cells to switch *in vitro* offers the opportunity to study the mechanism of templated insertions and to engineer B cells by manipulating the factors involved in DNA repair and by offering different substrates.

Online Content Methods, along with any additional Extended Data display items and Source Data, are available in the online version of the paper; references unique to these sections appear only in the online paper.

Received 4 April; accepted 25 July 2017.
Published online 23 August 2017.

1. Meyaard, L. The inhibitory collagen receptor LAIR-1 (CD305). *J. Leukoc. Biol.* **83,** 799–803 (2008).
2. Tan, J. *et al.* A *LAIR1* insertion generates broadly reactive antibodies against malaria variant antigens. *Nature* **529,** 105–109 (2016).
3. Mwakasungula, S. *et al.* Red blood cell indices and prevalence of hemoglobinopathies and glucose 6 phosphate dehydrogenase deficiencies in male Tanzanian residents of Dar es Salaam. *Int. J. Mol. Epidemiol. Genet.* **5,** 185–194 (2014).
4. Tran, T. M. *et al.* An intensive longitudinal cohort study of Malian children and adults reveals no evidence of acquired immunity to *Plasmodium falciparum* infection. *Clin. Infect. Dis.* **57,** 40–47 (2013).
5. Muyldermans, S. Nanobodies: natural single-domain antibodies. *Annu. Rev. Biochem.* **82,** 775–797 (2013).
6. Piccoli, L. *et al.* Neutralization and clearance of GM-CSF by autoantibodies in pulmonary alveolar proteinosis. *Nat. Commun.* **6,** 7375 (2015).
7. Reed, J. H., Jackson, J., Christ, D. & Goodnow, C. C. Clonal redemption of autoantibodies by somatic hypermutation away from self-reactivity during human immunization. *J. Exp. Med.* **213,** 1255–1265 (2016).
8. Long, M., Betrán, E., Thornton, K. & Wang, W. The origin of new genes: glimpses from the young and old. *Nat. Rev. Genet.* **4,** 865–875 (2003).
9. Kolkman, J. A. & Stemmer, W. P. Directed evolution of proteins by exon shuffling. *Nat. Biotechnol.* **19,** 423–428 (2001).
10. Jain, M. *et al.* Improved data analysis for the MinION nanopore sequencer. *Nat. Methods* **12,** 351–356 (2015).
11. Robbiani, D. F. *et al. Plasmodium* infection promotes genomic instability and AID-dependent B cell lymphoma. *Cell* **162,** 727–737 (2015).
12. Keskin, H. *et al.* Transcript-RNA-templated DNA recombination and repair. *Nature* **515,** 436–439 (2014).
13. Chakraborty, A. *et al.* Classical non-homologous end-joining pathway utilizes nascent RNA for error-free double-strand break repair of transcribed genes. *Nat. Commun.* **7,** 13049 (2016).
14. Onozawa, M. *et al.* Repair of DNA double-strand breaks by templated nucleotide sequence insertions derived from distant regions of the genome. *Proc. Natl Acad. Sci. USA* **111,** 7729–7734 (2014).
15. Onozawa, M., Goldberg, L. & Aplan, P. D. Landscape of insertion polymorphisms in the human genome. *Genome Biol. Evol.* **7,** 960–968 (2015).
16. Rommel, P. C., Oliveira, T. Y., Nussenzweig, M. C. & Robbiani, D. F. RAG1/2 induces genomic insertions by mobilizing DNA into RAG1/2-independent breaks. *J. Exp. Med.* **214,** 815–831 (2017).

Supplementary Information is available in the online version of the paper.

Acknowledgements We thank M. Nussenzweig and H. Wardemann for reagents for antibody cloning and expression. This work was supported by the Swiss Vaccine Research Institute and by the Fondazione Aldo e Cele Daccò. The work on the healthy European blood donors was supported by the European Research Council (grant no. 670955 BROADimmune). The Mali study was funded by the Division of Intramural Research, National Institute of Allergy and Infectious Diseases, National Institutes of Health. A.L. and F.S. are supported by the Helmut Horten Foundation. This paper is published with the permission of the Director of KEMRI.

Author Contributions K.P. characterized genomic DNA, analysed the data and wrote the manuscript; J.T. isolated new LAIR1-containing antibodies, analysed the data and wrote the manuscript; L.P. produced mutant antibodies, analysed the data and wrote the manuscript; M.F. performed bioinformatics analysis; S.B. sequenced and expressed antibodies; Y.C. helped with genomic sequencing; C.S.-F. immortalized memory B cells; T.W. helped with MinION sequencing; D.J. performed cell sorting and analysis; M.A. performed protein analysis; A.A. performed *P. falciparum* culture; F.M.N., S.J., O.K.D., B.T., I.Z., C.D. and P.C.B. provided cohort samples; T.M.T. and P.D.C. provided cohort samples and analysed the relationship between LAIR1-containing antibodies and malaria risk; F.S. provided supervision; A.L. provided overall supervision, analysed the data and wrote the manuscript.

Author Information Reprints and permissions information is available at www.nature.com/reprints. The authors declare competing financial interests: details are available in the online version of the paper. Readers are welcome to comment on the online version of the paper. Publisher's note: Springer Nature remains neutral with regard to jurisdictional claims in published maps and institutional affiliations. Correspondence and requests for materials should be addressed to A.L. (lanzavecchia@irb.usi.ch).

Reviewer Information *Nature* thanks P. Preiser, M. Wahlgren and the other anonymous reviewer(s) for their contribution to the peer review of this work.

METHODS

No statistical methods were used to predetermine sample size. The experiments were not randomized and the investigators were not blinded to allocation during experiments and outcome assessment.

Serum and plasma samples. Kenyan plasma samples were obtained from adults living in a malaria-endemic region within Kilifi County. Tanzanian serum and plasma samples were obtained from healthy male volunteers, malaria negative at study enrolment and during peripheral blood mononuclear cell (PBMC) collection, HIV and hepatitis B and C negative, age 25.4 ± 2.8 years (mean ± s.d.)[3]. The Mali study was conducted in the rural village of Kalifabougou where intense *P. falciparum* transmission occurs from June to December each year. Six hundred and ten individuals (310 males and 300 females) were enrolled, ranging in age from 1 to 26 years (mean 9 years). The cohort has been described in detail elsewhere[4]. A smaller number of serum samples was also obtained from adults in the Fulani and Dogon ethnic groups in Mantéourou, Mali. Forty-eight individuals (28 males and 20 females) were enrolled, ranging in age from 21 to 57 years (mean 39.7 years).

Ethics approval. In all cases, written informed consent was obtained from the participants (or guardians of participating children) before inclusion in the study. The acquisition and use of the Kenyan plasma samples were approved by the Kenya Medical Research Institute Scientific and Ethics Review Unit (protocol number: KEMRI-SERU 3149), as well as the Oxford Tropical Research Ethics Committee. The Tanzanian samples were obtained with informed consent from the trial participants. The clinical trial was conducted according to good clinical practice and with authorization from the Institutional Review Boards of the Ifakara Health Institute, the National Institute for Medical Research Tanzania, the Tanzanian Food and Drugs Authority and the Commission cantonale d'éthique de la recherche sur l'être humain du canton de Vaud, Switzerland. The trial is registered at https://clinicaltrials.gov/ with identifier: NCT01949909. The Mali study was approved by The Ethics Committee of the Faculty of Medicine, Pharmacy and Dentistry at the University of Sciences, Technique and Technology of Bamako, and the Institutional Review Board of the National Institute of Allergy and Infectious Diseases, National Institutes of Health. Written informed consent was obtained from participants or parents or guardians of participating children before inclusion in the Mali study.

Parasite culture. *P. falciparum* parasites were initially obtained from children who were diagnosed with malaria in Kilifi County, Kenya. The parasites were adapted to *in vitro* culture and cultivated using standard protocols[17]. The *P. falciparum* laboratory line 3D7 was also cultured under the same conditions. $3D7^{D21}$ was derived by enrichment of 3D7 parasites reactive with the LAIR1-containing monoclonal antibody MGD21. Parasites were cryopreserved at the late trophozoite stage in small aliquots for subsequent use in assays.

Screening of serum or plasma with bead-based immunoassay. Serum and plasma were tested for the presence of LAIR1-containing antibodies using a two-determinant bead-based immunoassay. Anti-goat IgG microbeads (Spherotech) were coated with goat anti-human LAIR1 (R&D Systems, AF2664) and 40 × SYBR Green I (ThermoFisher Scientific) or with goat anti-human EGF (R&D Systems, AF-259-NA) without SYBR Green I for 20 min at room temperature. The beads were washed, mixed, and incubated with the serum at a 1/30 dilution for 1 h at room temperature under shaking conditions. Beads coated with anti-LAIR1 were differentiated from control beads coated with anti-EGF based on SYBR green staining. Serum antibody binding was detected using 2.5 μg ml^{-1} Alexa Fluor 647-conjugated donkey anti-human IgG (Jackson ImmunoResearch, 709-606-098) or Alexa Fluor 647-conjugated donkey anti-human IgM (Jackson ImmunoResearch, 709-606-073). FACS Diva (version 6.2) was used for acquisition of samples and Flow-Jo (version 10.1) was used for flow cytometry analysis. ΔMFI was calculated by subtracting the MFI of the anti-EGF control beads from that of the anti-LAIR1 beads in the IgG or IgM channel.

B-cell immortalization and isolation of monoclonal antibodies. IgM or IgG memory B cells were isolated from frozen PBMCs by magnetic cell sorting with anti-CD19-PECy7 antibodies (BD, 341113) and mouse anti-PE microbeads (Miltenyi Biotec, 130-048-081), followed by fluorescence-activated cell sorting (FACS) using goat Alexa Fluor 647-conjugated anti-human IgG (Jackson ImmunoResearch, 109-606-170) or anti-human IgM (Jackson ImmunoResearch, 109-606-129) and PE-labelled anti-human IgD (BD, 555779). As previously described[18], sorted B cells were immortalized with Epstein-Barr virus (EBV) and plated in single cell cultures in the presence of CpG-DNA (2.5 μg ml^{-1}) and irradiated PBMC-feeder cells. Two weeks after immortalization, the culture supernatants were tested (at a 2/3 dilution) for the presence of LAIR1-containing antibodies using the bead-based immunoassay described above. For several donors, the culture supernatants were also tested for the ability to bind to infected erythrocytes from a mixture of four parasite isolates (3D7-MGD21^{+}, 9106, 9605 and 11019) by flow cytometry. In brief, cryopreserved infected erythrocytes were thawed, stained with 10 × SYBR Green I for 30 min at room temperature, and incubated with the B-cell supernatants for 1 h at 4 °C. Detection of antibody binding was done with 2.5 μg ml^{-1} Alexa Fluor 647-conjugated goat anti-human IgG.

Sequence analysis of antibody cDNA. cDNA was synthesized from selected B cell cultures and both heavy chain and light chain variable regions (VH and VL) were sequenced as previously described[19]. The usage of VH and VL genes and the number of somatic mutations were determined by analysing the homology of VH and VL sequences of monoclonal antibodies to known human *V*, *D* and *J* genes in the IMGT database[20]. Antibody-encoding sequences were amplified and sequenced with primers specific for the V and J regions of the given antibody. Sequences were aligned with Clustal Omega[21].

Mutation analysis of *LAIR1* inserts. The number of somatic mutations in the *LAIR1* inserts was obtained by analysing the homology of the inserts to the original *LAIR1* genomic sequence (sequence from Ensembl genome database: ENSG00000167613). Amino acid sequences of *LAIR1* inserts of all the antibodies discovered were grouped for each donor and aligned to the original unmutated LAIR1 sequence using Clustal Omega[21]. The replacement to silent mutation ratio (R/S) values were calculated at each codon for each donor. Mean (R/S) values above 2.9, indicative of positive selection, were used to highlight hot spots in the LAIR1 extracellular domain (PDB 3RP1) using the BioLuminate software (Schrödinger, LLC, 2016 v.2.4).

Production of recombinant antibodies, antibody variants and fusion proteins. Antibody heavy and light chains were cloned into human IgG1, Igκ and Igλ expression vectors and expressed by transient transfection of Expi293F cells (ThermoFisher Scientific) using polyethylenimine (PEI). Cell lines were routinely tested for mycoplasma contamination. The antibodies were affinity purified by protein A chromatography (GE Healthcare). Variants of the GCE536, MGD21, MGM1 and MGJ5 antibodies were produced by inserting or exchanging the mutated or unmutated *LAIR1* sequences or by substituting these sequences with the Ig-like domains of *PD1* and *SLAM* genes (sequences from Ensembl genome database: ENSG00000188389 and ENSG00000117090, respectively). The antibody constructs were tested for staining of 9,215 infected erythrocytes and binding values (%) at 1 μg ml^{-1} antibody concentration were calculated by interpolation of binding curves fitted to a sigmoidal curve model (Graphpad Prism 7).

Amplification of antibody gDNA. Genomic DNA was isolated from B cell clones with a commercial kit (QIAGEN). For analysis of the camel-like antibody MGB47, 3′ rapid amplification of cDNA ends (RACE)[22] with the CH2-γ-REV1 primer (GAGACCTTGCACTTGTACTCCTTGCC) was used for amplification of truncated heavy chain mRNAs. Heavy-chain variable-to-constant gDNA of MGB47 was amplified using an upstream 5′ VH3-21 primer (GGGTCCATATTGTGATCCT GAGTCTGGG) and CH2-γ-REV1 as the reverse primer. After PCR amplification with LongAmp Taq Polymerase (New England Biolabs), the 6,000-bp amplicon was cloned into a vector using the TOPO XL PCR cloning kit (ThermoFisher) and sequenced by plasmid-NGS sequencing (Microsynth, Switzerland). All other *LAIR1* switch and V-DJ inserts were analysed by PCR amplification of gDNA and Sanger Sequencing using donor-specific forward and universal reverse primers: donE_FW (CCTGGAGGGTCTTCTGCTTGCTGGC), donF_FW (CCTCCTGCTGGTGG CAGCTCCC), donJ/M_FW1 (ATGGAGTTTGGGCTGAGCTGGGTTTTCC), donJ_FW2 (GTGAGTGAACACGAGTGAGAGAAACAGTGG), donM_FW2 (GAGTGAACATGAGTGAGAAAAACTGGATTTGTGTGG), donO/Q_FW (ATGAAACATCTGTGGTTCTT), 3′J6_REV (GGCATCGGAAAATCCA CAGAGGCTCC), IgG_CH1_REV1 (TCTTGTCCACCTTGGTGTTGCT), IgG_CH1_REV2 (GTAGTCCTTGACCAGGCAGC), IgM_CH2_REV1 (GGACACCTGAATCTGCCGGGGACTGAAACCC), and IgM_CH2_REV2 (CTGGTCACCTTGTAGGTCGTGGGCCCAG).

Switch region PCR and Illumina sequencing. gDNA was isolated from FACS-sorted human naive (CD19^{+} CD27^{-} IgM^{+}) or memory B cells (CD19^{+} CD27^{+} IgG^{+}/IgA^{+}) using a commercial kit (QIAGEN). Switch region PCRs on memory B cell gDNA were performed using LongAmp Taq Polymerase (New England Biolabs) in 50 μl reaction volumes with incubation for 3 min at 95 °C, followed by 30 cycles of 95 °C for 40 s, 60 °C for 30 s, 65 °C for 3 min and a final extension for 10 min at 65 °C. The upstream switch-μ forward primer S-μ-FW (CACCCTTGAAAGTAGCCCATGCCTTCC) was combined with different reverse primers. IgG-switched B cell DNA was amplified using S-γ-REV (CCTGCCTCCCAGTGTCCTGCATTACTTCTG)[23], which binds 3′ of switch-γ regions, or CH2-γ-REV1, which binds in the IgG-CH2 constant region, to allow amplification of alleles carrying a CH1 deletion. DNA deriving from IgA^{+}-sorted cells was amplified with primer S-α-REV (CTCAGTCCAACACCCACCACTCC). All reverse primers mentioned were designed to allow amplification of various IgG and IgA subclasses. The switch-μ region of naive B cell gDNA was amplified combining the S-μ-FW primer with S-μ-REV (GGAACGCAGTGTAGACT CAGCTGAGG). The PCR reaction was performed using Herculase II Fusion DNA Polymerases (Agilent) with 1 M betaine and 3% DMSO in a 50 μl volume at 98 °C

for 4 min followed by 30 cycles of 98 °C for 40 s, 58 °C for 30 s and 72 °C for 4 min, with a final extension for 10 min at 72 °C. Size-selected, purified switch amplicons were sent to GATC Biotech (Germany) for library preparation, barcoding, and Illumina MiSeq sequencing.

MinION sequencing. Oxford Nanopore Technology (ONT) was used to generate biological and technical replicates of Illumina MiSeq sequencing runs. For biological replicates, barcodes were introduced by the addition of recommended BC-sequences to S-μ and S-γ primers and PCR amplification. The sequencing library was prepared using the Nanopore 2D sequencing kit SQK-LSK207, followed by loading onto Nanopore flow cells FLO-MIN106 and sequencing with the MinION Mk1B sequencer for up to 20 h.

Infected erythrocyte binding assays. Recombinant monoclonal antibodies were produced in Expi293F cells and tested for the ability to stain 3D7-MGD21^{+} and eight Kenyan parasite isolates[2] by flow cytometry. Cryopreserved infected erythrocytes were thawed, stained with 10 × SYBR Green I for 30 min at room temperature, and incubated with serial dilutions of the recombinant antibodies for 20 min at room temperature. Antibody binding was detected with 2.5 μg ml^{-1} goat Alexa Fluor 647-conjugated anti-human IgG.

Selected sera were screened for the presence of LAIR1-containing antibodies that could bind to infected erythrocytes. A mixture of four parasite isolates (3D7-MGD21^{+}, 9106, 9605 and 11019) was stained with 10 μg ml^{-1} DAPI for 30 min at room temperature and incubated with test sera at a 1/30 dilution for 20 min at room temperature. The infected erythrocytes were then incubated with goat anti-human LAIR1 (R&D Systems, AF2664) for 20 min at room temperature. The binding of LAIR1-containing antibodies to the infected erythrocyte surface was detected by the simultaneous addition of Alexa Fluor 488-conjugated donkey anti-goat IgG (Jackson ImmunoResearch, 705-546-147) and Alexa Fluor 647-conjugated donkey anti-human IgG (Jackson ImmunoResearch, 709-606-098).

ELISA. Total IgGs were quantified using 96-well MaxiSorp plates (Nunc) coated with goat anti-human IgG (SouthernBiotech, 2040-01) using Certified Reference Material 470 (ERMs-DA470, Sigma-Aldrich) as a standard. To test specific binding of antibody constructs, ELISA plates were coated with 2 μg ml^{-1} of type I recombinant human collagen (Millipore, CC050), 2 μg ml^{-1} of an anti-human LAIR1 antibody (clone DX26, BD Biosciences 550810), 1 μg ml^{-1} of recombinant human GM-CSF (Gentaur), 2 μg ml^{-1} of an anti-PD1 or an anti-SLAM antibody (R&D Systems, AF1086 and AF164). Plates were blocked with 1% bovine serum albumin (BSA) and incubated with titrated antibodies, followed by AP-conjugated goat anti-human IgG, Fcγ fragment specific (Jackson Immuno Research, 109-056-098). Plates were then washed, substrate (p-NPP, Sigma) was added and plates were read at 405 nm.

Western blots. B cell supernatants containing secreted antibodies were diluted in H_2O, 4× sample loading buffer (Life Technologies) and 10× sample reducing agent (Life Technologies) and loaded onto precast gels with a 4–12% acrylamide gradient (Invitrogen). The iBlot2 apparatus (Life Technologies) was used for protein transfer to PVDF membranes followed by blocking for 1 h at room temperature with 3% BSA in TBS. The membrane was incubated with different combinations of primary and secondary antibodies diluted in TBS/1% BSA for 1 h at room temperature with 2 sequential TBS incubations to wash the membrane between incubations. For detection of IgG, anti-human IgG-biotinylated antibody (Southern Biotech, 2040-08) was used at 1 μg ml^{-1}, followed by 25 ng ml^{-1} streptavidin-horseradish peroxidase (HRP) (Jackson ImmunoResearch, 016-030-084). IgM isotypes were stained with 10 μg ml^{-1} unlabelled goat anti-human IgM (Southern Biotech, 2020-01) and 8 ng ml^{-1} donkey anti-goat HRP (Jackson ImmunoResearch, 705-036-147). To detect LAIR1-containing antibodies, a polyclonal goat anti-human LAIR1 antibody (R&D) at 2 μg ml^{-1} was combined with secondary donkey anti-goat HRP. Membranes were developed with ECL-substrate on a Las4000 imager (General Electric Company).

Surface staining of B cell lines. EBV immortalized B cells were stained with different fluorescently labelled antibodies to detect surface immunoglobulin expression and LAIR1 co-staining (Alexa Fluor 647-conjugated anti-human IgG, Jackson ImmunoResearch, 109-606-170; FITC-conjugated anti-human kappa, DAKO, F0434, PE-conjugated anti-human lambda, DAKO, R0437; PE-conjugated anti-human LAIR1 clone DX26, BD Bioscience, 550811). Cells were analysed by flow cytometry and FlowJo software. Dead cells were excluded from the analysis by 4′,6-diamidine-2′-phenylindole dihydrochloride (DAPI) staining. The time point of the analysis was selected for optimal BCR expression levels and for downregulation of the original LAIR1 receptor, because EBV cell lines downregulate the inhibitory receptor LAIR1 at an early time point after immortalization but may also decrease surface-Ig levels after certain passages.

Genomic insertion analysis after Illumina sequencing. We generated a computational pipeline to analyse targeted amplicons of 300 bp paired-end (PE) reads obtained by MiSeq Illumina sequencing methodology (Extended Data Fig. 5). Raw sequences reads were trimmed to remove adaptor contamination and poor-quality base calls using Trim Galore (http://www.bioinformatics.babraham.ac.uk/projects/trim_galore/, v.0.4.2, parameters–Illumina–paired -q 20–length 99). In addition, assessment of the PE reads was performed by average quality score per base position, using FastQC (http://www.bioinformatics.babraham.ac.uk/projects/fastqc/). Trimmed reads were aligned in paired-end mode to the GRCh37 human genome assembly using Burrows–Wheeler Alignment tool (v.0.7.12, parameters: bwa mem)[24]. The switch region of the IgH locus was defined on GRCh37, with the following coordinates: chr14:106050000–106337000. To find insertions in the IgH switch region locus, we selected genomic ranges when sequence coverage was above 2 reads and/or above 40 reads, thus, generating two respective and separated workflows, with a sequence length comprises between 50 bp and 2,000 bp. Genome coverage was processed using Bedtools (http://bedtools.readthedocs.io/en/latest/index.html, v.2.26.0) and a dedicated python script using pysam (https://github.com/pysam-developers/pysam) was written to identify potential insert. In brief, in both workflows (2 and 40 reads), potential inserts were assigned if they fulfilled the following criteria: (i) one mapping read in 5′ end is chimaeric with the switch region; (ii) one mapping read in 3′ end is chimaeric with the switch region; (iii) two discordant reads have their mates read mapped in the switch region. Afterwards, inserts coming from 2 and 40 minimum reads coverage were merged according to the following rule: if the difference between two inserts that overlap was equal or below 10 bp, we kept the shortest one, otherwise the longest one was kept. The list of potential inserts was annotated using GENCODE v.19[25] and BEDOPS tools[26] and individually validated by a *de novo* assembly of the contig sequence. Non-chimaeric, but properly paired reads mapping the insert coordinates and chimaeric reads corresponding to the encompassing mate pairs and spanning mate pairs, were extracted using SAMtools[27]. Reads mapping to the switch region were extracted only if they were spanning mate pairs related to the insert coordinates. Selected reads were uniquely mapped to the region of interest (no XA tag), with a minimum mapping quality of 5. Original read sequences were retrieved, pulled together and used as input files to perform a *de novo* assembly using the Trinity software[28]. Finally, to validate a contig sequence for each insert, we used BLAST[29] (command-line version, v.2.5.0+). The consensus insert sequences were 'blasted' against the switch region and we removed the inserts that had an alignment with at least half of their sequence length at a minimum 80% identity (parameters: -task megablast -dust no -perc_identity 80). Then, we blasted each contig sequence against the switch region sequence and the consensus insert sequence (parameters: -task blastn -dust no -perc_identity 70) to confirm whether the contig was made of the complete insert sequence and contained two flanking sequences of at least 50 bp that matched the switch region. The shortest contig that fulfilled the criteria mentioned above was selected for each insert.

Bioinformatic analysis of MinION sequencing. To analyse targeted amplicon 2–4-kb reads obtained by ONT sequencing methodology, we developed a pipeline (Extended Data Fig. 6). Raw sequences reads were quality-filtered using Metrichor basecaller (https://metrichor.com/s/). 2D reads with a sequence length above 1,000 bp (or 2,000 bp depending on the primers used for the amplification) were aligned against GRCh37 human genome assembly with LAST software[30] (parameters: last-train and lastal -p ONT_fasta_sequences.par last-split -m1e-6). Then we parsed LAST output and selected reads that contain an insert (minimum 50 bp length), two flanking regions of minimum 100 bp mapping to the switch region (switch locus defined as chr14:106050000–106337000) and allowing a gap of 100 bp maximum between the insert and the switch region. Finally, we merged the insert coordinates of the overlapping inserts with bedtools and annotated the inserts list with GENCODE v.19[25] using BEDOPS tool[26]. Scripts are available at MinION and Illumina inserts coordinates were merged with Bedtools (merge command with default parameter). The circular genomic representation of the inserts has been generated using the Circos software[31]. Switch inserts with genic (intron or exon–intron) origin were subjected to an enrichment analysis using EnrichR and the Human Gene Atlas as the gene-set library[32,33].

Statistical analysis. The number *n* described in the figure legends refers to the number of independent experiments. The analysis of the relationship between the presence of LAIR1-containing antibodies and protection from malaria was performed in the R statistical environment (v.3.2.5). Two-tailed Fisher's exact tests were performed to investigate the association between LAIR1-containing antibodies and protection from febrile malaria.

Code availability. Scripts for Illumina and MinION sequence analysis are available at https://bitbucket.org/mathildefog/switchillumina and https://bitbucket.org/mathildefog/switchminion, respectively.

Data availability. Sequence data for the monoclonal antibodies isolated in this study have been deposited in GenBank (https://www.ncbi.nlm.nih.gov/genbank/) with the accession codes indicated in Supplementary Table 1. The NGS data for switch region sequencing are deposited in NCBI Sequence Read Archive (SRA) with the accession code PRJNA382214. The analyses of these sequences are provided in Supplementary Tables 2–4.

17. Trager, W. & Jensen, J. B. Human malaria parasites in continuous culture. *Science* **193,** 673–675 (1976).
18. Traggiai, E. *et al.* An efficient method to make human monoclonal antibodies from memory B cells: potent neutralization of SARS coronavirus. *Nat. Med.* **10,** 871–875 (2004).
19. Tiller, T. *et al.* Efficient generation of monoclonal antibodies from single human B cells by single cell RT–PCR and expression vector cloning. *J. Immunol. Methods* **329,** 112–124 (2008).
20. Lefranc, M.-P. *et al.* IMGT, the international ImMunoGeneTics information system. *Nucleic Acids Res.* **37,** D1006–D1012 (2009).
21. Goujon, M. *et al.* A new bioinformatics analysis tools framework at EMBL-EBI. *Nucleic Acids Res.* **38,** W695–W699 (2010).
22. Picelli, S. *et al.* Full-length RNA-seq from single cells using Smart-seq2. *Nat. Protocols* **9,** 171–181 (2014).
23. Mills, F. C., Mitchell, M. P., Harindranath, N. & Max, E. E. Human Ig S gamma regions and their participation in sequential switching to IgE. *J. Immunol.* **155,** 3021–3036 (1995).
24. Li, H. Aligning sequence reads, clone sequences and assembly contigs with BWA-MEM. Preprint at https://arxiv.org/abs/1303.3997 (2013).
25. Harrow, J. *et al.* GENCODE: the reference human genome annotation for The ENCODE Project. *Genome Res.* **22,** 1760–1774 (2012).
26. Neph, S. *et al.* BEDOPS: high-performance genomic feature operations. *Bioinformatics* **28,** 1919–1920 (2012).
27. Li, H. *et al.* The Sequence Alignment/Map format and SAMtools. *Bioinformatics* **25,** 2078–2079 (2009).
28. Haas, B. J. *et al. De novo* transcript sequence reconstruction from RNA-seq using the Trinity platform for reference generation and analysis. *Nat. Protocols* **8,** 1494–1512 (2013).
29. Camacho, C. *et al.* BLAST+: architecture and applications. *BMC Bioinformatics* **10,** 421 (2009).
30. Kiełbasa, S. M., Wan, R., Sato, K., Horton, P. & Frith, M. C. Adaptive seeds tame genomic sequence comparison. *Genome Res.* **21,** 487–493 (2011).
31. Krzywinski, M. *et al.* Circos: an information aesthetic for comparative genomics. *Genome Res.* **19,** 1639–1645 (2009).
32. Chen, E. Y. *et al.* Enrichr: interactive and collaborative HTML5 gene list enrichment analysis tool. *BMC Bioinformatics* **14,** 128 (2013).
33. Kuleshov, M. V. *et al.* Enrichr: a comprehensive gene set enrichment analysis web server 2016 update. *Nucleic Acids Res.* **44,** W90–W97 (2016).

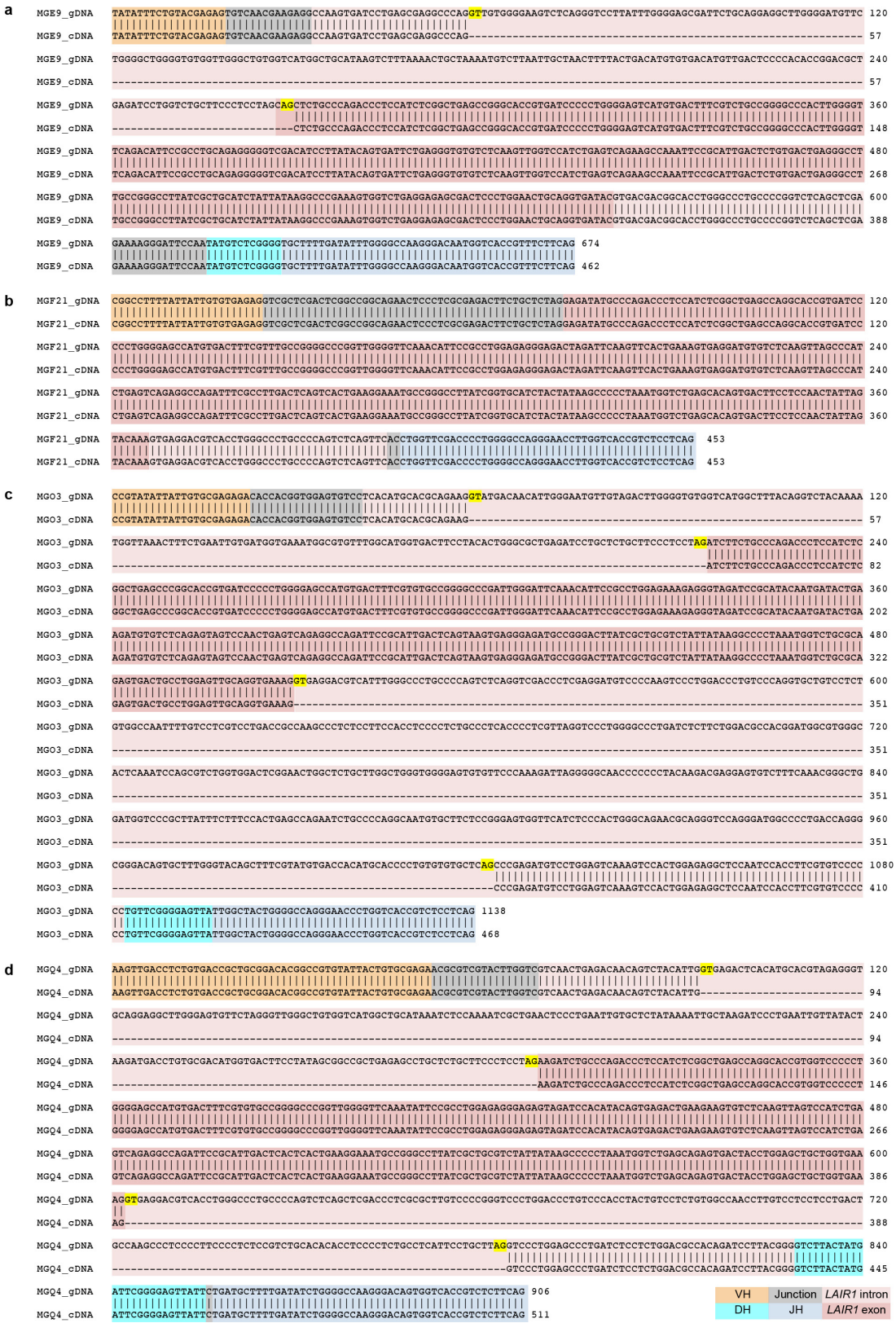

Extended Data Figure 1 | Alignment of gDNA and cDNA sequences of LAIR1-containing antibodies. Shown is one representative antibody from each donor. **a**, MGE9 (donor E); **b**, MGF21 (donor F); **c**, MGO3 (donor O); **d**, MGQ4 (donor Q).

a MMJ5

GGCTGAGCTAACCTGGGCTGGGCTCAGCTGAGCTGAGCTACGCTGGGCTGGGCTGGGCTGAGCCGAGCTGAACTGGGCTGAGCAGG
CTGTGTCGGGCTGAGCCAAGCTGGGCCGAGCTCAGCAGAGCTGAGCCGAGCTGAGCTTAGCTGGGCTGAGCTAACCAGGGCTGGGC
TGAGCTGGGCTGAGCTGAGCTGAGCTGAACTGGGCTGAAGGACGCTGAGATCCTGCTCTGCTTCCCTCCTAGAAGATCTGCCCAGA
ATTCCGCCTGGAGAGGGAGAGTAGATCCACATACAATGAAACTGAAGATGTGTCTCAAGTTAGTCCATCTGAGTCAGAGGCCAGAT
TCCGCATTGACTCAGTAAGTGAAGGAAATGCCGGGCCTTATCGCTGCATCTATTATAAGCCCCCTAAATGGTCTGAGCAGAGTGAC
TACCTGGAGCTGCTGGTGAAAGGTGAGGACGTCACCTGGGCCCTGCCCCAGTTGAGCAGAGCTAAGCCGAGGCTGGGCTGGGCTAA
CCTGGGCTGGGCCGAGCTGAGCAGAGCTAAGCCGAGGCTGGGCTGGGCTAACCTGGGCTGGGCTGAGCTGAGCTGGGTTGGGCTGG
GCTGGGCTGGGCTGAGCTAAGCTGAACT

Position in reference genome (Chr 14, GRCh37.p13 assembly):
A = 106325639
T = 106325613

b MGM5

GAGCTAACCTGGACTGGGGCTGAACTAACCTGGGCAGAGCTGAGCTGGGCTGAGCTAACCTGGGCTGGGGCTGAGCTAACCTGGGG
TGGGCTCAGCTGAGCTGAGCTACGCTGGGCTGGGCTGGGCTGAGCCGAGCTGAACTGGGCTGAGCAGGCTGTGTCGGGCTGAGCCA
AGCTGGGCCGAGCTCAGCAGAGCTGAGCCGAGCTAAGCTTACCTGGGCTGCCTGCTCTGCTTCCCTCCTAGAAGATCTGCCCAGAC
CCTCCATCTCGGCTGAGCCAGGCACCGTGATCCCCCTGGGGAGCCATGTGACTTTCGTGTGCCGGGGCCCGGTTGGGGTTCAAACA
TTCCGCCTGGAGAGGGAGAGTAGATCCACATACAATGATACTGAAGATGTGTCTCAAGCTAGTCCATCTGAGTCAGAGGCCAGATT
CCGCATTGACTCAGTAAGTGAAGGAAATGCCGGGCCTTATCGCTGCGTCTATTATAAGCCCCCTAAATGGTCTGAGCAGAGTGACT
ACCTGGAGCTGCTGGTGAAAGGTGAGGACGTCACCTGGGCCCTGCCCCAGTGCTGGGCTGAGCTGGGCTGAGCTGAGCTGAGCTGA
ACTGGGCTGAACGGGCTTAGACGAGCAGGGCCGAGCTGAGCAGAGCTAAGCCGAGGCTGGGCTGGGCTAACCTGGGCTGGGCCGAG
CTGAGCAGAGCTAAGCCGAGGCTGGGCTGGGCTAACCTGGGCTGGGCTGAACTGAGC

Position in reference genome (Chr 14, GRCh37.p13 assembly):
G = 106325696
G = 106325685

c MGB47

GAGCTGACCTAGGCTGGGCTGGGCTGGGCTGGGCTGGGCTGAGTCAAACTGAAACGGGTTGTGCGTGCTGTGATGGGCTGAGCCAA
GCTAGGCTGAGCTGAGCCAAGTTGAACTTAACTGGGCTGAGCTAACCTGGACAAGGCTGAGCTGGGCTGAGCTAACCTGGACTGGG
GCTGAGCTAACCTGGGCAGACCTGAGCTGAGGTAACCAGGACTGGGGCTGACCTAACCTGGGCAGAGCTGAACTGGGCTGAGCTAA
CCTGGGCTGGGGCTAAATTCCCTGAATTGTGATGCTAACATGACGTGTGTGGCATGGTGACTTCCTACAGTGGACGCTGAGATCCT
GCTCTGCTTCCCTCCTAGAAGATCTGCCCAGACCCTCCATCTCGGCTGAGCCAGGCACCGTGATCCCCCTGGGGAGCCATGTGACT
TTCGTGTGCCGGGGCCCGGTTGGGGTTCAAACATTCCGCCTGGAGAGGGAGAGTAGATCCAGATACACTGAAACTGAAGATGTGTC
TCAAACTAGTCCATCTGAGTCAGAGGCCAGATTCCGCATTGACTCAGTAAGTGAAGGAAATGCCGGGCCTTATCGCTGCCTCTATT
ATAAGCCCCCTAAATGGTCTGAGCAGAGTGACTTCCTGGAGCTGCTGGTGAAAGGTGAGGACGTCTCCGGAGATGAGCTTAGCTGG
GCTGAGCTAACCAGGGCTGGGCTGAGCTGGGCTGAGCTGAGCTGAGCTGATCTGGGCTGCACGGGCTGAGGCGAGCAGGGCCGAGC
TGAGCAGAGCTAAGCCGAGGCTGGGCTGGGCTAACCTGGGCTGGGCCGAGCTGAGCAGAGCTAAGCCGAGGCTGGGCTGGGCTAAC
CTGGGCTGGGCTGAGCTGAGCTGGGTTGGACAGGGCTGGGCTGGGCTGAGCTAA

Position in reference genome (Chr 14, GRCh37.p13 assembly):
G = 106325856
G = 106325716

LAIR1 intron
LAIR1 exon
Sμ

Extended Data Figure 2 | Genomic sequences of switch regions containing *LAIR1* inserts. Shown is one representative antibody for each donor; **a**, MMJ5 (donor J); **b**, MGM5 (donor M); **c**, MGB47 (donor B). The chromosome coordinates of the insertion sites are indicated in blue and green.

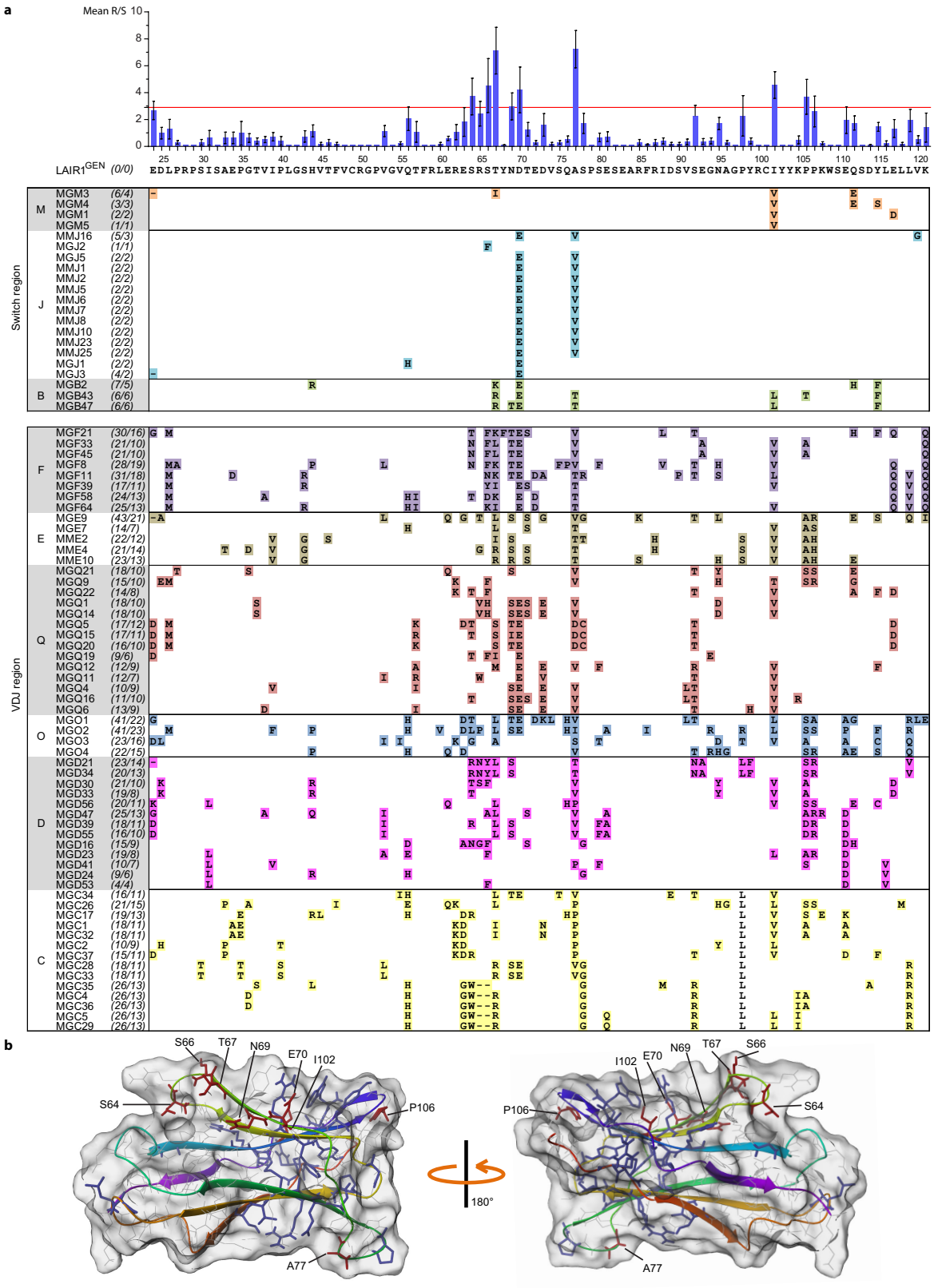

Extended Data Figure 3 | Somatically mutated and conserved regions in the LAIR1 domains inserted in the VDJ or in the switch region. **a**, Amino acid substitutions in antibodies isolated from different donors and mean R/S ratios at each residue. The mutational analysis takes into consideration the germline LAIR1 alleles found in each donor. In donor C, the P98L substitution is uncoloured because it may arise from polymorphism, since the donor is heterozygous at this position. The number of nucleotide mutations and amino acid substitutions are reported in brackets next to the antibody names. **b**, Graphic representation of mutational hot spots (red) and of most conserved regions (blue).

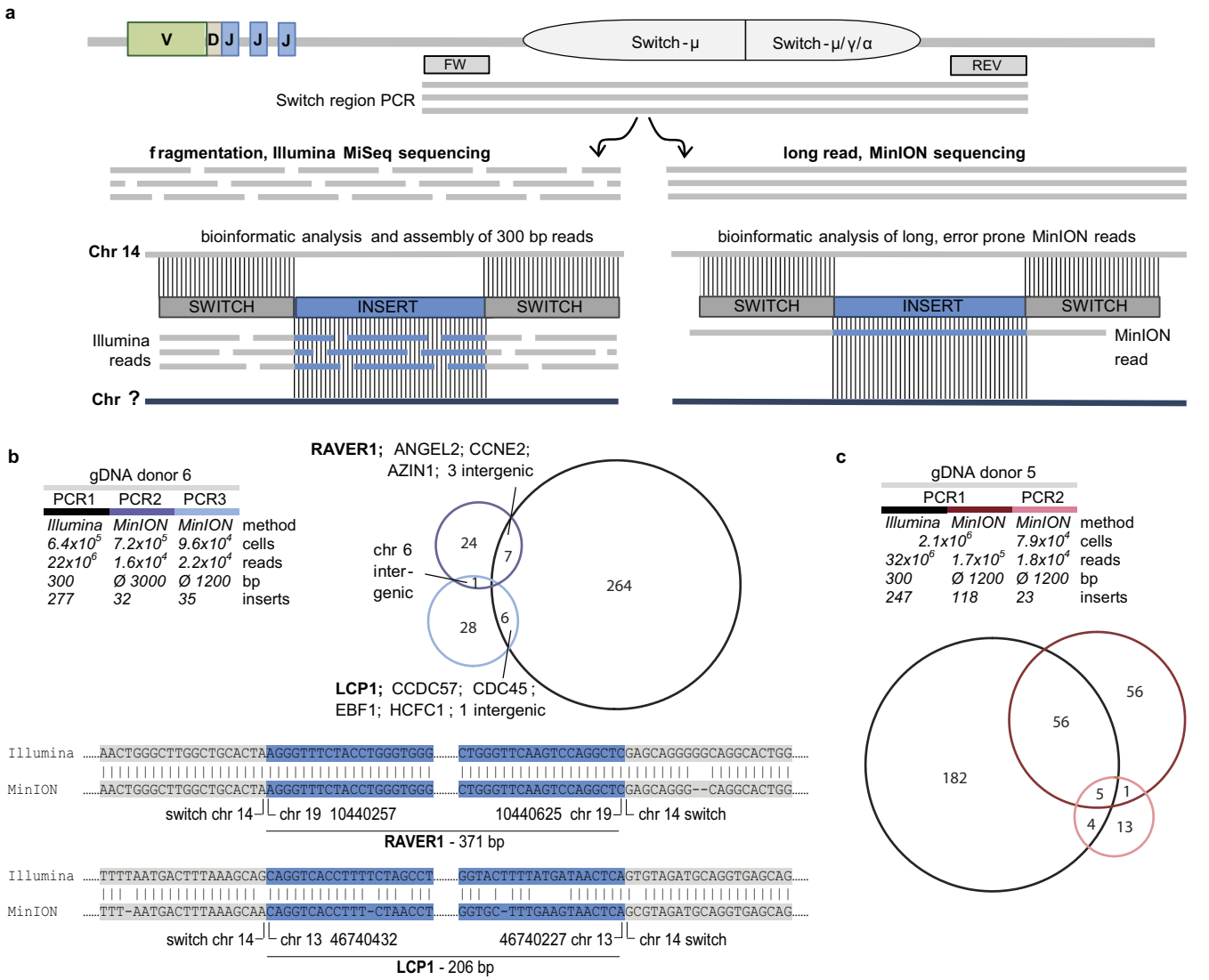

Extended Data Figure 4 | Validation of switch region inserts combining Illumina and MinION technologies. a, Illumina and MinION workflows. Switch regions of polyclonal naive or IgG/IgA switched B cells were amplified by PCR. For Illumina sequencing, PCR amplicons were fragmented, re-amplified during library preparation and sequenced using the 2 × 300 bp MiSeq system. The bioinformatic analysis included the assembly of contiguous, chimaeric reads. For insert confirmation, independently generated PCR-barcoded primary products were sequenced with MinION technology and analysed with a different bioinformatic approach for long, error-prone MinION reads. **b**, Multiple identical switch inserts for donor 6 were confirmed in biological replicate experiments with independent technical and analytical setups. Shown are the experimental designs, shared and unique reads in a Venn diagram and an alignment of Illumina and MinION sequences covering the switch insertion sites for two examples (*LCP1, RAVER1*). **c**, Shared and unique switch inserts in technical and biological replicate experiments of donor 5.

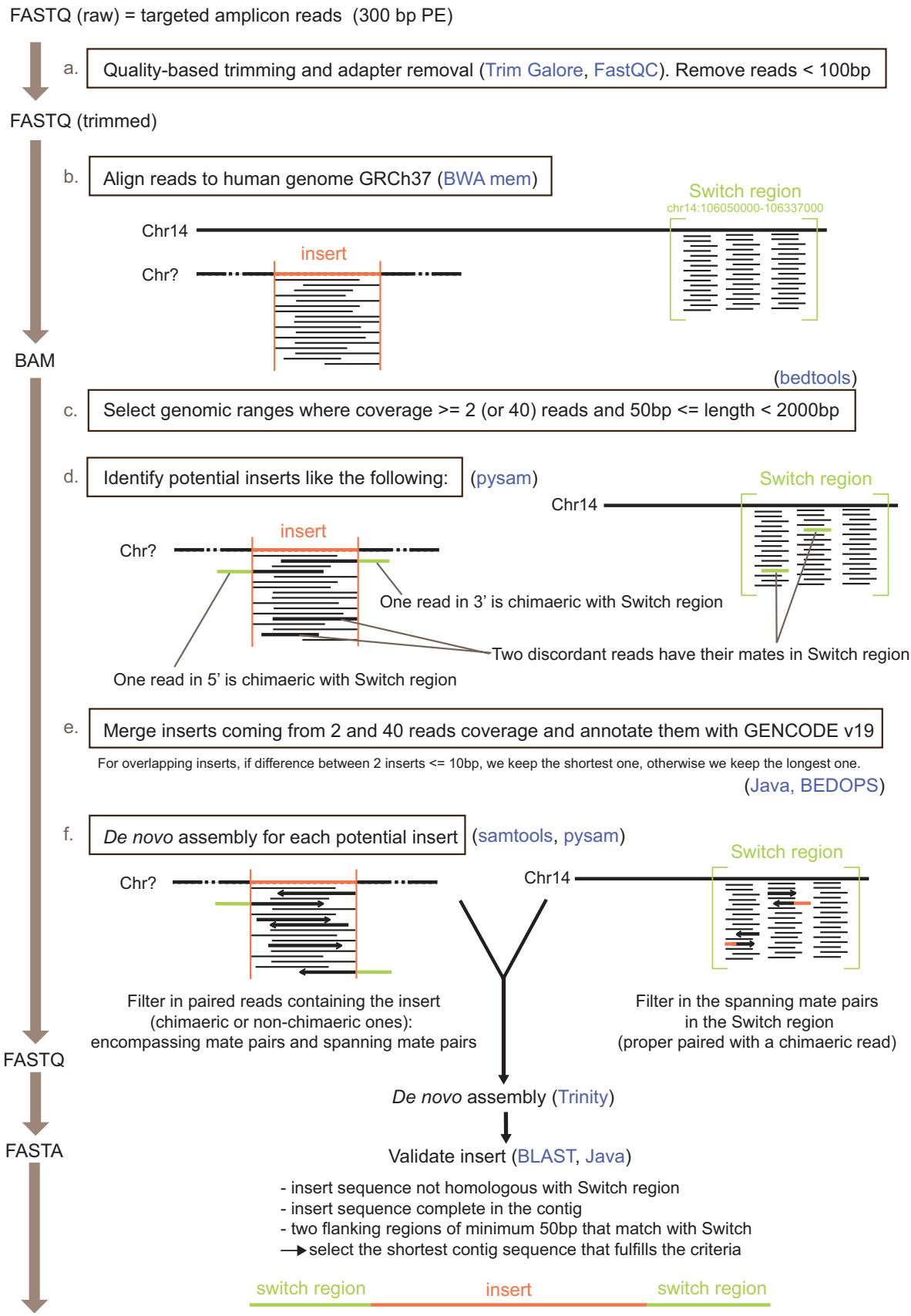

Extended Data Figure 5 | Pipeline for data analysis using the Illumina platform. Shown is the scheme of the bioinformatics workflow used for the analysis of Illumina sequences.

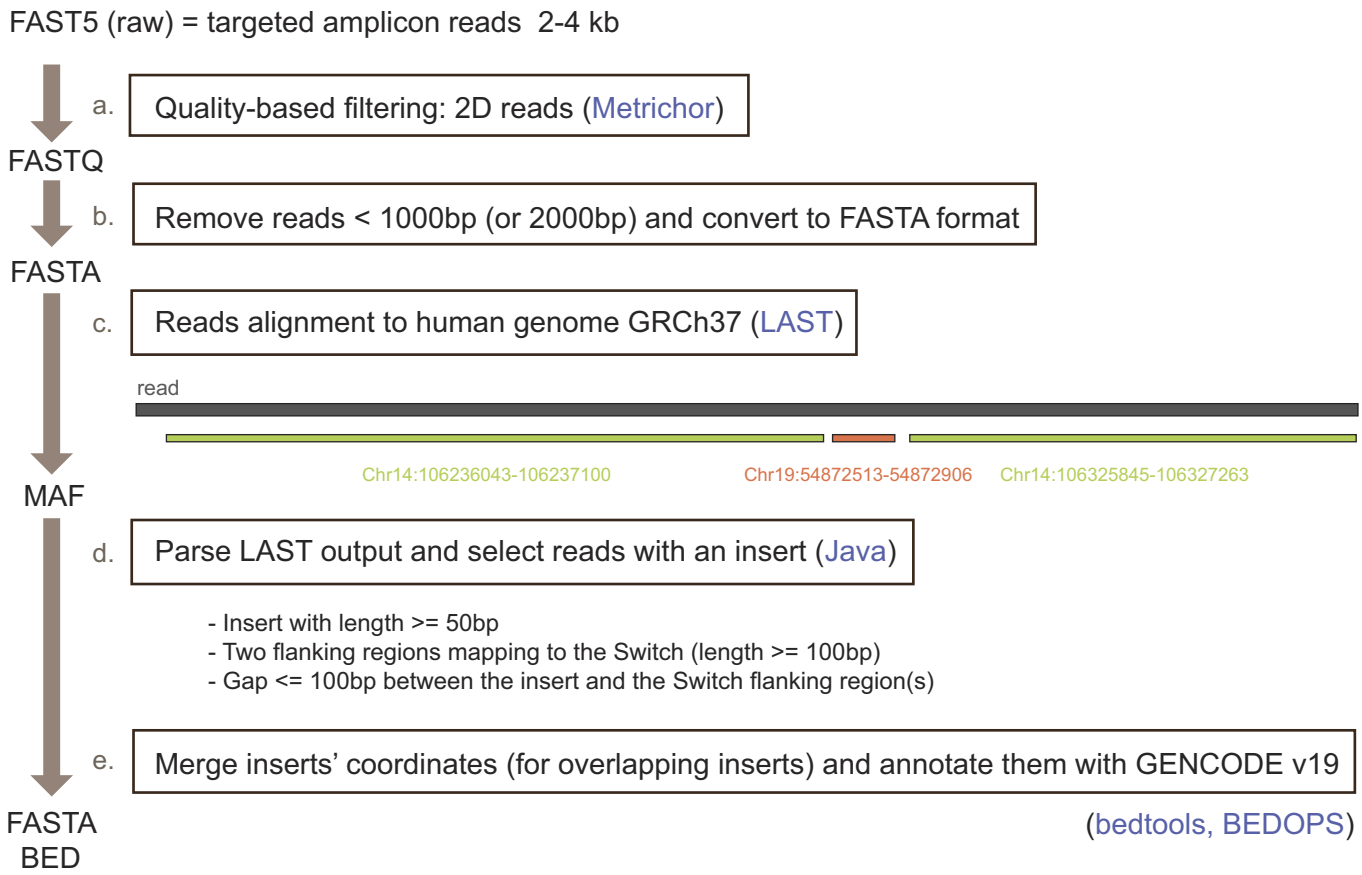

Extended Data Figure 6 | Pipeline for data analysis using the MinION technology. Shown is the scheme of the bioinformatics workflow used for the analysis.

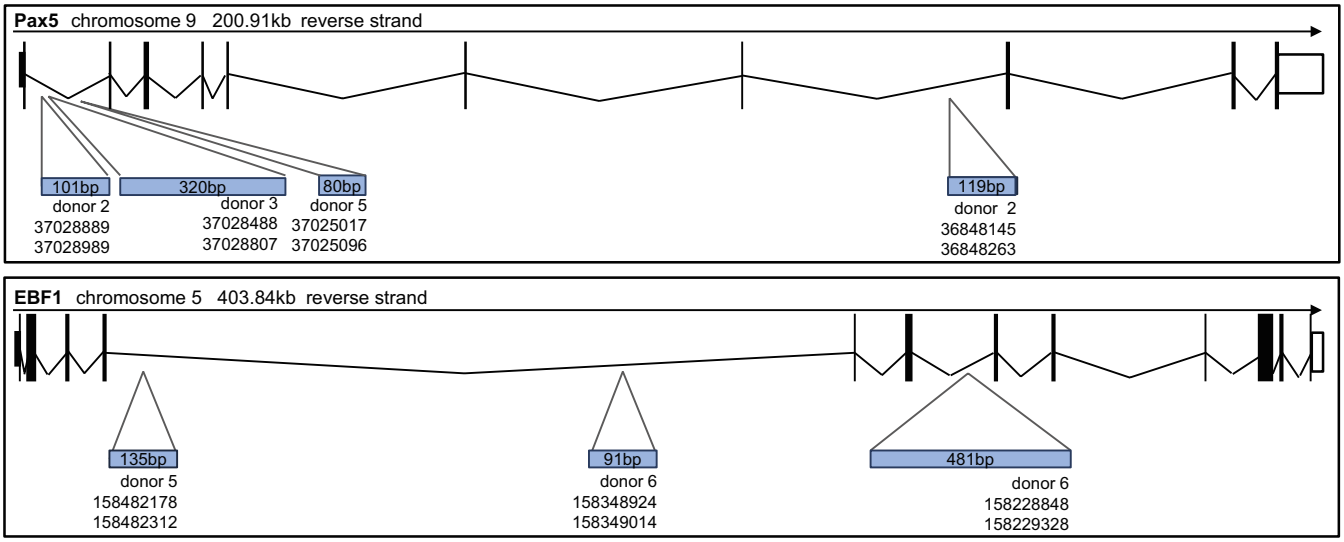

multiple insert-donor genes	
6 inserts	*SNHG1*
5 inserts	*MALAT1*
4 inserts	*CUX1, PAX5, LMNA, IRF8, AFF3, ACTB, AC010976.2*
3 inserts	*TXNDC11, SLC20A1, SETBP1, EBF1, SNHG5, SND1, SETX, RPL28, PACS1, NEAT1, ENO1, CSNK1E, BCL11A, AC096579.13*
2 inserts	*PRKD2, LCP, IKZF3, GAS2L1, FBXO11, ATG16L2, ACTG1, DGKH, HECTD4, HNRNPA1, SLAMF1, EIF3B, KDM2B, MBP, PPP2R5C, SCAPER, SNAPC4, ZNF423, ZZEF1, TCF4, RUFY3, RPTOR, RP11-63A11.1, MGRN1, INPP5D, HMGB1, ETS1, CDT1, FAM53B, HUWE1, RCC1, ST3GAL3, FANCA, L3MBTL2, MKNK2, RAB26, RPL36, ARHGEF2, CASKIN1, CSK, EEFSEC, EIF4A2, ESR2, IKZF1, MYC, NRXN2, NUP214, PKIG, RCC2, ZC3H7A, WDR66, AC096579.7, AFTPH, MAML3, PHF12, WIPF2*

Extended Data Figure 7 | Examples of genes that donate multiple inserts. Shown is the original position of the inserts donated by *PAX5* and *EBF1* as well as a list of genes that donated two or more inserts.

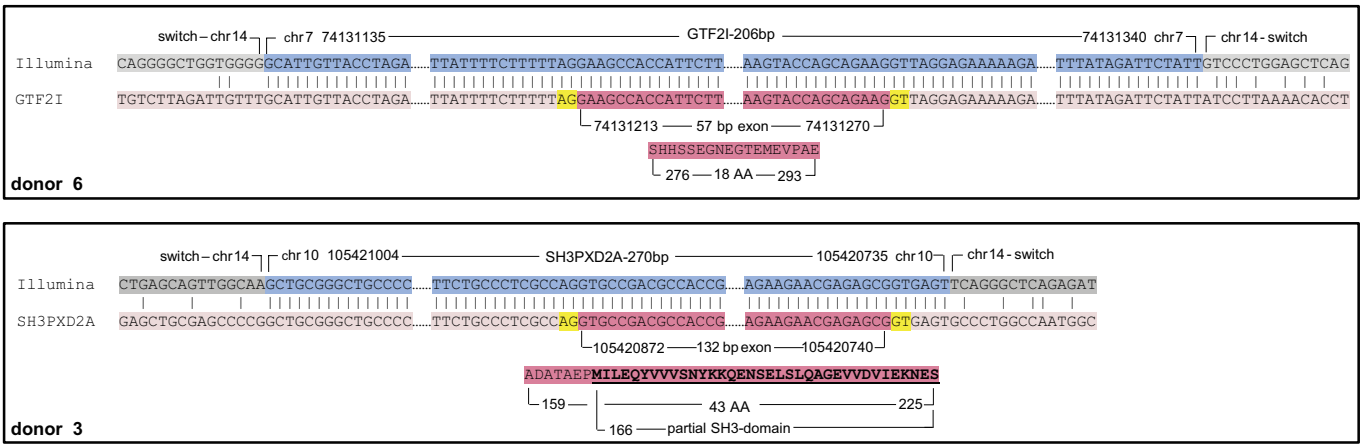

Extended Data Figure 8 | Examples of potentially functional inserts. Shown is the alignment of the contig sequence and the genomic region from which the insert was derived, as well as the potential amino acid sequence inserted between the VH and CH1.

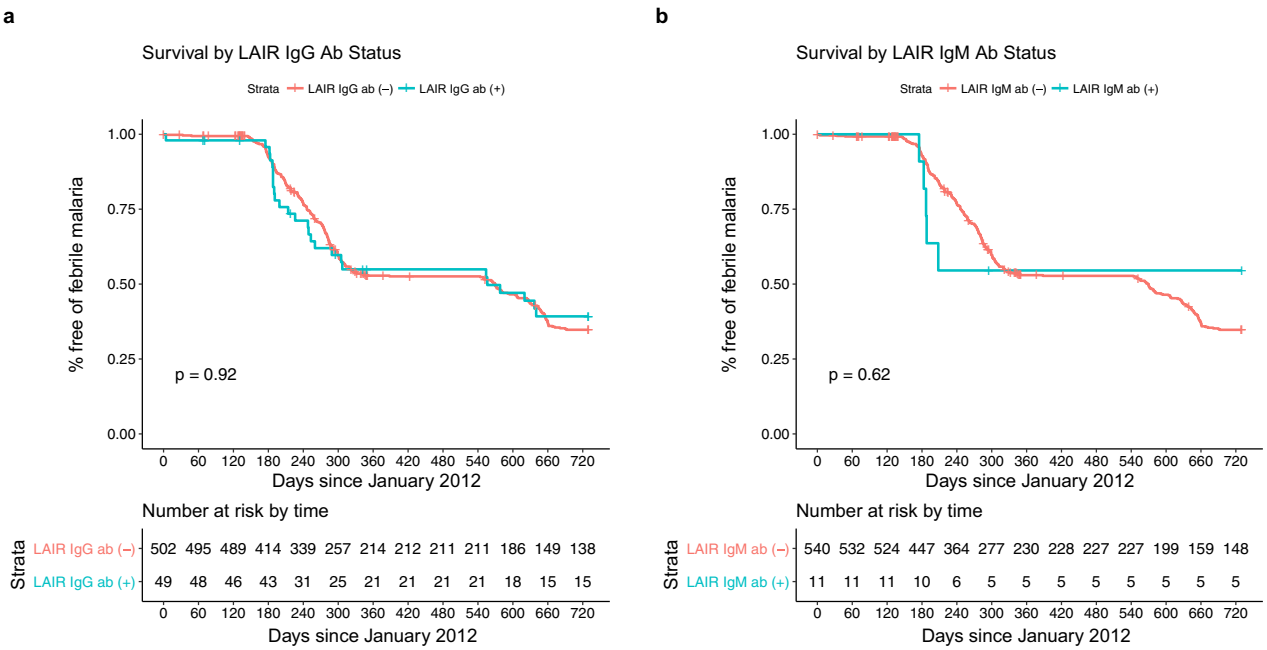

Extended Data Figure 9 | Relationship between LAIR1-IgG or LAIR1-IgM status and protection from febrile malaria. Shown is the clinical status of 551 members of the Malian cohort, stratified by LAIR1-containing IgG (**a**) or LAIR1-containing IgM (**b**) status, over the years 2012 and 2013. Febrile malaria is defined as parasite density $\geq$2,500 asexual parasites per microlitre of blood and an axillary temperature of $\geq$37.5 °C.

Extended Data Table 1 | *V* gene and insert usage of LAIR1-containing antibodies

	Donor	mAb	Isotype		Heavy chain VDJ genes (% identity to GL)					Light chain VJ genes (% identity to GL)				*LAIR1* mutations (% identity to GL)
Switch region	M (Malian)	MGM1	IgG1	λ	*VH3-30*	(79.5)	*D3-16*	*JH4*	(89.4)	*VL3-10*	(88.2)	*JL1*	(81.1)	(99.3)
		MGM3	IgG1	λ	*VH3-30*	(86.8)	*D3-16*	*JH4*	(87.2)	*VL3-10*	(88.5)	*JL1*	(78.4)	(98.0)
		MGM4	IgG1	λ	*VH3-30*	(93.4)	*D3-16*	*JH4*	(91.5)	*VL3-10*	(97.1)	*JL1*	(83.8)	(99.0)
		MGM5	IgG1	λ	*VH3-30*	(88.5)	*D3-16*	*JH4*	(83.0)	*VL3-10*	(91.0)	*JL1*	(81.1)	(99.7)
	J (Tanzanian)	MGJ1	IgG1	κ	*VH3-20*	(83.0)	*D6-25*	*JH3*	(87.8)	*VK1-5*	(89.3)	*JK3*	(91.9)	(99.3)
		MGJ2	IgG3	κ	*VH3-20*	(90.6)	*D6-19*	*JH3*	(91.8)	*VK1-5*	(96.1)	*JK3*	(91.9)	(99.7)
		MGJ3	IgG1	κ	*VH3-20*	(85.4)	*D2-21*	*JH3*	(89.8)	*VK1-5*	(88.5)	*JK3*	(89.2)	(98.6)
		MGJ5	IgG1	κ	*VH3-20*	(87.5)	*D6-19*	*JH3*	(89.8)	*VK1-5*	(98.9)	*JK3*	(97.4)	(99.3)
		MMJ1	IgM	κ	*VH3-20*	(88.2)	*D6-19*	*JH3*	(85.7)	*VK1-5*	(90.0)	*JK3*	(86.5)	(99.3)
		MMJ2	IgM	κ	*VH3-20*	(90.6)	*D6-19*	*JH3*	(81.6)	*VK1-5*	(93.2)	*JK3*	(86.5)	(99.3)
		MMJ5	IgM	κ	*VH3-20*	(91.7)	*D6-19*	*JH3*	(83.7)	*VK1-5*	(92.5)	*JK3*	(86.5)	(99.3)
		MMJ6	IgM	κ	*VH3-20*	(91.0)	*D6-19*	*JH3*	(79.6)	*VK1-5*	(91.4)	*JK3*	(86.5)	(99.3)
		MMJ7	IgM	κ	*VH3-20*	(90.6)	*D6-19*	*JH3*	(81.6)	*VK1-5*	(92.8)	*JK3*	(86.5)	(99.3)
		MMJ8	IgM	κ	*VH3-20*	(90.6)	*D6-19*	*JH3*	(81.6)	*VK1-5*	(93.2)	*JK3*	(86.5)	(99.3)
		MMJ10	IgM	κ	*VH3-20*	(90.6)	*D6-19*	*JH3*	(81.6)	*VK1-5*	(93.2)	*JK3*	(86.8)	(99.3)
		MMJ16	IgM	κ	*VH3-20*	(90.6)	*D6-19*	*JH3*	(81.6)	*VK1-5*	(93.2)	*JK3*	(86.5)	(98.3)
		MMJ23	IgM	κ	*VH3-20*	(91.7)	*D6-19*	*JH3*	(83.7)	*VK1-5*	(92.5)	*JK3*	(86.5)	(99.3)
		MMJ25	IgM	κ	*VH3-20*	(90.6)	*D6-19*	*JH3*	(83.7)	*VK1-5*	(92.1)	*JK3*	(86.5)	(99.3)
	B (Kenyan)	MGB2	IgG3	nd	*nd*	(nd)	*nd*	*nd*	(nd)	*nd*	(nd)	*nd*	(nd)	(97.6)
		MGB43	IgG3	nd	*nd*	(nd)	*nd*	*nd*	(nd)	*nd*	(nd)	*nd*	(nd)	(98.0)
		MGB47	IgG3	nd	*nd*	(nd)	*nd*	*nd*	(nd)	*nd*	(nd)	*nd*	(nd)	(98.0)
VDJ region	E (Tanzanian)	MGE7	IgG1	λ	*VH1-46*	(89.9)	*D2-15*	*JH3*	(85.7)	*VL2-14*	(91.3)	*JL7*	(86.5)	(95.2)
		MGE9	IgG1	λ	*VH1-46*	(88.5)	*D3-10*	*JH3*	(91.8)	*VL2-14*	(93.4)	*JL7*	(91.9)	(85.4)
		MME2	IgM	λ	*VH1-46*	(86.1)	*D1-26*	*JH3*	(87.8)	*VL2-14*	(94.4)	*JL7*	(91.7)	(92.5)
		MME4	IgM	λ	*VH1-46*	(86.8)	*D2-21*	*JH3*	(91.8)	*VL2-14*	(93.4)	*JL7*	(85.7)	(92.9)
		MME10	IgM	λ	*VH1-46*	(86.8)	*D1-26*	*JH3*	(91.8)	*VL2-14*	(92.4)	*JL7*	(88.6)	(92.2)
	F (Tanzanian)	MGF8	IgG2	κ	*VH4-38-2*	(93.8)	*D5-18*	*JH5*	(90.0)	*VK3-15*	(94.3)	*JK2*	(92.1)	(90.5)
		MGF11	IgG1	κ	*VH4-38-2*	(92.4)	*D5-18*	*JH5*	(96.0)	*VK3-15*	(92.5)	*JK2*	(94.7)	(89.5)
		MGF21	IgG1	κ	*VH4-38-2*	(88.5)	*D7-27*	*JH5*	(92.0)	*VK3-15*	(92.8)	*JK2*	(92.1)	(89.8)
		MGF33	IgG1	κ	*VH4-38-2*	(91.3)	*D3-3*	*JH5*	(92.0)	*VK3-15*	(92.1)	*JK2*	(97.4)	(92.9)
		MGF39	IgG1	κ	*VH4-38-2*	(94.1)	*D5-18*	*JH5*	(96.0)	*VK3-15*	(95.0)	*JK2*	(92.3)	(94.2)
		MGF45	IgG1	κ	*VH4-38-2*	(91.3)	*D3-3*	*JH5*	(92.0)	*VK3-15*	(91.8)	*JK2*	(97.4)	(92.9)
		MGF58	IgG1	κ	*VH4-38-2*	(92.4)	*D5-18*	*JH5*	(92.0)	*VK3-20*	(97.2)	*JK2*	(97.4)	(91.8)
		MGF64	IgG1	κ	*VH4-38-2*	(91.3)	*D5-18*	*JH5*	(96.0)	*VK3-15*	(91.8)	*JK2*	(97.4)	(91.5)
	O (Malian)	MGO1	IgG1	κ	*VH4-59*	(87.4)	*D3-10*	*JH4*	(87.2)	*VK3D-20*	(90.4)	*JK5*	(100.0)	(86.1)
		MGO2	IgG1	κ	*VH4-59*	(89.8)	*D2-2*	*JH4*	(85.1)	*VK3D-20*	(94.0)	*JK5*	(97.3)	(86.1)
		MGO3	IgG1	κ	*VH4-59*	(89.1)	*D3-10*	*JH4*	(85.1)	*VK3D-20*	(90.8)	*JK5*	(92.1)	(92.2)
		MGO4	IgG1	κ	*VH4-59*	(91.6)	*D3-10*	*JH4*	(80.9)	*VK3D-20*	(94.3)	*JK5*	(97.3)	(92.5)
	Q (Malian)	MGQ1	IgG1	κ	*VH4-59*	(90.9)	*D3-10*	*JH3*	(98.0)	*VK2-30*	(95.9)	*JK1*	(94.1)	(93.9)
		MGQ4	IgG1	κ	*VH4-59*	(94.0)	*D3-10*	*JH3*	(98.0)	*VK2-30*	(94.2)	*JK1*	(91.2)	(96.6)
		MGQ5	IgG2	κ	*VH4-59*	(89.9)	*D3-10*	*JH3*	(100.0)	*VK2-30*	(91.8)	*JK1*	(85.3)	(94.2)
		MGQ6	IgG1	κ	*VH4-59*	(94.0)	*D3-10*	*JH3*	(98.0)	*VK2-30*	(95.6)	*JK1*	(94.1)	(95.6)
		MGQ9	IgG1	κ	*VH4-59*	(92.3)	*D3-10*	*JH3*	(100.0)	*VK2-30*	(95.6)	*JK1*	(97.1)	(94.9)
		MGQ11	IgG1	κ	*VH4-59*	(93.3)	*D3-10*	*JH3*	(95.9)	*VK2-30*	(95.9)	*JK1*	(100.0)	(95.9)
		MGQ12	IgG1	κ	*VH4-59*	(92.7)	*D3-10*	*JH3*	(100.0)	*VK2-30*	(94.2)	*JK1*	(94.1)	(95.9)
		MGQ14	IgG1	κ	*VH4-59*	(90.2)	*D3-10*	*JH3*	(98.0)	*VK2-30*	(95.6)	*JK1*	(94.1)	(93.9)
		MGQ15	IgG2	κ	*VH4-59*	(91.2)	*D3-10*	*JH3*	(100.0)	*VK2-30*	(92.5)	*JK1*	(85.3)	(94.2)
		MGQ16	IgG1	κ	*VH4-59*	(94.4)	*D3-10*	*JH3*	(98.0)	*VK2-30*	(96.3)	*JK1*	(97.1)	(96.3)
		MGQ19	IgG1	κ	*VH4-59*	(95.4)	*D3-10*	*JH3*	(95.4)	*VK2-30*	(97.3)	*JK1*	(97.1)	(96.9)
		MGQ20	IgG2	κ	*VH4-59*	(90.5)	*D3-10*	*JH3*	(100.0)	*VK2-30*	(95.9)	*JK1*	(91.2)	(94.6)
		MGQ21	IgG1	κ	*VH4-59*	(92.6)	*D3-10*	*JH3*	(100.0)	*VK2-30*	(97.6)	*JK1*	(100.0)	(93.9)
		MGQ22	IgG1	κ	*VH4-59*	(88.1)	*D3-10*	*JH3*	(100.0)	*VK2-30*	(93.8)	*JK1*	(100.0)	(95.2)

Isotype and *V(D)J* gene usage of heavy chain and light chain of mAbs containing LAIR1 in the switch or in the VDJ region. *D* genes of the monoclonal antibodies containing a V(D)J insert cannot always be properly predicted by IMGT. Mutations of the *LAIR1* insert are shown as % of identity to the genomic unmutated *LAIR1* exon. GL, germline; nd, not determined.